Agriculture, Pêcheries et Alimentation Québec

PRIME-VERT
UN PAS DE PLUS. POUR VOUS. POUR VOTRE COLLECTIVITÉ.

DIAGNOSTIC SIMULTANÉ DES GÈNES D'AVIRULENCE DE *PHYTOPHTHORA SOJAE* POUR UNE GESTION OPTIMALE DE LA LUTTE GÉNÉTIQUE CHEZ LE SOYA

19-002-2.2-C-ULAV

DURÉE DU PROJET : JUIN 2019 / AOÛT 2023

RAPPORT FINAL

Réalisé par :
Caroline Labbé, Université Laval
Richard R. Bélanger, Université Laval

DATE

31 JANVIER 2023

DIAGNOSTIC SIMULTANÉ DES GÈNES D'AVIRULENCE DE *PHYTOPHTHORA SOJAE* POUR UNE GESTION OPTIMALE DE LA LUTTE GÉNÉTIQUE CHEZ LE SOYA

19-002-2.2-C-ULAV

RÉSUMÉ DU PROJET

La lutte génétique contre les maladies des végétaux est l'une des méthodes les plus efficaces et sécuritaires pour l'environnement. Dans le cas du soya, une des grandes cultures les plus importantes mondialement, il existe des variétés exprimant des gènes de résistance contre la pourriture causée par l'agent pathogène *Phytophthora sojae*, un des fléaux liés à cette production. Cependant, pour que la lutte génétique fonctionne bien, il faut au préalable, connaître le génotype des facteurs dits d'avirulence (*Avr*) de la souche de *P. sojae* qui se trouve dans un champ particulier (pathotype). En effet, les gènes de résistance à *P. sojae* (*Rps*) exprimés par différentes variétés de soya, ne sont efficaces que contre certains gènes *Avr* de l'agent pathogène. C'est pourquoi il est important de déterminer le pathotype de *P. sojae* qui repose sur la capacité de cet agent pathogène à exprimer, ou non, les gènes *Avr* qui sont des protéines effectrices issues de la traduction de ces gènes. Les gènes *Avr*, préalablement identifiés et séquencés, montrent des divergences au niveau de leur ADN ce qui a permis l'identification des séquences génétiques soit, des tronçons d'ADN qui diffèrent entre l'haplotype virulent et l'haplotype avirulent, que l'on décrit plus tard dans le texte comme « marqueurs génétiques ». À l'aide de ces marqueurs, il a été possible de construire des amorces spécifiques dans le but de créer un protocole PCR qui permet de les discriminer et, du même coup, de déterminer, pour un isolat de *P. sojae* donné, son profil de virulence contre les gènes de résistance (*Rps*) du soya.
L'objectif du présent projet était de développer un outil moléculaire permettant d'obtenir et de caractériser le pathotype des isolats de l'agent pathogène *P. sojae* prélevés à partir d'échantillons de sols et/ou plantes récoltés dans des champs de soya au Québec et ailleurs. Ce faisant, suivant l'identification du pathotype de l'agent pathogène dans un champ donné, cela devait permettre de choisir de façon éclairée la variété de soya exprimant le bon gène de résistance pour contrer le pathotype de l'isolat présent.

OBJECTIFS ET APERÇU DE LA MÉTHODOLOGIE

L'objectif principal du projet était d'offrir aux producteurs et semenciers de soya un outil moléculaire de diagnostic rapide et précis permettant d'identifier de façon simultanée la présence/absence de l'allèle *Avr* (avirulent) pour les sept principaux gènes d'avirulence (effecteurs) connus chez *P. sojae* afin d'en établir le pathotype à partir d'échantillons de sol/plantes provenant de leurs champs. Cet objectif atteint, les producteurs et semenciers seraient en mesure de choisir, en toute connaissance de cause, les cultivars de soya possédant les gènes *Rps* appropriés pour leur culture. Pour ce faire, notre laboratoire a tout d'abord identifié des marqueurs moléculaires (ou génétiques), i.e. des variations d'ADN qui divergeaient entre les formes avirulente (*Avr*) et virulente (*avr*) pour les différents facteurs d'avirulence à l'étude chez *P. sojae*. Les résultats de ce travail ont été publiés par Arsenault-Labrecque *et al*. en 2018. En ayant établi les divergences génétiques entre les allèles virulent et avirulent, il était alors possible de créer un outil moléculaire basé sur l'utilisation de la technologie PCR.

Objectif 1. Le premier objectif de ce projet était d'optimiser le test PCR multiplexe. Cette technique consiste à amplifier, de façon simultanée, tous les allèles *Avr* des gènes à l'étude et ce, dans une seule réaction PCR. À l'aide des marqueurs génétiques préalablement identifiés, il a fallu élaborer des jeux d'amorces permettant de détecter, avec un minimum de réactions PCR (multiplexe), la présence ou non de l'allèle avirulent chez des souches de *P. sojae* sélectionnées et ce, pour sept différents gènes d'avirulence (*Avr1a*, *1b, 1c*, *1d, 1k, 3a* et *6*). Tout d'abord, il fallait créer des amorces qui amplifiaient correctement les allèles *Avr* des différents gènes de façon individuelle (PCR uniplexe). Il a ensuite été

nécessaire d'établir différentes combinaisons de ces amorces dans un mélange avec lequel il était possible, sans interférence, d'amplifier la totalité des gènes *Avr* à l'étude.

Le deuxième objectif (**Objectif 2**) consistait à valider l'efficacité des marqueurs génétiques retenus pour le test de génotypage (PCR multiplexe). Brièvement, pour chaque pathotype obtenu par génotypage sur des isolats de *P. sojae* inconnus, il fallait le comparer et, ultimement, le valider avec un pathotypage effectué en serre selon la méthode de Lebreton *et al.,* 2018, qui consistait à tester différentes accessions de soya qui exprimaient chacune un gène *Rps* (*Rps1a, Rps1b, Rps1c, Rps1d, Rps1k, Rps3a* et *Rps6*) en présence d'un isolat de *P. sojae* à virulence inconnue. À la suite du bioessai mené en bassins hydroponiques, le pathotype de l'agent pathogène est alors obtenu en comparant l'intensité des symptômes des différentes lignées du différentiel *Rps* avec le cultivar *rps* i.e. qui ne contient aucun gène de résistance. Enfin, afin d'établir ou non la présence d'haplotypes supplémentaires non répertoriés chez les gènes *Avr* étudiés, nous avons utilisé 23 isolats supplémentaires de *P. sojae* pour lesquels les données de phénotypage en bassin hydroponique avaient été obtenues et nous les avons séquencés. Cette analyse de séquençage devait également permettre de découvrir l'haplotype des allèles *Avr/avr* pour les gènes *Avr3b* et *Avr3c.* Lors de ce travail, les souches de *P. sojae* utilisées provenaient du Québec, de l'Ontario, et du Manitoba.

Objectif 3. Le troisième objectif visait à mettre au point une méthode d'extraction d'ADN directement à partir d'échantillons de sols ou encore, à partir de plantes présentant la pourriture phytophthoréenne dans le but de fournir au LEDP une approche rapide de diagnostic sur plantes et à une compagnie, une approche avec sol. Cet objectif servait à développer un protocole d'utilisation de l'outil moléculaire suffisamment performant pour espérer obtenir le diagnostic (pathotype) du champ dans des temps inférieurs à deux semaines, ce qui semblait raisonnable au vu des trois à quatre mois nécessaires à l'isolement de souches purifiées à partir d'échantillons de sol. Lors de ces travaux, une méthodologie (*speed-baiting*) a été développée. Elle consistait à faire flotter de petits morceaux de feuilles de soya à la surface d'échantillons de sols (contaminés potentiellement par *P. sojae*) saturés en eau. Après 24-48 heures, les morceaux de feuilles étaient récoltés et lyophilisés avant d'en faire l'extraction d'ADN. En parallèle, différents kits d'extraction d'ADN pour les sols et plantes ont été testés afin d'effectuer directement la PCR multiplexe sur l'ADN obtenu.

Enfin, l'**Objectif 4** consistait à transférer le test moléculaire (PCR multiplexe) conventionnel en test q-PCR. L'utilisation de la PCR quantitative en temps réel est effectivement un outil qui pourrait permettre non seulement de détecter la présence de l'agent pathogène via l'amplification de ses gènes *Avr* mais aussi, de quantifier le niveau de contamination d'un échantillon de sol donné. Suite aux résultats obtenus à l'objectif 3, il a fallu adapter ce test car la détection des haplotypes des gènes *Avr* de *P. sojae* à partir de l'ADN provenant d'échantillons de sols ou encore de plantes/d'appâts foliaires était impossible en raison de l'interférence de la grande quantité d'ADN étranger avec la PCR multiplexe. En conséquence, un test rt-PCR (real-time PCR) en uniplexe pour chaque gène *Avr* a été développé. Brièvement, des amorces permettant d'amplifier la zone variable (marqueurs génétiques) pour chaque gène *Avr* ont été conçues et utilisées. Le produit d'amplification obtenu pouvait ensuite être analysé par HRM (*high resolution melting* curve) en exploitant le fait que les allèles *Avr* et *avr* présentaient des courbes de fusion différentes. Il est ainsi possible de déterminer directement l'haplotype de l'amplicon obtenu suite à l'amplification.

RÉSULTATS SIGNIFICATIFS OBTENUS ET DISCUSSION

Objectif 1. Optimisation du test PCR multiplexe. Une méthodologie PCR multiplexe a été développée afin de déterminer l'haplotype des gènes d'avirulence suivants dans des isolats de *Phytophthora sojae* : *Avr1a, 1b, 1c, 1d, 1k, 3a* et *6*. Les résultats de ces travaux ont été publiés par Dussault-Benoit, *et al*. 2020 (Annexe 1). Brièvement, des amorces spécifiques ont été développées pour identifier les allèles avirulents (*Avr*) des gènes à l'étude. La concentration des amorces dans le *master mix*, les températures d'appariement pour la PCR, la taille de l'amplicon obtenu pour chacun des gènes, étaient les contraintes à optimiser pour l'obtention d'un protocole de PCR multiplexe. Lors de ces travaux, deux protocoles de réactions PCR ont été développés : un test PCR multiplexe pour les gènes *Avr1a, 1b, 1d, 1k, 3a* et *6* et un test PCR unique pour *Avr1c* car les amorces permettant de discriminer la forme virulente de la forme avirulente pour ce gène interféraient avec les autres amorces dans le test multiplexe. Les résultats obtenus avec le protocole sont présentés à la Figure 1.

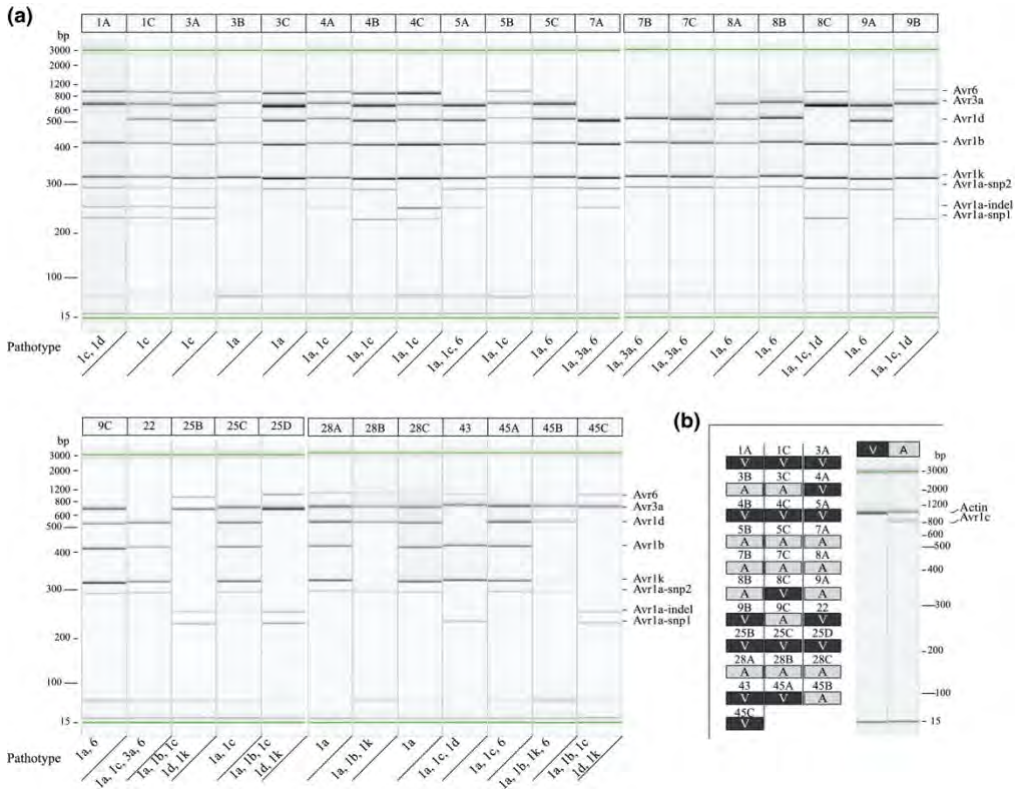

Figure 1. a) PCR multiplexe permettant d'amplifier l'allèle *Avr* (avirulent) des gènes *Avr1a, 1b, 1d, 1k, 3a* et *6* effectuée sur 31 isolats de *Phytophthora sojae* afin d'en établir le pathotype. B) PCR uniplexe pour le gène *Avr1c*.
Pour les deux tests, lorsque l'amplicon est présent, le pathotype est avirulent pour le gène associé.

Objectif 2. Validation des marqueurs génétiques retenus. Les résultats obtenus lors de l'utilisation de l'outil moléculaire ont été comparés avec les phénotypes obtenus par bioessais hydroponiques. Plus de 360 pathotypages par phénotypage ont été effectués pour répondre à cet objectif durant le projet. Les résultats de validation présentés au **Tableau 1**, sont issus des phénotypages (130) pour lesquels les accessions Williams *Rps1c* et Williams *Rps3a* ont été utilisées lors des bio-essais. En résumé, une validation moyenne de 93% a été obtenue pour l'ensemble des interactions *Avr/Rps* à l'étude. De fait, pour l'interaction *Avr3a/Rps3a*, un score parfait a été obtenu lorsque le bon différentiel a été utilisé. De plus, Arsenault-Labrecque *et al.* (2022) ont démontré que *Avr3a* pouvait être utilisé contre *Rps8* (annexe II).

Tableau 1. Validation du test génétique avec les résultats de pathotypage par phénotypage (bioessai hydroponique) sur 130 isolats de *Phytophthora sojae* de diverses provenances géographiques (2019-2022). N.B. l'ensemble des résultats est présenté à l'Annexe III du présent document.

Gène pour gène	Confirmation	Outliers	Confirmation (%)
Avr1a/Rps1a	118	12	91%
Avr1b/Rps1b	120	10	92%
Avr1c/Rps1c	119	11	92%
Avr1d/Rps1d	119	11	92%
Avr1k/Rps1k	119	11	92%
Avr3a/Rps3a	130	0	100%
Avr6/Rps6	125	5	96%

Les rares cas de disparité entre génotypes et phénotypes peuvent s'expliquer par des facteurs externes qui affectent parfois la résolution du bioessai hydroponique (Annexe IV). En effet, le degré de virulence des souches et les conditions environnementales sont des paramètres difficiles à gérer par l'expérimentateur. Par exemple, les gènes *Rps1b* et *Rps1k*, montrent des résultats intermédiaires dans certains cas au niveau du bioessai alors qu'il est beaucoup plus simple d'interpréter le résultat PCR, ce qui peut expliquer les quelques disparités observées pour ces deux gènes (Fig. 2 A, B, C; Fig. 3 A, B, C). Par exemple, pour *Rps1b* et *Rps1k*, les souches 603 et 778 seraient classées virulentes en phénotypage alors que le génotype est *Avr* (Fig. 2A; Fig. 3).

Afin de déterminer si de nouveaux pathotypes étaient présents dans les souches testées, un séquençage complet (WGS) a été effectué avec la technologie Illumina 150PE sur 23 isolats de *P. sojae*, en sus des séquençages pour les 31 isolats déjà disponibles. Ce travail avait pour objectif la recherche de nouveaux haplotypes chez les gènes *Avr* déjà à l'étude en plus de la recherche de marqueurs pour de nouveaux gènes *Avr* tels que *Avr3b* et *Avr3c*. Après les analyses en bio-informatique (mapping, analyse de variants), il a été possible de trouver de nouveaux marqueurs génétiques notamment pour le gène *Avr6*. En effet, l'étude bio-informatique des 23 isolats précédents a révélé que si le locus du gène *Avr3c* était utilisé à la place du marqueur pour le gène *Avr6*, les discordances entre génotype et phénotype étaient complètement éliminées (Figures 4 A, B et 5 A, B). Par exemple, la souche 778 qui présentait un génotype avirulent pour le marqueur *Avr6*, présentait un phénotype virulent, résultat corroboré par le marqueur du gène *Avr3c* (Fig. 4A et 5B). De même, la souche 556 qui avait été classée virulente à *Rps6* selon le marqueur *avr6*, a été re-classifiée *Avr* avec le marqueur du gène *Avr3c* (Fig. 4B et 5A). Comme ces deux gènes font partie du même « linkage group » (Dong *et al.,* 2009), il est plausible que le gène d'avirulence/virulence à *Rps6* et *Rps3c* soit l'effecteur *Avh27* (*Avr3c*). Enfin, ce qui milite également en faveur du *Avr3c* comme unique facteur d'avirulence dans cette région est que les mutations associées aux différents phénotypes sont situées dans la CDS alors qu'il n'y a pas de mutation dans la CDS de *Avr6*.

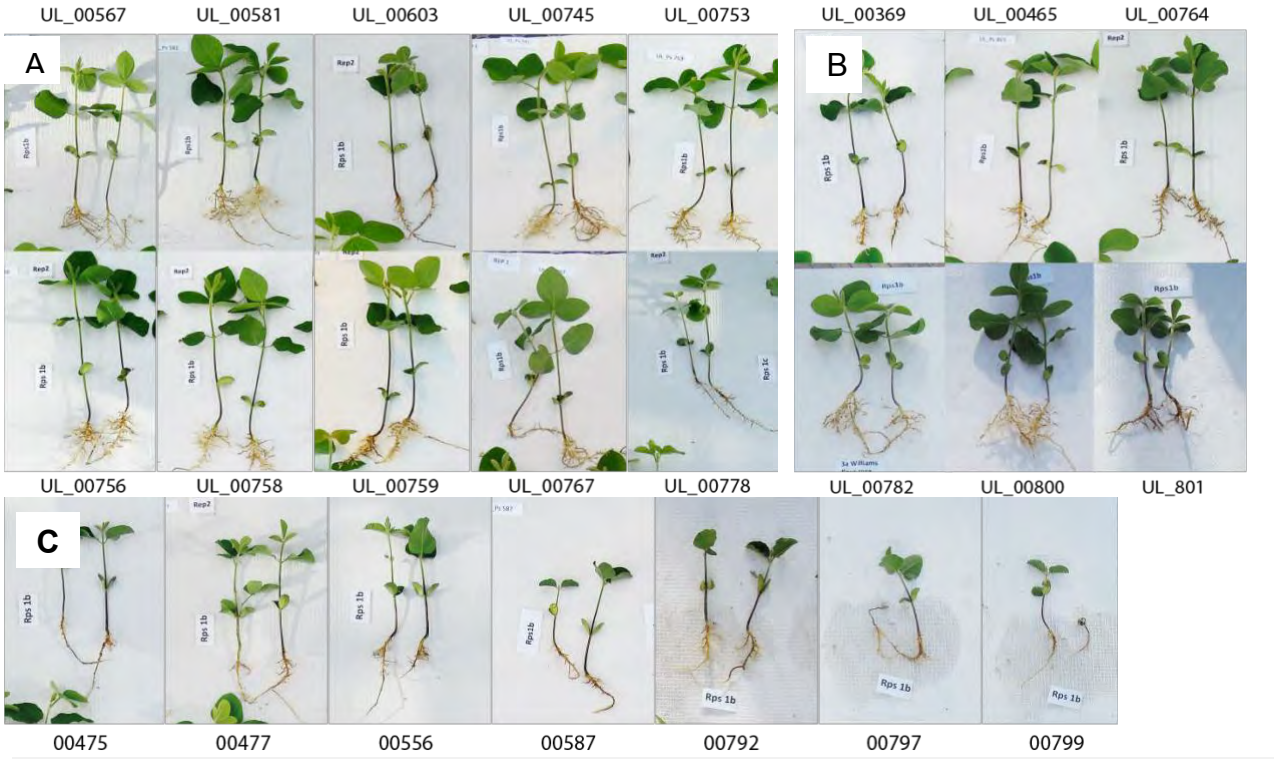

Figure 2. Phénotypes observés sur 23 isolats de *Phytophthora sojae*, pour le gène *Rps1b* selon les génotypes analysés (3 allèles différents A, B et C). A et B génotype avirulent (*Avr*). C. génotype virulent

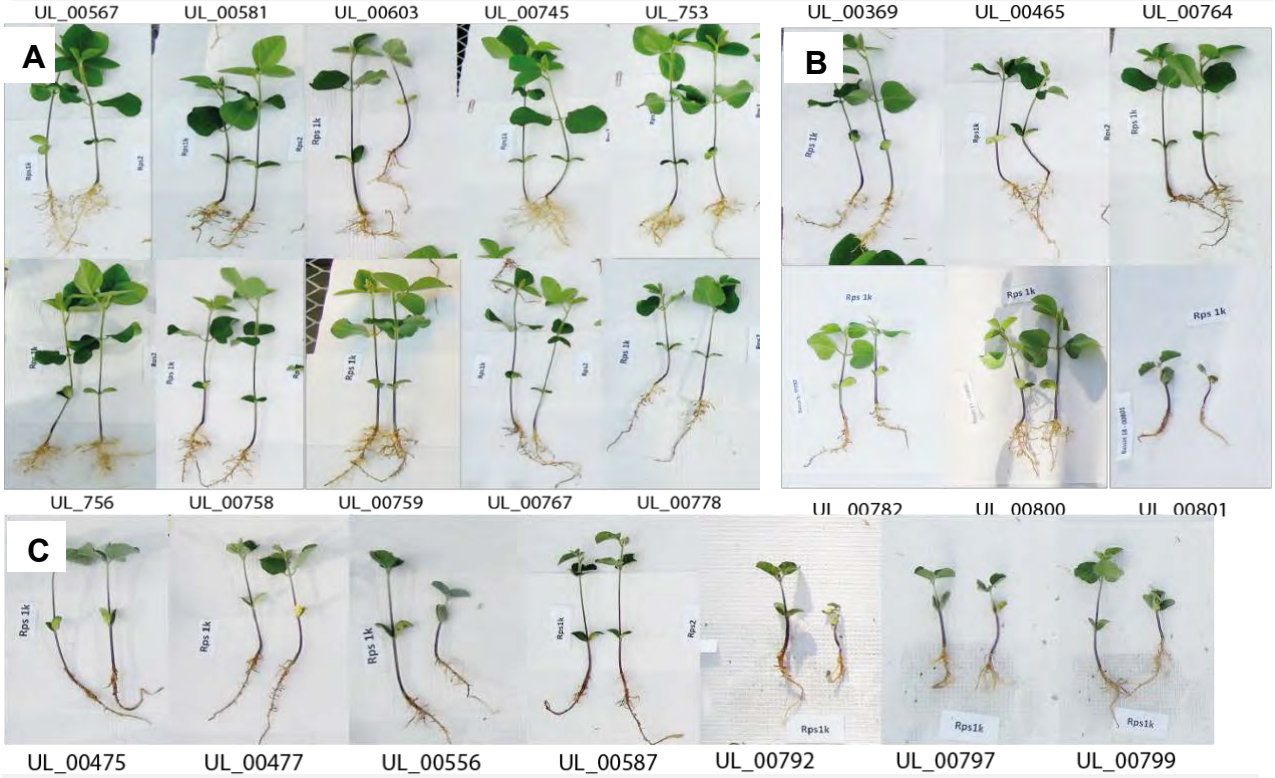

Figure 3. Phénotypes observés sur 23 isolats de *Phytophthora sojae* pour le gène *Rps1k* selon les génotypes analysés (3 allèles différents **A**, **B** et **C**). **A**, **B.** Génotype avirulent (*Avr*). **C**. Génotype virulent (*avr*).

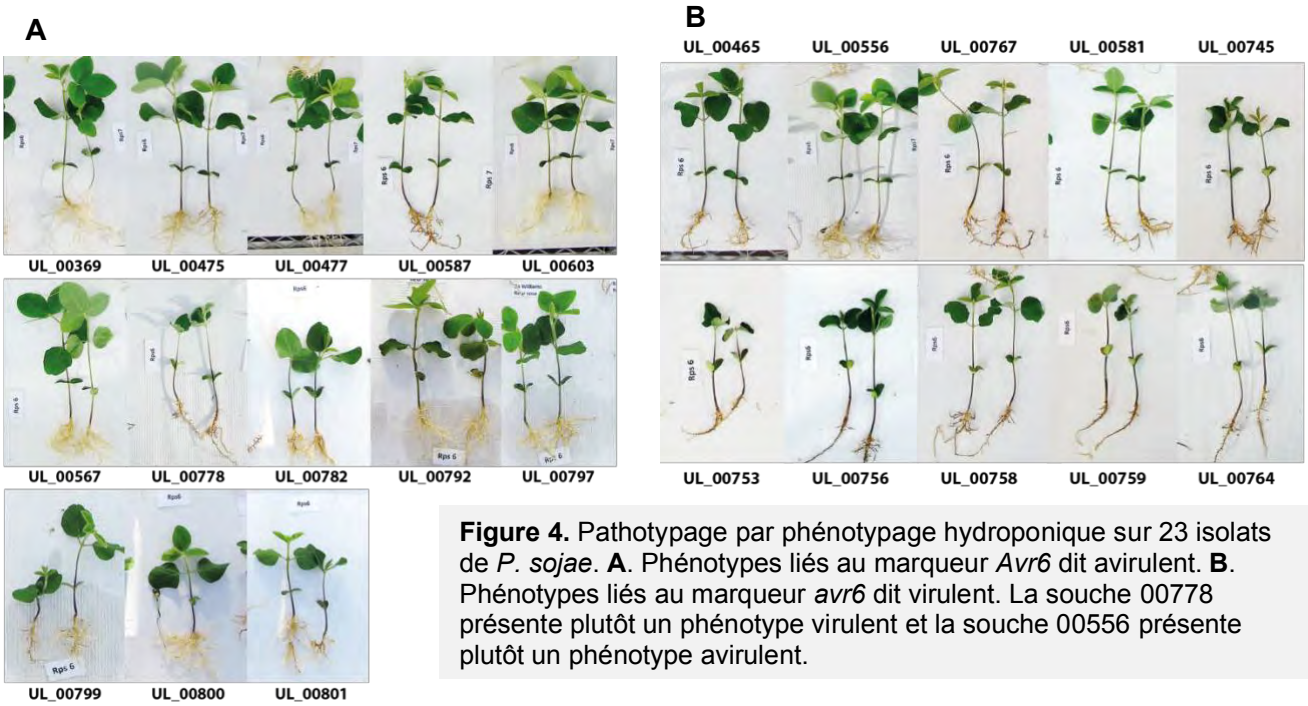

Figure 4. Pathotypage par phénotypage hydroponique sur 23 isolats de *P. sojae*. **A**. Phénotypes liés au marqueur *Avr6* dit avirulent. **B**. Phénotypes liés au marqueur *avr6* dit virulent. La souche 00778 présente plutôt un phénotype virulent et la souche 00556 présente plutôt un phénotype avirulent.

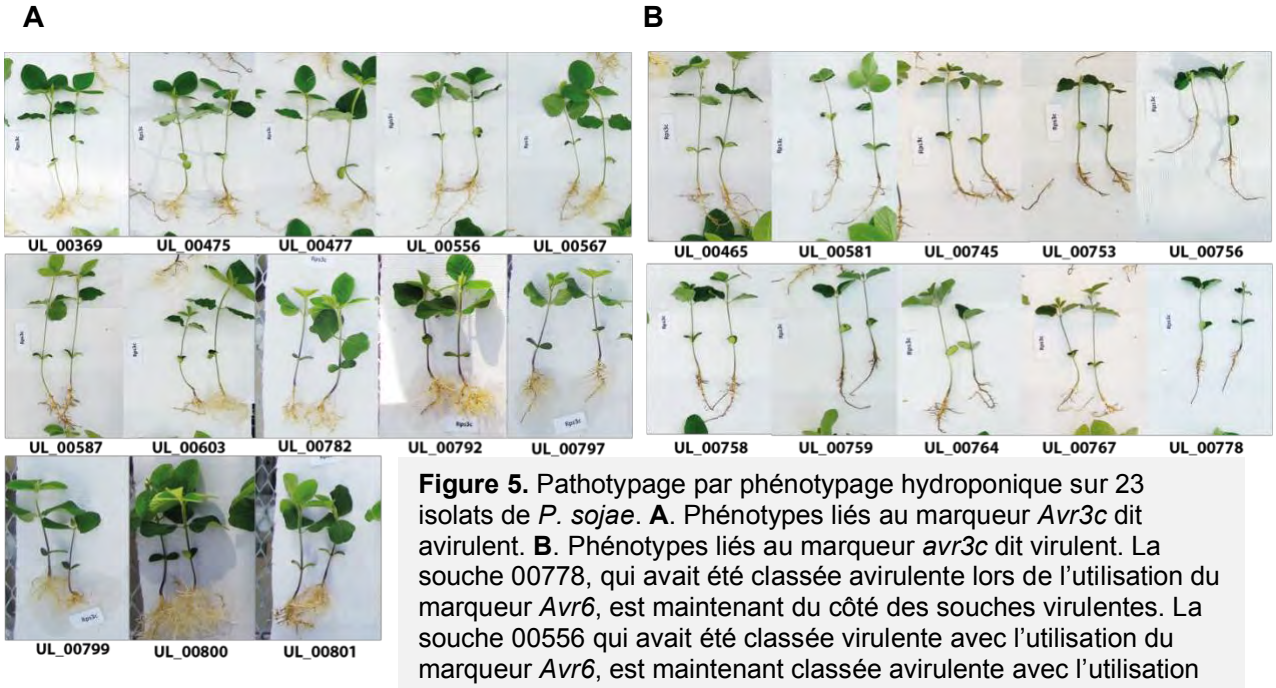

Figure 5. Pathotypage par phénotypage hydroponique sur 23 isolats de *P. sojae*. **A**. Phénotypes liés au marqueur *Avr3c* dit avirulent. **B**. Phénotypes liés au marqueur *avr3c* dit virulent. La souche 00778, qui avait été classée avirulente lors de l'utilisation du marqueur *Avr6*, est maintenant du côté des souches virulentes. La souche 00556 qui avait été classée virulente avec l'utilisation du marqueur *Avr6*, est maintenant classée avirulente avec l'utilisation du marqueur *Avr3c*.

Le travail au niveau des marqueurs génétiques a particulièrement bien progressé au cours de la dernière année. Ainsi, les marqueurs pour *Avr3b* et *Avr3c* ont pu être identifiés, ce qui a permis d'élargir le spectre de gènes *Avr* pouvant être testés. Par ailleurs, les différents haplotypes des gènes *Avr1a* et *Avr1c* mériteraient d'être étudiés plus en détails. En effet, la manifestation de l'allèle *Avr* demeure très rare chez ces gènes en raison de la pression de sélection exercée depuis quelques décennies

(Tremblay *et al.,* 2021). En effet les deux gènes sont très près l'un de l'autre sur le génome (moins de 5Kb), et sont situés dans une région très riche en ADN répété ce qui complique grandement la tâche bio-informatique. Dans les prochains mois, un séquençage sera effectué à l'aide de la technologie Minion (Oxford Nanopore), sur trois souches ciblées et pour lesquelles le phénotype avirulent pour *Avr1a* et *Avr1c* est bien clair afin d'établir la structure du génotype à l'aide de longs « *reads* », séquences normalement obtenues par l'utilisation de cette technologie.

Objectif 3. Le troisième objectif visait à mettre au point une méthode d'extraction d'ADN directement à partir d'échantillons de sols ou encore de plantes présentant la pourriture phytophthoréenne.
Plusieurs protocoles pour extraire l'ADN directement des sols ont été essayés au courant des derniers mois. Que ce soit par l'utilisation de protocoles publiés ou bien par l'utilisation de kits commerciaux (Qiagen, MP Biomedicals, OmegaBiotek,…), il n'a pas été possible de détecter les gènes *Avr* par PCR multiplexe ou uniplexe à partir des extractions d'ADN obtenu. Ceci s'explique facilement par la quantité trop faible d'ADN de *P. sojae* à l'intérieur d'échantillons complexes et la présence d'inhibiteurs de PCR présents en trop grande quantité dans les sols. Afin de pallier cette situation, un protocole d'enrichissement pour le *P. sojae* a dû être développé. Il consiste à prendre des morceaux de feuilles de soya (environ 1cm^2) et de les faire flotter sur les échantillons de sols saturés en eau entre 24 et 48h dans une chambre de croissance (Fig.6). Les morceaux de feuilles sont ensuite lyophilisés en vue de l'extraction subséquente d'ADN. Cette méthode, nommée « speed-baiting », permet de *1)* s'affranchir des inhibiteurs de PCR et *2)* enrichir les extraits d'ADN avec *P. sojae* si présent dans le sol. Il s'agit d'une avancée importante dans ce projet parce qu'elle résout à la fois, les problèmes d'extraction de l'ADN à partir d'échantillons de plantes et réduit considérablement le temps pour le diagnostic dans un contexte commercial. Deux rapports décrivant en détail ces protocoles ont été préparés et transmis au LEDP (Annexes V et VI).

Figure 6. Test de « speed-baiting » effectué sur un sol. Les échantillons de feuilles sont incubés pendant 24-48h et sont utilisés pour l'extraction d'ADN.

Pour ce qui est des échantillons de sols, l'extraction d'ADN représentait encore un plus grand défi en raison de la tentative d'extraire directement l'ADN de *P. sojae* dans un échantillon microbiologiquement complexe et faible en ADN sans le bénéfice d'une isolation ciblée par le speed baiting. Toutes tentatives d'amplification des gènes *Avr* par multiplexe PCR sur ces extraits se sont avérées vaines. Dans le but d'atteindre l'ultime approche qui permettrait un diagnostic direct à partir d'échantillons de sol, il a été résolu d'optimiser une analyse PCR emboîtée (*nested* PCR). En effet, cette technique est désirable lorsque l'ADN cible est en quantité trop faible dans l'échantillon d'ADN et pour lequel une grande spécificité est requise. Alors que cette alternative n'était pas initialement prévue dans les objectifs de ce projet, beaucoup de détermination au sein du groupe a mené à des résultats encourageants. À la lumière d'une résolution très satisfaisante pour un gène *Avr* utilisé comme preuve de concept, les efforts seront poursuivis pour optimiser cette approche.

Objectif 4. Lors de cet objectif, il était question de transférer le test moléculaire PCR conventionnel en test q-PCR avec la technologie *real time* PCR. Au départ, il était question de quantifier l'abondance de *P. sojae* à partir d'un échantillon de sol en vue d'établir un niveau de base à partir duquel la présence de l'agent pathogène pouvait causer des problèmes dans un champ de soya. Suite à la difficulté éprouvée pour détecter la présence de l'agent pathogène tel que décrit plus haut, cet objectif de quantification a été délaissé pour un protocole rt-PCR. Ce dernier a été développé dans le but de générer, avec des amorces spécifiques aux gènes *Avr1b, 1c, 1k, 3a* et 6, des amplicons englobant la

région des marqueurs génétiques qui permettraient de détecter l'haplotype du gène *Avr* correspondant en une seule étape. Brièvement, des amorces ont été construites de part et d'autre des zones des marqueurs spécifiques et utilisées en PCR emboîtée, le tout suivi par une analyse des fragments en HRM (*High Resolution Melting*) après amplification. Comme les amplicons obtenus avaient des différences génétiques (SNP, délétions) selon leur haplotype, l'analyse de fusion a permis de déterminer directement la forme *Avr* ou *avr* du gène. Les résultats typiques de cette technique sont présentés à la Figure 7. À l'aide d'ADN témoin pour chaque génotype, des analyses rt-PCR ont été effectuées sur des ADN provenant de souches purifiées de *P. sojae*, pour lesquelles le génotype était connu. Cette étude a permis de montrer qu'il était effectivement possible, après analyse des « melting curves » de discriminer les allèles pour chaque gène d'avirulence. Cette méthode permet donc d'amplifier, de confirmer la présence ou non de *P. sojae* dans l'échantillon et 2) de déterminer si la séquence est celle d'une souche *Avr* ou *avr* pour un gène d'avirulence donné. Une publication de cette méthodologie est sur le point d'être soumise (Annexe VII).

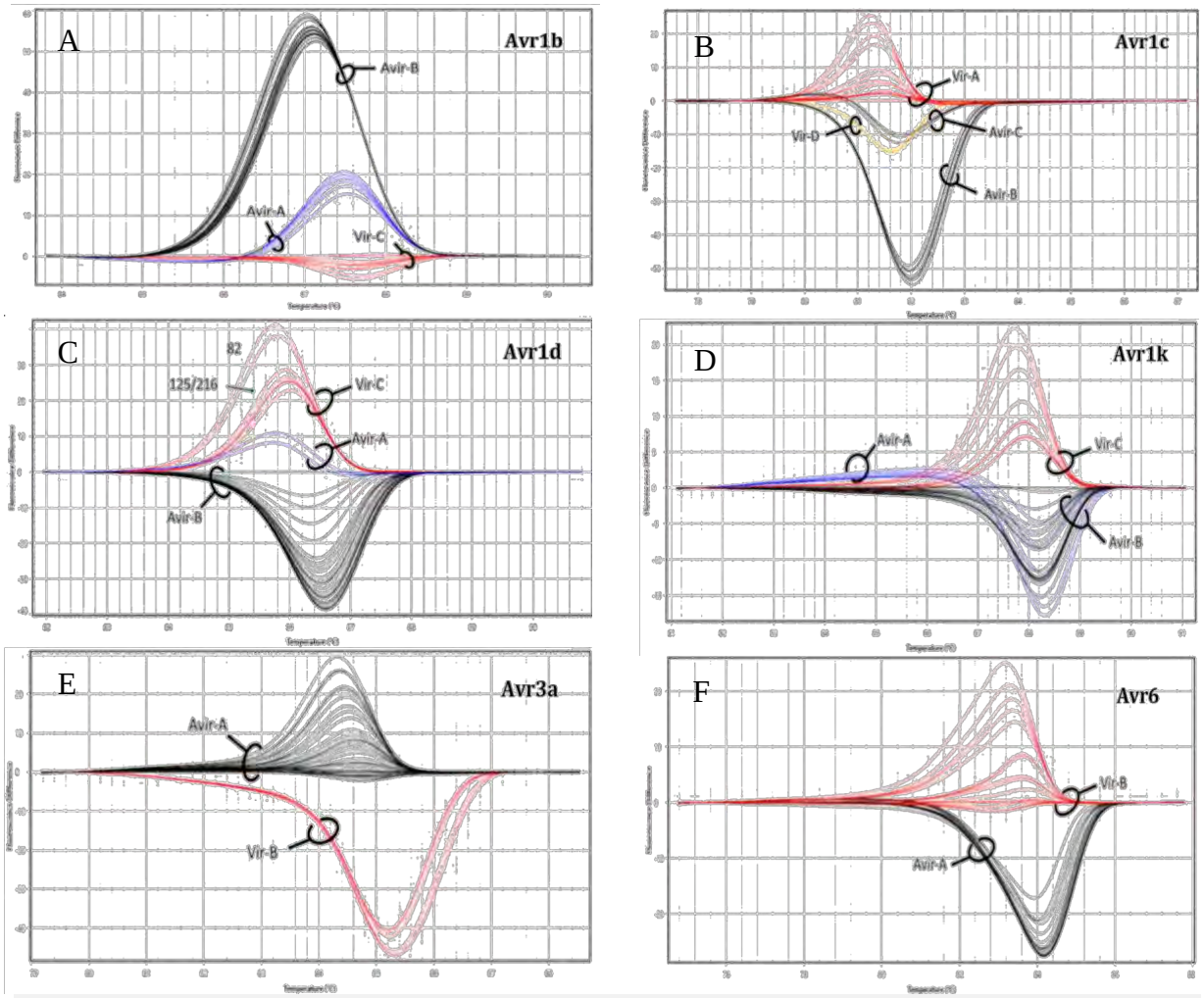

Figure 7. Analyse HRM pour les différents allèles des gènes *Avr* de *Phytophthora sojae*. Les courbes de différentes couleurs représentent l'ensemble des allèles *Avr* et *avr* retrouvés dans différents isolats de l'agent pathogène. Ces résultats ont été effectués sur des ADN provenant d'isolats purifiés de *P. sojae*.

DISCUSSION

Dans le cadre de ce projet, quatre grands objectifs avaient été définis. Le premier objectif visait à optimiser le test PCR multiplexe dans le but d'identifier les gènes d'avirulence de *P. sojae*. À cette fin, les efforts ont porté sur le développement d'un essai moléculaire en multiplexe PCR permettant d'identifier le pathotype (race) de souches de *P. sojae* à partir d'isolats obtenus de sols ou de plantes malades. Cet essai a permis d'éliminer toute la procédure longue et fastidieuse de l'essai biologique tel que le test de l'hypocotyle ou encore, le test en hydroponique. La puissance de cette méthode réside dans sa rapidité et sa précision sans la difficulté d'interprétation inhérente aux tests biologiques. Dans le cadre de l'objectif 2, plusieurs travaux de validation ont été effectués pour démontrer la fiabilité des marqueurs génétiques à l'égard des phénotypes anticipés. Ces résultats ont donné un taux de corroboration de 93%, pourcentage qui dépasse l'efficacité de tests commerciaux. De plus, dans le contexte de cet objectif, il a été possible de dépasser les objectifs en définissant de nouveaux marqueurs plus efficaces pour certains gènes ainsi que des marqueurs pour des gènes encore non identifiés (ex. 3b et 3c). Le troisième objectif cherchait à assurer le transfert technologique de ce travail en rendait l'utilisation du test plus conviviale. En effet, à la base, le test n'est efficace qu'avec des extraits d'ADN obtenus d'isolats purifiés de *P. sojae*. Pour contourner cette limitation, une toute nouvelle méthodologie d'analyse est en phase de développement avec l'utilisation de la PCR emboîtée. Cette méthode, une fois optimisée, permettra d'obtenir les amplicons désirés directement à partir de l'ADN de plante ou encore de sols. Cette technique demande plus de ressources au niveau de l'analyse PCR mais permet un affranchissement de la purification de *P. sojae* par « baiting » classique qui, selon notre expérience, requiert entre un et trois mois avant d'obtenir un isolat prêt à analyser. C'est une avancée non négligeable vers le développement de l'outil moléculaire. En effet, à partir du *speed-baiting*, il faut dorénavant une semaine avant d'avoir le pathotype d'un échantillon de sol.
Pour l'objectif 4, une toute nouvelle approche q-PCR a été développée afin de s'affranchir des étapes d'analyse sur gel ou en électrophorèse capillaire pour interpréter les résultats suivant l'amplification. Grâce à la conception d'amorces permettant d'amplifier la zone variable (marqueurs) pour chaque gène *Avr* de *P. sojae*, il est maintenant possible de déterminer le pathotype par analyse HRM puisque les différents allèles donnent des amplicons ayant des courbes de fusion différentes.

DOCUMENTS TRANSMIS au LEDP et TRANSFERT TECHNOLOGIQUE

Formation sur l'utilisation de la méthode PCR multiplexe.
Marqueurs moléculaires pour Avr1a, Avr1b, Avr1c, Avr1d, Avr1k, Avr3a et Avr6.
Souches types des gènes *Avr* de *P. sojae.*

ANNEXES

Annexe I : Dussault-Benoit, *et al*. 2020.
Annexe II : Arsenault-Labrecque, *et al*. 2022.
Annexe III : Tableau : Ensemble des résultats de pathotypage, par phénotypage et génotypage, ayant servi à valider l'efficacité des marqueurs génétiques utilisés dans l'outil moléculaire PCR multiplexe
Annexe IV : Figure illustrant les types de résultats de l'essai hydroponique
Annexe V : Protocole Speed baiting.
Annexe VI : Protocole extraction d'ADN à partir d'échantillons de plantes.
Annexe VII : Santhanam et al., 2023
Formation sur l'utilisation des différentes méthodes prévue pour le printemps 2023

APPLICATIONS POSSIBLES POUR L'INDUSTRIE

Les travaux liés à ce projet ont permis de développer une méthode de détection du pathotype de *Phytophthora sojae* à partir d'échantillons de feuilles de soya utilisées comme appâts à l'aide de la technique de PCR emboîtée. De plus, cette technique pourrait éventuellement fonctionner avec des extraits d'ADN de sols. Pour l'industrie, cela permettra de mettre au point un outil avec lequel il sera possible d'obtenir le pathotype de *P. sojae* associé à un champ particulier aussi rapidement qu'en quelques jours voire, quelques heures. Cette méthodologie est adaptée pour tous les types de laboratoire : analytiques, privés ou publiques. Enfin, pour l'Industrie agricole et les semenciers de soya, il sera possible à coût modeste, d'obtenir à l'aide du test moléculaire un portrait des pathotypes de *P. sojae* dans les champs et de ce fait, être en mesure de choisir des cultivars de soya résistants à la maladie.

POINT DE CONTACT POUR INFORMATION

Richard Bélanger, Université Laval
Caroline Labbé, Université Laval

REMERCIEMENTS AUX PARTENAIRES FINANCIERS

Ce projet a été réalisé dans le cadre du volet 2 du programme Prime-Vert – Approche régionale et interrégionale avec une aide financière du ministère de l'Agriculture, des Pêcheries et de l'Alimentation. Un merci tout spécial au MAPAQ!

Le projet Primevert, ainsi qu'une subvention du CFCRA, ont également servi de force motrice pour une subvention Génome-Québec/Génome-Canada dans le cadre du programme GAPP. Ces trois projets ont été effectués en synergie et nous remercions grandement tous les collaborateurs pour leur aide financière qui a permis l'exécution de ce travail.

Littérature citée.

1. Arsenault-Labrecque, G., Sonah H., Lebreton A., Labbé C., Marchand G., Xue A., Belzile F., Knaus B.J., Grünwald N.J., Belanger R.R. (2018). Stable predictive markers for *Phytophthora sojae* avirulence genes that impair infection of soybean uncovered by whole genome sequencing of 31 isolates. BMC Biology. 18:80. https://bmcbiol.biomedcentral.com/articles/10.1186/s12915-018-0549-9.

2. Arsenault-Labrecque, G., Santhanam, P., Asselin, Y., Cinget, B., Lebreton, A., Labbé, C., ... & Bélanger, R. R. (2022). RXLR effector gene *Avr3a* from *Phytophthora sojae* is recognized by *Rps8* in soybean. *Molecular Plant Pathology*, *23*(5), 693-706.

3. Dong, S., Qutob, D., Tedman-Jones, J., Kuflu, K., Wang, Y., Tyler, B.M., Gijzen, M. (2009). The Phytophthora sojae avirulence locus *Avr3c* encodes a multi-copy RXLR effector with sequence polymorphisms among pathogen strains. Plos One. Vol. 4, e5556. https://doi.org/10.1371/journal.pone.0005556

4. Dussault-Benoit, C., Arsenault-Labrecque, G., Sonah, H., Belzile, F., Bélanger, R.R. (2020). Discriminant haplotypes of avirulence genes of *Phytophthora sojae* lead to a molecular assay to predict phenotypes. Plant Molecular Pathology. 21:318-329.

5. Lebreton, A., Labbé, C., de Ronne, M., Xue, A., Marchand, G., Bélanger, R.R. (2018). Development of a simple hydroponic assay to study vertical and horizontal resistance of soybean and pathotypes of *Phytophthora sojae*. Plant Disease. 102: 114-123.

6. Tremblay, V., McLaren, D.L., Kim, Y.M., Strelkov, S.E., Conner, R.L., Wally, O., Bélanger, R.R. (2021). Molecular assessment of pathotype diversity of *Phytophthora sojae* in Canada highlights declining sources of resistance in soybean. Plant Disease. https://doi.org/10.1094/PDIS-04-21-0762-RE

ANNEXE I

Dussault-Benoit, C., Arsenault-Labrecque, G., Sonah, H., Belzile, F., Bélanger, R.R. (2020). Discriminant haplotypes of avirulence genes of *Phytophthora sojae* lead to a molecular assay to predict phenotypes. Plant Molecular Pathology. 21:318-329.

Janvier 2023

Received: 26 July 2019 | Revised: 27 November 2019 | Accepted: 28 November 2019

DOI: 10.1111/mpp.12898

ORIGINAL ARTICLE

Molecular Plant Pathology WILEY

Discriminant haplotypes of avirulence genes of *Phytophthora sojae* lead to a molecular assay to predict phenotypes

Chloé Dussault-Benoit[1] | Geneviève Arsenault-Labrecque[1] | Humira Sonah[1,2] | François Belzile[1] | Richard R. Bélanger[1]

[1]Department of Phytology, Université Laval, Québec, QC, Canada

[2]National Agri-Food Biotechnology Institute (NABI), Mohali, India

Correspondence
Richard R. Bélanger, Department of Phytology, Université Laval, Québec, QC, Canada.
Email: Richard.Belanger@fsaa.ulaval.ca

Funding information
Natural Sciences and Engineering Research Council of Canada; Fonds de Recherche du Québec - Nature et Technologies; Genome Canada; Western Grains Research Foundation; Agriculture and Agri-Food Canada; University of Guelph; Empresa Brasileira de Pesquisa Agropecuária; Natural Sciences and Engineering Research Council of Canada; Canada Research Chairs; Université Laval

Abstract

The soybean–*Phytophthora sojae* interaction operates on a gene-for-gene relationship, where the product of a resistance gene (*Rps*) in the host recognizes that of an avirulence gene (*Avr*) in the pathogen to generate an incompatible reaction. To exploit this form of resistance, one must match with precision the appropriate *Rps* gene with the corresponding *Avr* gene. Currently, this association is evaluated by phenotyping assays that are labour-intensive and often imprecise. To circumvent this limitation, we sought to develop a molecular assay that would reveal the avirulence allele of the seven main *Avr* genes (*Avr1a*, *Avr1b*, *Avr1c*, *Avr1d*, *Avr1k*, *Avr3a*, and *Avr6*) in order to diagnose with precision the pathotypes of *P. sojae* isolates. For this purpose, we analysed the genomic regions of these *Avr* genes in 31 recently sequenced isolates with different virulence profiles and identified discriminant mutations between avirulence and virulence alleles. Specific primers were designed to generate amplicons of a distinct size, and polymerase chain reaction conditions were optimized in a final assay of two parallel runs. When tested on the 31 isolates of known virulence, the assay accurately revealed all avirulence alleles. The test was further assessed and compared to a phenotyping assay on 25 isolates of unknown virulence. The two assays matched in 97% (170/175) of the interactions studied. Interestingly, the sole cases of discrepancy were obtained with *Avr3a*, which suggests a possible imperfect interaction with *Rps3a*. This molecular assay offers a powerful and reliable tool to exploit and study with greater precision soybean resistance against *P. sojae*.

KEYWORDS

Avr genes, effectors, multiplex polymerase chain reaction, plant pathogen, phytophthora root rot (PRR), *Rps* genes, soybean diseases

1 | INTRODUCTION

Soybean (*Glycine max*) production has steadily increased all over the world and particularly in Canada over the last decade, and it is now the third most important crop in the country, covering more than 3 million hectares (Statistics Canada, 2018). This rapid expansion has led to increased disease pressure from a variety of pathogens. Among them, *Phytophthora sojae*, the causal agent of phytophthora

root rot (PRR), is arguably the most economically important soybean pathogen in Canada (Xue *et al*., 2015). *P. sojae* is an oomycete belonging to the kingdom of Stramenopiles. It is a filamentous eukaryotic organism related to brown algae, but it does not perform photosynthesis. Like other oomycetes, morphologically it strongly resembles fungi (Tyler, 2007), but its hyphae, unlike those of fungi, are non-partitioned and consist of cellulose rather than chitin (Bartnicki-Garcia, 1968).

The pathogen can infect soybean at all growth stages, from seed to adult plants (Tyler, 2007), and can cause damage at any time in the season. Symptoms include seed rot, damping-off, browning, and death of the roots and stem. Sometimes the foliage can turn brown and wither. Conditions favourable to the development of this disease are poor drainage, frequent in clay soils, which can easily be flooded for a longer period. Under favourable conditions, the oospores, the survival structure of *P. sojae*, will germinate into sporangia containing zoospores that can move easily in water with their two flagella. These motile spores are attracted to the root exudates of soybean by chemotaxis. Once they reach the roots, the zoospores are able to penetrate and invade the root cells with a structure called a haustorium. Following sexual reproduction in the root cortex, new oospores are formed and can survive in the dead plant or tissues for many years even under adverse conditions (Tyler, 2007).

Currently, the most effective method to curb the devastating impact of *P. sojae* is genetic resistance in the host. Complete (or vertical) resistance against *P. sojae* is conferred by single genes named *Rps* (resistance to *Phytophthora sojae*). These resistance genes act by recognizing the products of avirulence (*Avr*) genes of the pathogen in a traditional gene-for-gene relationship. The *Avr* genes of *P. sojae* encode effector proteins, most with RxLR (Arg-X-Leu-Arg) motifs, and these effectors are recognized by proteins having nucleotide-binding site and leucine-rich repeat (NLR receptors) motifs, encoded by the *Rps* genes (Tyler and Gijzen, 2014).

The presence of *Rps* genes in soybean cultivars has resulted in an increased selection pressure, which in turn has led to the development of new pathotypes, of which 200 combinations have been reported in populations of *P. sojae* (Kaitany *et al*., 2001; Dorrance *et al*., 2004; Tyler and Gijzen, 2014). These new pathotypes reflect the occurrence of mutations in *P. sojae Avr* genes, whereby the latter are no longer recognized by *Rps* genes, opening the way to new infections (Shan *et al*., 2004; Rasoolizadeh *et al*., 2018). Typically, an *Rps* gene can be overcome and cease to be effective when the pathogen loses the ability to produce the corresponding Avr protein, following deletion or altered expression of an *Avr* gene, or alters its structure through point mutations or indels in the gene, making it unrecognizable by the product of the *Rps* gene (Tyler and Gijzen, 2014). Currently, there are approximately 25 known *Rps* genes in soybean, of which six have been introgressed internationally into commercial soybean varieties (*Rps1a*, *Rps1b*, *Rps1c*, *Rps1k*, *Rps3a*, and *Rps6*), concordant with *Avr* genes in *P. sojae* (Sugimoto *et al*., 2012; Abeysekara *et al*., 2016).

To properly exploit *Rps* genes against *P. sojae*, deployment of soybean cultivars with an appropriate combination of *Rps* genes, to match *Avr* genes present in field isolates, is essential. It is thus imperative to identify the virulence profile or pathotypes of these isolates present in a given environment by precisely detecting the presence or absence of functional *Avr* genes. For this purpose, phenotyping assays with soybean differentials carrying a single *Rps* gene have typically been exploited. The hypocotyl assay has been historically the most commonly used because of its simple protocol (Kaufmann and Gerdemann, 1958; Dorrance *et al*., 2008). However, problems with false positives, intermediate responses, and stability of *Avr* genes/expression over time have hampered its reliability. More recently, Lebreton *et al*. (2018) proposed a new assay to phenotype the isolates of *P. sojae* that relied on zoospore inoculation in hydroponic solutions to more closely reproduce the natural course of infection. While this bioassay appears to eliminate some of the shortcomings of the hypocotyl assay, it remains labour-intensive and requires several weeks to complete.

In a recent effort to associate phenotypes with genotypes, Arsenault-Labrecque *et al*. (2018) sequenced 31 *P. sojae* isolates collected from Canadian fields and analysed the sequences and variants of the seven most common *Avr* genes: *1a*, *1b*, *1c*, *1d*, *1k*, *3a*, and *6*. They were able to define specific haplotypes for each *Avr* gene and further show, through the use of the hydroponic assay, that each haplotype corresponded to a distinct virulence profile. This suggests that genomic signatures can be used as accurate predictors of phenotypes and could potentially be exploited as diagnostic tools to identify pathotypes in *P. sojae* isolates. On the basis of this hypothesis, the objectives of the present study were (a) to identify unique sequences based on the haplotypes identified by Arsenault-Labrecque *et al*. (2018) that are specific and discriminant to detect the presence of the allele(s) conferring avirulence for each of the seven *Avr* genes, (b) to design primers from these sequences and to develop a molecular approach combining all the specific pairs of primers needed to amplify the seven avirulence alleles, and (c) to test the efficiency of the molecular tool by comparing the results with those obtained with a phenotyping assay. Here we describe a novel and unique diagnostic tool that defines with unprecedented precision the virulence profiles of *P. sojae* isolates. This tool can find direct applications in the study of functionality of *Avr* and *Rps* genes and in the development and selection of germplasm resistant to *P. sojae*.

2 | RESULTS

2.1 | Gene-specific PCR-based markers for seven *Avr* genes in *P. sojae*

For all seven *Avr* genes under study, all primers were designed to amplify sequences associated with the avirulence allele of the genes (Figure 1). In some cases, markers defined by Arsenault-Labrecque *et al*. (2018) were used directly, and in cases where markers were

(a)

		Scaffold position of the markers				
Avr1a		Avr1a-snp1 Fwd		Avr1a-indel Fwd	Avr1a-snp Rev	
Haplotypes	Phenotypes	7:2263686	7:2263687	7:2042427-2042445	7:1799779	7:1799780
A	A	C	A	no deletion	G	A
B	V	C	A	no deletion	**A**	**C**
C-D	V	**G**	**G**	no deletion	G	A
E	V	C	A	**deletion**	G	A

(b)

Avr1b		Avr1b Fwd				
Haplotypes	Phenotypes	6:3146466	6:3146467	6:3146468	6:3146477	6:3146481
A-B	A	G	G	G	T	TAAG
C	V	**A**	**A**	**A**	**TGCA**	**T**

(c)

Avr1c		Avr1c Fwd		Avr1c Rev			
Haplotypes	Phenotypes	7:2046037	7:2046038	7:2046815	7:2046817	7:2046819	7:2046821
B-C	A	**G**	**A**	**G**	**A**	**G**	**C**
A	V	C	C	A	T	A	A
D	V	-	-	**G**	**A**	**G**	**C**
E	V	-	-	-	-	-	-

(d)

Avr1d		Avr1d Fwd
Haplotypes	Phenotypes	5:5919167-5922387
A-B	A	no deletion
C	V	**deletion**

(e)

Avr1k		Avr1k Fwd	
Haplotypes	Phenotypes	6:3142512	6:3142519
A-B	A	T	C
C	V	**C**	**G**

(f)

Avr3a		Avr3a Fwd
Haplotypes	Phenotypes	9:615329
A	A	CAAAGAT
B	V	**C**

(g)

Avr6		Avr6 Rev
Haplotypes	Phenotypes	4:7223782
A	A	AGAGCCTCAAGCTTG
B	V	**A**

FIGURE 1 Discriminant haplotypes associated with distinct phenotypes in seven avirulence genes of *Phytophthora sojae* used to build discriminant primers: (a) *Avr1a*, (b) *Avr1b*, (c) *Avr1c*, (d) *Avr1d*, (e) *Avr1k*, (f) *Avr3a*, and (g) *Avr6*. A = avirulent and V = virulent. Haplotype letters refer to those previously identified by Arsenault-Labrecque *et al*. (2018). Scaffold positions refer to the position of the markers used as per the *P. sojae* reference genome v. 3.0

not discriminant enough for polymerase chain reaction (PCR) (e.g., one single nucleotide polymorphism [SNP]), additional markers associated with the same alleles were used for the design of the primers. In other cases where the discriminant variants were located outside of the coding region, the primers were developed based on the specific haplotype linked to the avirulence allele. The positions of all the amplified regions are shown in Table 1.

For *Avr1a*, multiple variants were found on alleles conferring virulence on soybean lines carrying the *Rps1a* gene (Figure 1a). One such variant was an 18-bp deletion conferring virulence to all isolates carrying it. For those virulent isolates lacking the deletion, they were distinguished from the avirulent ones on the basis of two adjacent SNPs found in two separate regions (Avr1a-snp1 and Avr1a-snp2).

In the case of *Avr1b*, a combination of SNPs and indels, located within 15 bp of each other, was found to discriminate the avirulence allele (Figure 1b). A forward primer was thus designed in that region to encompass all five variants. Sequence alignments with isolates P6497, P7064, P7074, and P7076 showed that the primers would accurately predict the phenotypes for the latter three isolates (Figure S1), isolate P6497 being a rare outlier as reported by Arsenault-Labrecque *et al*. (2018).

The *Avr1c* avirulence allele could be discriminated from the virulence form on the basis of two SNPs situated at the 3′ end of the forward primer and four SNPs positioned at the 5′ end of the reverse primer (Figure 1c). This design allowed the avirulent haplotypes to be targeted specifically against several other haplotypes linked to virulence. When the reverse primer was aligned against the new haplotypes recently reported in Chinese isolates (Yang *et al*., 2019), our results demonstrated that it was specific to all avirulence alleles. In addition, it was specific to virulence allele *Avr1c-4* but it is unknown if it would be amplified because we could not compare in silico alignment of the forward primer in absence of the sequences located outside the genic region.

In the case of *P. sojae* isolates carrying *Avr1d*, they were easily distinguished from those with pathotype 1d on the basis of a complete deletion of the gene (Figure 1d). Primers were thus simply designed to amplify a region within the gene.

For *Avr1k*, two SNPs were selected within 7 bp of each other that discriminated the avirulence allele from the virulence one to design the primers (Figure 1e).

Based on two distinct haplotypes, the avirulence allele of *Avr3a* presented an extra sequence of six nucleotides (Figure 1f). This area was therefore selected to design discriminant primers.

TABLE 1 Primer sequences, with their genomic positions, amplicon size and concentrations, used for the detection of seven *Avr* genes in the *Phytophthora sojae* genome

Primer names	Amplicon position[a]	Product size	Forward sequence[b]	Reverse sequence	Concentrations F and R primers (μM)
Avr1a-indel	Scaffold_7:2,042,431–2,042,664	234	GAAAGTGGACGGATATTTTCAAC	CAAGGACGGACTGGTACAGA	0.100
Avr1a-snp1	Scaffold_7: 2,263,667–2,263,879	213	CTTAGTGTGCACCAACAGCCA	ACCACACTTCACGGAGCATT	0.100
Avr1a-snp2	Scaffold_7: 1,799,519–1,799,796	278	GCTTTTCATCCAACGCTCAT	AATGATTGGCGGCAGATC	0.150
Avr1b	Scaffold_6:3,146,464–3,146,866	403	AAGGGGTACAGCCTGGATAAG	CTTGCGCTGTGAAGTGTCAT	0.150
Avr1c	Scaffold_7:2,046,020–2,046,821	802	CGGCAGAAGTTCTGGAAGA	GCCTTCCTTTGTCAGATTCG	0.250
Avr1d	Scaffold_5:5,919,385–5,919,881	497	CACGAGCAATGTCCTGTACG	CGAGCGTCCGATTTATAACTGG	0.075
Avr1k	Scaffold_6: 3,142,499–3,142,801	303	CTGTTCAGAAACTTCCGGTGC	CATGAAAAAGTCGGGGTTTG	0.150
Avr3a	Scaffold_9: 615,324–615,930	607	CTAGGCAAAGATGTCACCTG	ATCATGGCAAGCACCAATCT	0.100
Avr6	Scaffold_4: 7,223,071–7,223,796	726	GTCGTGCTGCATACTCTTGG	CAAGCTTGAGGCTCTGTGCT	0.100

[a]Amplicon position is based on *P. sojae* reference genome v. 3.0.

[b]Underlined nucleotides indicate discriminant nucleotide positions used to design primers.

Finally, a 15-bp deletion upstream of *Avr6* was consistently observed in all virulent isolates (Figure 1g). As it was consistently associated with a phenotype of virulence, it was used for primer design.

2.2 | Analysis of genetic diversity

Based on availability of sequences covering the zones defined by our primers, *Avr1k* and *Avr6* were compared between isolates used in this study with those of isolates from China and the United States. This phylogenetic analysis revealed that they encompassed the genetic diversity currently reported for those genes (Figure S2). Interestingly, all outside isolates used for comparison matched the expected virulent phenotype except for a single isolate, which was reported as virulent (with the hypocotyl assay) despite carrying the avirulence allele.

2.3 | Uniplex PCR amplification and specificity

The results showed that successful amplification of the functional version of the *Avr* genes matched perfectly the expected phenotype for each of the seven *Avr* genes, thus confirming the specificity of the primers for the targeted region (Figure 2). For six of the seven genes, a single set of primers was sufficient to discriminate the haplotypes leading to a virulent or avirulent reaction. In the case of *Avr1a*, four different haplotypes were exploited so three different pairs of primers had to be designed and included in the molecular assay to cover the spectrum of possible haplotypes: Avr1a-indel, Avr1a-snp1, and Avr1a-snp2 (Figure 2). As explained above, only the simultaneous presence of all three amplicons indicated avirulence.

2.4 | Multiplex PCR and specificity

Following optimization of the PCR conditions, the molecular assay was carried out in two parallel runs: one multiplex assay for the detection of *Avr1a*, *Avr1b*, *Avr1d*, *Avr1k*, *Avr3a*, and *Avr6*, and one singleplex assay for *Avr1c*. The presence of a band, or three in case of *Avr1a*, of a specific size as described in Table 1 indicates that the tested isolate carries the avirulence allele associated with the amplicon of the *Avr* gene of that size. Conversely, the absence of an amplicon for a given gene indicates that the isolate carries the corresponding virulence allele. For instance, Figure 3 presents results from the multiplex PCR assay on the 31 known isolates with their corresponding pathotype based on a phenotypic assay (Arsenault-Labrecque *et al*., 2018). Results show that the pathotype, as expressed by the absence of an amplicon for a given gene, is accurately predicted by the molecular assay. As an illustration, isolate 1A shows amplicons for *Avr1a*, *1b*, *1k*, *3a* and *6* (Figure 3a) and none for *1d* and *1c* (Figure 3b), which translates into pathotype 1c and 1d.

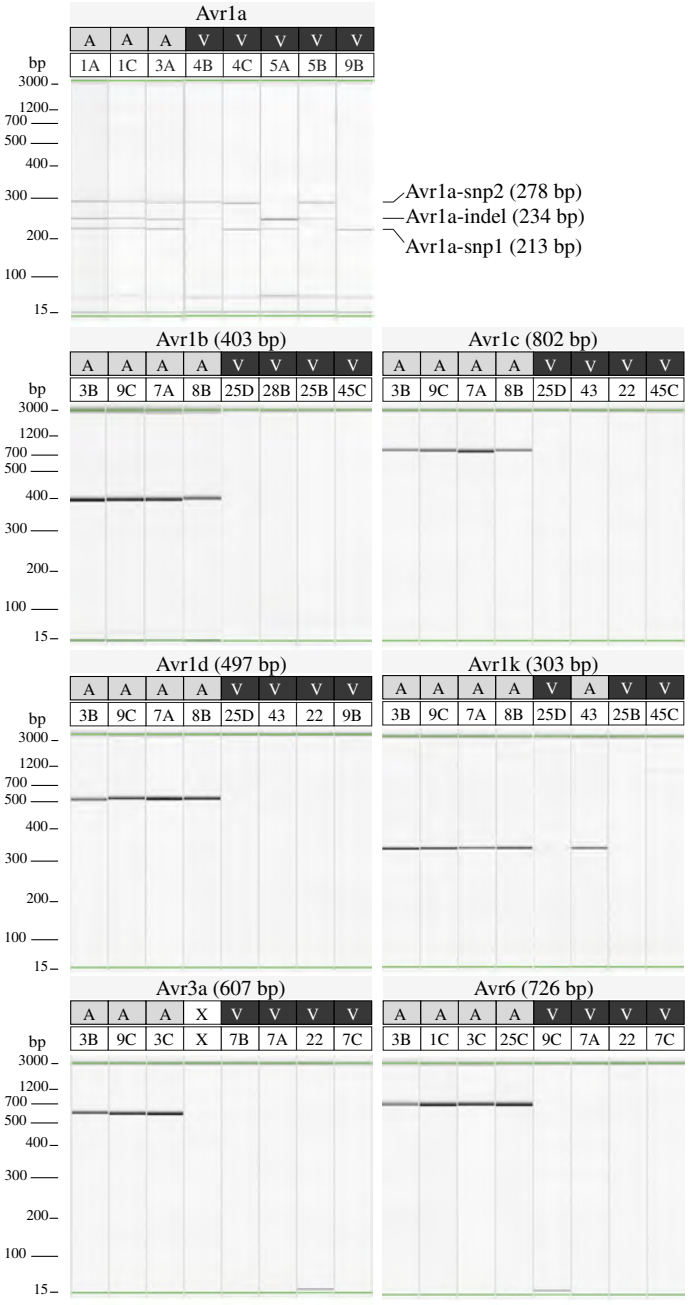

FIGURE 2 Gel images of uniplex polymerase chain reaction amplifications of discriminant regions associated with avirulence alleles for seven *Avr* genes in *Phytophthora sojae*. For each *Avr* gene, the expected phenotype (A = avirulent and V = virulent) against the corresponding *Rps* gene for each of the eight isolates tested is indicated at the top of the gel. The expected size of the amplicon is noted in parentheses next to each *Avr* gene, except for *Avr1a*. For *Avr1a*, three distinct regions, Avr1a-indel, Avr1a-snp1, and Avr1a-snp2, must amplify to detect a phenotype of avirulence

2.5 | Genotyping and phenotyping of isolates with unknown pathotype

After validation of the multiplex PCR assay with the 31 known isolates, 25 uncharacterized isolates were randomly selected to confirm the effectiveness of the assay. Representative results obtained following the molecular and hydroponic assays are presented for two isolates (Figure 4). The seedlings were scored and values compared to those of Haro (susceptible control) using Dunnett's test to determine if they were susceptible or resistant (Figure S3). As seen in Figure 4a, the presence of amplicons for *Avr1b*, *Avr1d*, and *Avr1k* on the gel is indicative that isolate 2012–82 should have pathotype 1a, 1c, 3a, 6. When compared with the bioassay (Figure 4b), the phenotypes obtained clearly corroborated the molecular assay where a compatible interaction was observed between the isolate and differentials *Rps1a*, *1c*, *3a*, and *6*. In the other example with isolate 2012–156 (Figure 4c), the molecular assay showed amplification for *Avr1a* (Avr1a-snp1, Avr1a-indel, Avr1a-snp2), *1b*, *1k*, *3a*, and *6*, which leads to a diagnostic of pathotype 1c, 1d for that isolate. Interestingly, the phenotypic assay shown in Figure 4d confirmed the compatible interaction with differentials *Rps1c* and *1d* but also suggested one with *Rps3a*, despite the molecular assay clearly showing an amplicon for *Avr3a*. As a matter of fact, when results were combined for all 25 isolates and seven *Avr* genes (175 interactions), there was only a single and similar discrepancy when the molecular assay and the phenotypes did not match perfectly (Table 2). Indeed, in five cases a compatible interaction was observed with *Rps3a* in the hydroponic assay despite the presence of an amplicon for the avirulence allele

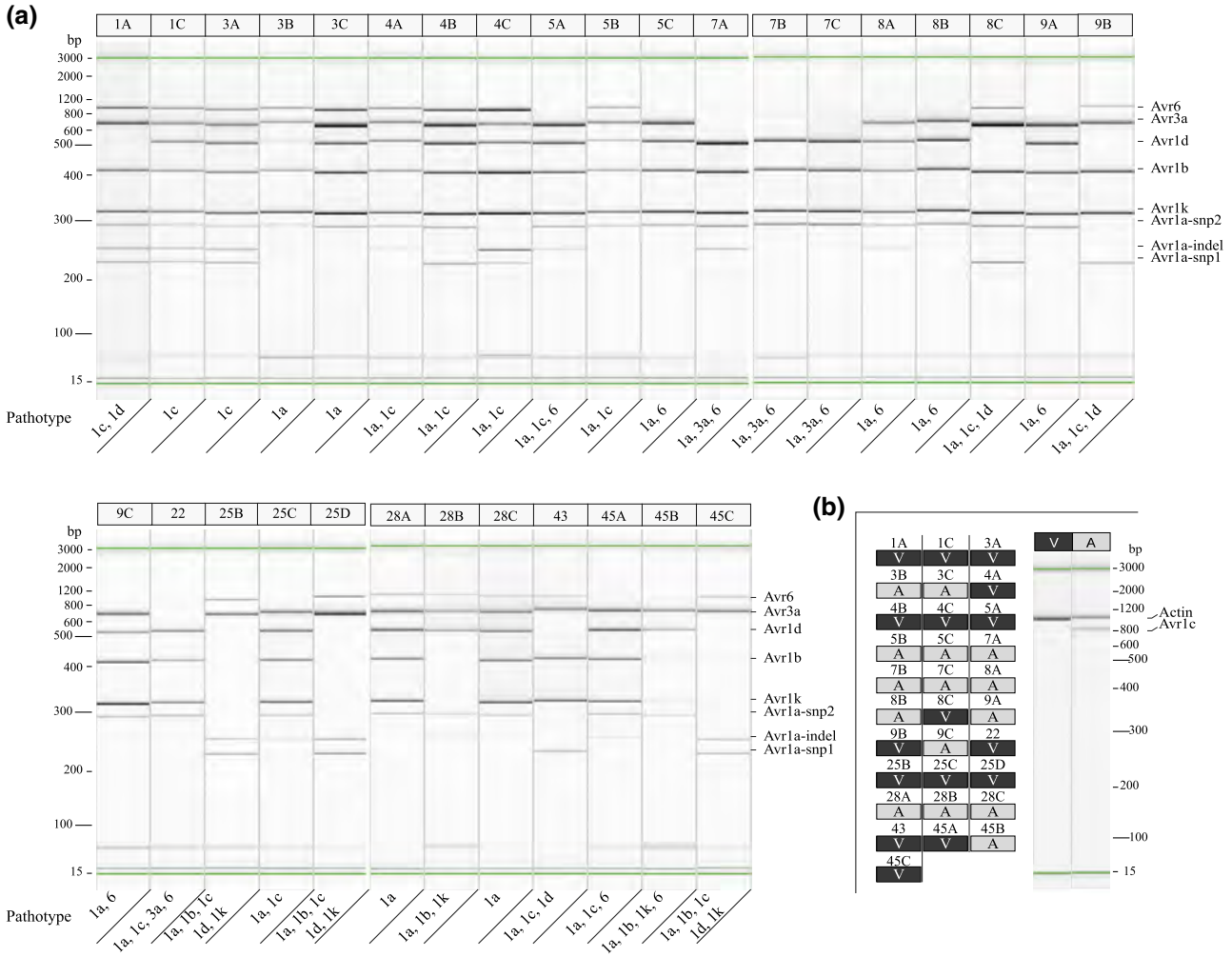

FIGURE 3 Gel images of multiplex polymerase chain reaction (PCR) amplifications of discriminant regions associated with avirulence alleles for seven *Avr* genes in *Phytophthora sojae*. (a) Results obtained with 31 isolates with a known pathotype, as indicated at the bottom of the gel, for *Avr1a*, *1b*, *1d*, *1k*, *3a*, and *6*. The expected size of the amplicon for each *Avr* gene is indicated on the right. (b) Complementary gel of PCR amplification of discriminant region associated with the avirulence allele for *Avr1c* (right) along with results obtained for the 31 isolates (A = avirulent and V = virulent) where A or V indicates presence or absence of the amplicon, respectively. For each isolate, the pathotype should correspond to the absence of an amplicon for each corresponding gene

of *Avr3a*. All other interactions generated a perfect match between the molecular and the phenotyping assay for a prediction accuracy of 97% (170/175).

3 | DISCUSSION

In recent years, molecular techniques have revolutionized and greatly facilitated the diagnostic of plant pathogens (Kostov *et al*., 2016; Michalecka *et al*., 2016; Reich *et al*., 2016; Silva *et al*., 2017; Burbank and Ortega, 2018). Among other applications, they have allowed the precise identification of the causal agents of diseases caused by a complex of fungi (Conti *et al*., 2019), the fulfillment of Koch's postulates with closely related species such as *Fusarium* spp. (Moine *et al*., 2014), and the diagnosis of the presence and identity of a pathogen from levels that were hitherto undetectable (Rollins *et al*., 2016; Haudenshield *et al*., 2017). In most cases, those PCR-based assays have exploited conserved regions such as the internal transcribed spacers (ITS) (Bruns and Shefferson, 2004) or the translation elongation factor 1α (TEF1-α) to develop diagnostic tools able to identify a given pathogen (Raja *et al*., 2017; Marin-Felix *et al*., 2019). By contrast, to our knowledge, this study presents the first molecular assay aimed at identifying *Avr* genes for the purpose of diagnosing the virulence profile of a plant pathogen. To this end, this assay necessitated access to the full genome sequences of many isolates of *P. sojae* in order to capture the spectrum of diversity within each *Avr* gene under study. Indeed, genetic control of *P. sojae* through introgression of *Rps* genes in soybean presupposes a thorough understanding and knowledge of the pathotype diversity of *P. sojae* isolates in the specific area where the *Rps* genes are deployed. Up to this point, the only way to determine the pathotype of a given isolate was through cumbersome and long phenotyping procedures, each with its own shortcomings (Dorrance *et al*., 2008; Lebreton *et al*., 2018). Through this unique molecular assay, based on discriminant

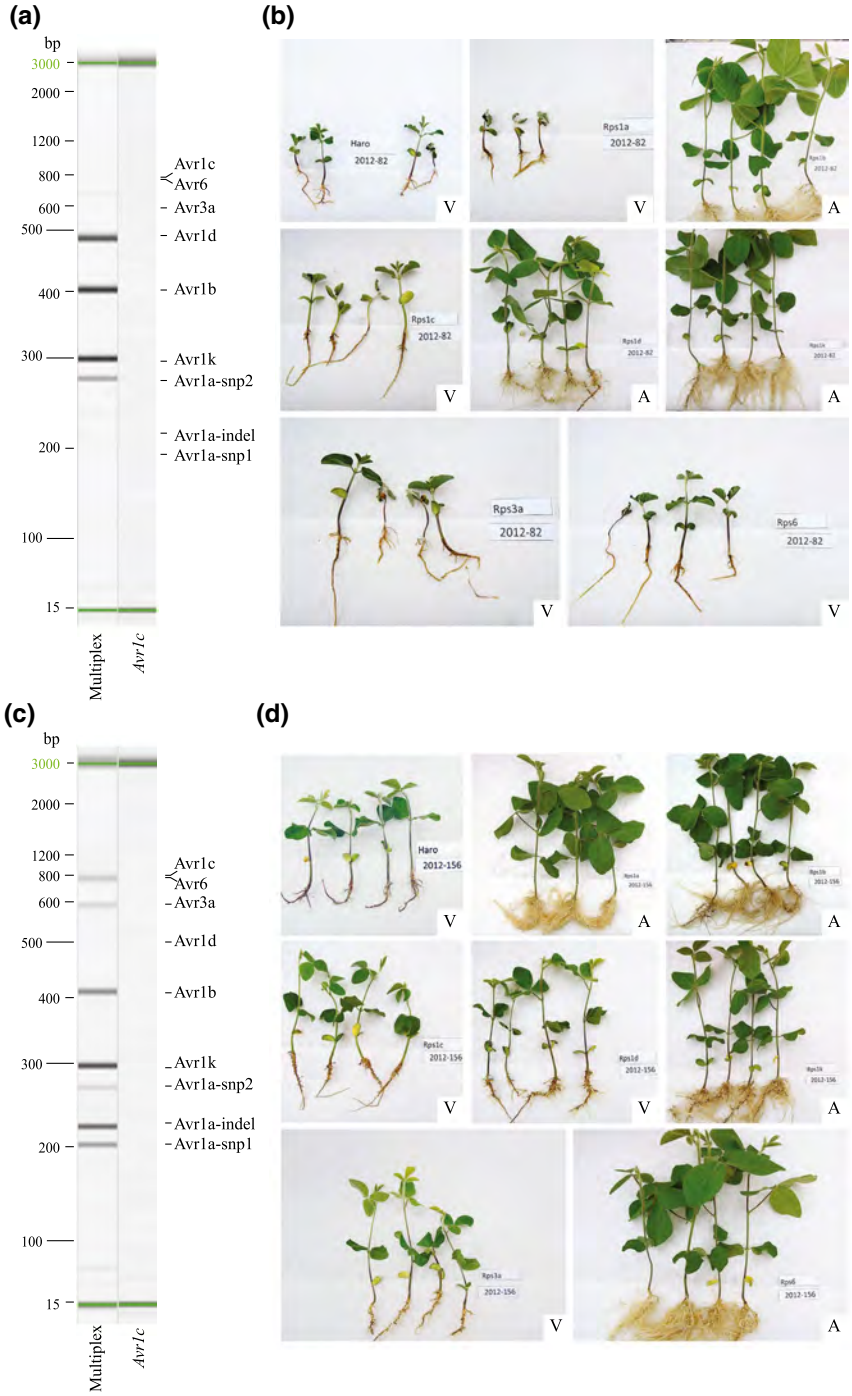

FIGURE 4 Comparison of molecular and phenotyping assays to determine the pathotypes of *Phytophthora sojae* isolates. (a) Gel image of multiplex polymerase chain reaction (PCR) amplifications of discriminant regions associated with avirulence alleles for seven *Avr* genes in *P. sojae* isolate 2012–82. Presence of amplicons for *Avr1b*, *1d*, and *1k* predicts a pathotype 1a, 1c, 3a, and 6. (b) Phenotyping results for isolate 2012–82 indicates a compatible interaction with Harosoy (*rps*), *Rps1a*, *Rps1c*, *Rps3a*, and *Rps6* and an incompatible interaction with *Rps1b*, *Rps1d*, and *Rps1k*, thereby assessing a pathotype 1a, 1c, 3a, and 6, similar to the molecular assay. A = avirulent and V = virulent (see Figure S3). (c) Gel image of multiplex PCR amplifications of discriminant regions associated with avirulence alleles for seven *Avr* genes in *P. sojae* isolate 2012–156. Presence of amplicons for *Avr1b*, *1k*, *3a*, and *6* and all three amplicons for *Avr1a* predicts a pathotype 1c and 1d. (d) Phenotyping results for isolate 2012–156 indicates a compatible interaction with Harosoy (*rps*), *Rps1c*, *Rps1d*, and *Rps3a* and an incompatible interaction with *Rps1a*, *Rps1b*, *Rps1k*, and *Rps6* thereby assessing a pathotype 1c, 1d, and 3a, with 3a being the only interaction at odds with the molecular assay. A = avirulent and V = virulent (see Figure S3)

haplotypes for seven *Avr* genes of *P. sojae*, it should now be possible to obtain a rapid and accurate identification of the virulence profile of isolates in order to precisely select soybean material carrying the appropriate *Rps* genes.

Since the intentional deployment of the first *Rps* gene in soybean, *Rps1a*, *P. sojae* has demonstrated a very strong resilience and ability to adapt to selection pressure through rapid mutations of *Avr* genes (Keeling, 1984; Layton *et al*., 1986; Drenth *et al*., 1996; Kaitany *et al*., 2001). As a result, the pathogen has evolved a staggering pathotype diversity (Dorrance *et al*., 2003; Sugimoto *et al*., 2012; Dorrance *et al*., 2016; Dorrance, 2018) that threatens current efforts to control its spread through genetic approaches. For instance, in a survey of *P. sojae* isolate diversity in Canada, Xue *et al*. (2015) reported an important shift in virulence over time, whereas most isolates now overcome *Rps1k*, the most recently introduced *Rps* gene, while this pathotype was completely absent in Canadian fields 20 years ago. This ability to alter *Avr* genes appears to be based on mutations that range from complete deletion of the gene or copy number variation, to presence of indels or single point mutations within or in close proximity to the gene (Qutob *et al*., 2009; Tyler and Gijzen, 2014). Recently, Arsenault-Labrecque *et al*. (2018) provided an exhaustive description and comparison

TABLE 2 Comparative results of predicted pathotypes between the molecular assay and the hydroponic assay for 25 isolates of *Phytophthora sojae*

Isolate	Predicted pathotype (molecular assay)	Observed pathotype[a] (hydroponic assay)
2010–29	1a, 1c	1a, 1c, 3a
2010–32	1a, 1c	1a, 1c
2010–42	1a, 1c	1a, 1c
2010–44	1a, 1c	1a, 1c, 3a
2011–35	1a, 1c, 3a	1a, 1c, 3a
2011–40	1a, 1b, 1c, 1k	1a, 1b, 1c, 1k
2012–01	1a, 1c, 3a, 6	1a, 1c, 3a, 6
2012–120	1a, 1c, 6	1a, 1c, 6
2012–127	1a, 1c	1a, 1c
2012–136	1a, 1c, 6	1a, 1c, 6
2012–156	1c, 1d	1c, 1d, 3a
2012–40	1a, 1c, 6	1a, 1c, 6
2012–57	1a, 1c, 1d	1a, 1c, 1d
2012–76	1a, 1c	1a, 1c, 3a
2012–82	1a, 1c, 3a, 6	1a, 1c, 3a, 6
2016–20	1a, 1b, 1c, 1d, 1k	1a, 1b, 1c, 1k, 1d
2018–01	1a, 1c, 1d, 3a	1a, 1c, 1d, 3a
2018–02	1a, 1b, 1c, 1d, 1k	1a, 1b, 1c, 1d, 1k
2018–03	1a, 1b, 1c, 1d, 1k	1a, 1b, 1c, 1d, 1k, 3a
2018–04	1a,1b, 1c, 1d, 1k, 3a	1a, 1b, 1c, 1d, 1k, 3a
2018–05	1a, 1c, 1d, 3a	1a, 1c, 1d, 3a
2018–06	1a, 1b, 1c, 1d, 1k	1a, 1b, 1c, 1d, 1k
2018–07	1a, 1c, 1d, 3a	1a, 1c, 1d, 3a
2018–08	1a, 1b, 1c, 1d, 1k	1a, 1b, 1c, 1d, 1k
2018–09	1a, 1c, 1d, 3a	1a, 1c, 1d, 3a

[a]Underlined pathotype indicates discrepancy with the molecular assay.

of haplotype diversity for seven *Avr* genes (*1a*, *1b*, *1c*, *1d*, *1k*, *3a*, and *6*) of *P. sojae* through whole-genome sequencing of 31 isolates with different pathotypes. While all isolates for the study originated from Canada, their results showed that they had captured all the haplotype diversity previously reported (but for one rare allele in *Avr1b* [Shan *et al*., 2004]) and even expanded it for a few *Avr*s. In this work, we further compared the allelic diversity of two avirulence genes (*Avr1k* and *Avr6*) among isolates from China, the United States, and Canada and found that all alleles were well aligned with the predicted virulence, except for a single isolate phenotyped with the hypocotyl assay, indicating that the accuracy of the bioassay expands to most known *P. sojae* isolates, regardless of their origin (Figure S2). In the case of *Avr1b*, our study showed that out of the four strains P6497, P7064, P7074, and P7076, only P6497 carried a haplotype of avirulence and showed a phenotype of virulence (Figure S1). However, it is important to underline that P6497 represents a rare case of virulence against *Rps1b* and avirulence against *Rps1k*, and that its pathotype is uncommon in nature (Xue *et al*., 2015). For these reasons, the sequences obtained by Arsenault-Labrecque *et al*. (2018) offered a precise blueprint of the currently known sequence variation and conservation in each gene, results that we exploited to identify discriminant regions associated with different phenotypes.

In the process of trying to develop a molecular assay based on the discriminant haplotypes, several challenges were encountered at different stages of the study. First, it is known that the acquisition of virulence for a pathogen is often due to a partial or complete deletion of the *Avr* gene (Jones and Dangl, 2006; Guttman *et al*., 2014; Petit-Houdenot and Fudal, 2017). In our study, this phenomenon was only systematically observed in the case of *Avr1d*, which meant that we had to conduct an exhaustive analysis of the upstream and downstream regions of the other *Avr* genes to find SNPs/indels that would segregate haplotypes associated with avirulence from those associated with virulence. In certain instances, as for *Avr1a*, *1c*, and *6*, the discriminating regions were located outside of the coding region of the gene.

When the molecular assay was applied to the 31 isolates that had been previously phenotyped (Arsenault-Labrecque *et al*., 2018), we were able to show a near-perfect adequation between the two approaches. This confirms that the molecular assay constitutes a valid substitute to the long phenotyping assays and offers a much more practical approach to determine pathotypes of *P. sojae* isolates. It can thus find applications in delineating with precision the deployment of soybean lines carrying the proper *Rps* genes to overcome the pathotypes present in a given environment. Furthermore, as new resistance genes are discovered and introgressed into soybean, the test can be adapted to include new *Avr* genes and follow the evolution of new pathotypes over time. Finally, it can incite the development of similar diagnostic tools for other gene-for-gene dependent plant–pathogen interactions.

On testing the accuracy of the molecular assay with 25 isolates of unknown virulence, some interesting biological insights were highlighted with respect to some *Avr* genes. As a first observation, it was certainly validating to record a 97% (170/175) level of concordance between the molecular and the phenotyping assays. Of additional significance is the fact that the only five cases of discrepancy out of 175 interactions tested were related to *Avr3a*, which gave a false predicted phenotype, consistently erring on the side of a virulent response where avirulence was expected based on the molecular assay. This was in clear contrast with the study of Arsenault-Labrecque *et al*. (2018) where *Avr3a* was the only gene where the two haplotypes aligned perfectly with a phenotype of virulence or avirulence as determined by the hypocotyl assay. As a result, *P. sojae* isolates were never tested, until this study, with the hydroponic assay against a differential carrying *Rps3a*. Reasons as to why *Avr3a* appears so unpredictable in our study can fall into two categories. The first one is related to gene regulation, which would explain that presence of the *Avr* gene with repressed expression can lead to a virulent response (Shan *et al*., 2004). It is well known that *Avr* genes are under strong selection pressure and their expression can potentially be altered by a number of events (Wang *et al*., 2011).

Incidentally, Arsenault-Labrecque *et al*. (2018) did observe cases where lower expression of *Avr1c* led to a phenotype of virulence. In addition, Qutob, *et al*. (2013) showed that the level of expression of *Avr3a* could be altered by the presence of small RNAs that would lead to silencing of the gene. Gijzen *et al*. (2014), suggested that epigenetic factors could alter *Avr* gene expression. However, the literature is still rather scant with respect to expression of *Avr3a*, and this phenomenon, if common, needs to be further studied. Alternatively, another explanation could lie in the efficiency of *Rps3a*. *Rps3a* is the least deployed of *Rps* genes accounting for about only 0.3% in commercially released varieties (Slaminko *et al*., 2010). Field observations have also reported the somewhat random nature of its efficiency (Dorrance *et al*., 2003). The different phenotypes obtained between the hydroponic assay and the hypocotyl assay seem to indicate that *Rps3a*, if effective at the collar, does not confer good root resistance, which would also explain its irregular field performance. These results certainly open the way to investigate more precisely the nature of *Rps3a* and its interaction with *Avr3a*.

In a recent report, Yang *et al*. (2019) described new haplotypes of the *Avr1c* gene from isolates recovered in Chinese fields. It was therefore interesting to determine if the primers designed in this study would discriminate those new haplotypes. While in the absence of the sequences for the forward primer it is impossible to make a definitive conclusion, the reverse primer was nonetheless specific to all avirulence alleles. Only virulence allele *Avr1c-4* also showed specificity so it will be worthwhile to determine if the forward primer would discriminate it as is the case with the virulent haplotype D (Arsenault-Labrecque *et al*., 2018), which is also specific to the reverse primer but not the forward one. In the event that the existing forward primer would not discriminate *Avr1c-4*, another primer could easily be designed that captured both haplotype D and *Avr1c-4*.

In summary, this work describes a comprehensive molecular assay capable of defining the pathotypes of *P. sojae*, based on seven *Avr* genes, with unprecedented ease and precision. Its other advantages can be found in eliminating the shortcomings of the different phenotyping procedures while reducing time and resources involved in the process. The test could be further exploited to study and uncover the molecular phenomena underlying the disparity between absence/presence of avirulence alleles and expected phenotypes. It can also have practical applications for breeders and growers in management of the disease with a tailored deployment of use of *Rps* genes based on a precise and rapid determination of pathotypes present in a given area.

4 | EXPERIMENTAL PROCEDURES

4.1 | *Phytophthora sojae* isolates and DNA extraction

All *P. sojae* isolates used in this study, including 31 previously sequenced by Arsenault-Labrecque *et al*. (2018), were sampled across Quebec and Ontario (Canada) and their virulence profile was determined by the hypocotyl assay as reported by Xue *et al*. (2015). To determine if the avirulence genes of the isolates used in this study captured the genetic diversity of other isolates elsewhere in the world, we compared the sequences of two *Avr* genes by alignment and made phylogenetic trees using CLC Genomics Workbench (Qiagen). These two genes were selected because they offered the largest sequence diversity available in the literature and public database (Dou *et al*., 2010; Song *et al*., 2013; Arsenault-Labrecque *et al*., 2018). In addition, Yang *et al*. (2019) recently reported new haplotypes of the *Avr1c* gene from isolates recovered in Chinese fields. To verify if the primers created for *Avr1c* were discriminant for these new alleles, alignments were performed with CLC Genomics Workbench with the reverse primer only, because sequences for the forward primer, located outside the genic region, were not available.

The isolates were first subcultured on V8 agar medium (20% clarified V8) covered with wax paper to facilitate harvest of hyphae and spores. After 1 week, cultures were scraped off the paper with a scalpel and placed in 1.5-mL tubes with screw caps (OMNI International Inc.). The tubes were then kept in the freezer at −80 °C for 2–3 hr and lyophilized overnight. The lyophilized samples were crushed with an Omni Bead Ruptor 24 (OMNI International). The DNA was then extracted from the crushed samples using the E.Z.N.A Plant DNA kit following the manufacturer's protocol for dried samples with slight modifications.

4.2 | Sequence variations and allele-specific primer design

For designing allele-specific primers, the discriminant variations in the sequences of the different *Avr* genes of 31 isolates were studied and identified based on the *P.sojae* reference genome v. 3.0 and the genomic sequences available in the NCBI SRA repository, under the bioproject PRJNA434589 as reported by Arsenault-Labrecque *et al*. (2018). In all cases, we sought to obtain amplicons associated with the avirulence allele(s) and of different sizes such that primers could be used in a multiplex assay and the amplicons easily resolved via gel electrophoresis. Discriminant variations most convenient for marker development were selected to design the primer pairs for the seven *Avr* genes under study (*Avr1a*, *1b*, *1c*, *1d*, *1k*, *3a*, and *6*). In cases where deletions were present, at least one primer was positioned in the deletion such that the avirulence allele (i.e., without the deletion) could be amplified. If only SNPs differentiated the virulence and avirulence alleles, primers were designed in such a way that these variant positions were located at the 3′ extremity to maximize the specificity of amplification. Regions with two or more SNPs were preferentially selected to increase the allelic specificity. The primers were then synthesized by Thermo-Fisher Scientific. The details of the nine pairs of primers are presented in Table 1.

4.3 | Validation of primer specificity

A simple PCR was first conducted with each of the primer pairs individually to ascertain their specificity. The PCR was performed in a T Professional Thermocycler (Biometra) and was carried out in a reaction volume of 20 µL. Each primer was diluted at a concentration of 0.25 µM. The One Taq NEB (New England Biolabs) was used at 0.025 U/µL with 2 µL of DNA extracted from *P. sojae* at a concentration of 10 ng/µL, 5 × One Taq Standard reaction buffer (New England Biolabs), 0.2 mM dNTPs, and 2.5% DMSO (Sigma). The PCR conditions were as follows: an initial denaturation at 94 °C for 5 min followed by 30 cycles of denaturation at 94 °C for 30 s, annealing at 60 °C for 30 s, elongation at 68 °C for 1 min, and a final elongation at 68 °C for 5 min. DNA fragment analysis was performed using a QIAxcel Advanced System on a DNA high-resolution cartridge, based on method OH500 with alignment markers of 15 and 3,000 bp according to the manufacturer's instructions (Qiagen). A PCR was performed on each of the 31 isolates of *P. sojae* with a known pathotype to validate that the presence of the expected amplicon was associated with an avirulent response.

In addition, because *Avr1b* has been reported as potentially affecting the virulence of other avirulence genes (Dou *et al*., 2008), we performed in silico alignments with CLC Genomics Workbench to validate if the primer for *Avr1b* would accurately predict the phenotypes for the well-studied isolates P6497, P7064, P7074, and P7076 (Shan *et al*., 2004).

4.4 | Optimization of the multiplex PCR

Following optimization of primer concentration, annealing temperature, and dNTP concentration, primers were mixed together in a single PCR to check their compatibility in a multiplex PCR. It was found that the primers amplifying the *Avr1c* gene were not compatible with the other primers because, when mixed together, primer dimers were formed. Attempts to design alternative sets of primers were unsuccessful, so it was decided that the primers for *Avr1c* would be used in a separate assay in parallel with the multiplex assay. The multiplex PCR therefore contains the following eight primer sets: Avr1a-indel, Avr1a-snp1, Avr1a-snp2, Avr1b, Avr1d, Avr1k, Avr3a, and Avr6.

The optimal number of cycles for the reaction was 40. Furthermore, a temperature gradient revealed that the temperature obtaining the most intense and most distinct bands was 55 °C for the multiplex PCR and 60 °C for the uniplex PCR. The dNTP concentration chosen was 0.25 mM. The final PCR products were analysed with the QIAxcel Advanced System (Qiagen).

The PCRs were carried out in a reaction volume of 20 µL. Following several tests of dilution of the primers, each primer was diluted at the optimal concentration detailed in Table 1. The One Taq (New England Biolabs) was used at 0.025 U/µL with 2 µL of DNA at a concentration of 10 ng/µL, 5 × One Taq Standard reaction buffer (New England Biolabs), 0.25 mM dNTPs, and 2.5% DMSO (Sigma). The multiplex PCR conditions consisted of an initial denaturation at 94 °C for 5 min followed by 40 cycles of denaturation at 94 °C for 30 s, annealing at 55 °C for 30 s, elongation at 68 °C for 1 min, and a final elongation at 68 °C for 5 min. For the uniplex PCR (*Avr1c*), the conditions were the same, except for annealing at 60 °C.

4.5 | Detection limits of the multiplex PCR

To determine the lowest concentration of DNA at which the multiplex and the uniplex PCR worked, dilutions from 0.01 pg to 20 ng were tested with the two PCR conditions described above. It was determined that the PCR multiplex could detect a DNA concentration of up to 0.2 ng, while the primers tested individually could detect a DNA concentration of 0.2 pg.

4.6 | Specificity of the molecular tool and phenotyping

Once the multiplex PCR conditions were optimized, the 31 isolates with known haplotypes, previously sequenced by Arsenault-Labrecque *et al*. (2018), were analysed to test the efficiency of the molecular assay. Subsequently, 25 isolates collected in the Canadian provinces of Quebec and Ontario between 2010 and 2018 were tested with the multiplex PCR and phenotyped using the hydroponic assay developed by Lebreton *et al*. (2018). For the hydroponic assay, zoospores were inoculated into a hydroponic system containing a nutrient solution diluted in water. Seven differential soybean lines were grown in the hydroponic system with a susceptible control (cv. Harosoy), and the virulence profile of the isolate tested was determined on the basis of which *Rps* genes resulted in immunity. Phenotypic responses (resistance or susceptibility) were recorded 14 days post-inoculation. Plants were scored based on a 1 to 5 scale developed by Lebreton *et al*. (2018) where 1 = none to limited root symptoms and 5 = mortality and advanced root necrosis. A statistical comparison (Dunnett's test) was performed to determine the phenotype of each of the isolates. When values were statistically similar to the ones obtained with cv. Haro (*rps*), the isolate was considered virulent, and when values were statistically lower, the isolate was considered avirulent.

ACKNOWLEDGEMENTS

We would like to thank the following partners for their financial support: Genome Canada, Génome Québec, Ministère de l'Économie, Innovation et Exportation du Québec, Western Grains Research Foundation, Canadian Field Crop Research Alliance, Institut de Biologie Intégrative et des Systèmes (IBISULaval), Centre de recherche sur les grains (CEROM), Agriculture and Agri-Food Canada, the University of Guelph, Semences Prograin, Syngenta, Sevita Genetics, la Coop Fédérée, Producteurs de grains du Québec, Grain Farmers of Ontario, Manitoba Pulse and Soybean Growers, Saskatchewan Pulse Growers, Réseau d'avertissements phytosanitaires and Empresa Brasileira de Pesquisa Agropecuária (EMBRAPA).

This work was further supported by grants from the Natural Sciences and Engineering Research Council of Canada and the Canada Research Chairs Program to R.R.B. The financing supported totally or in part the salaries of the students and researchers involved in the project and the materials. The authors declare that the research was conducted in the absence of any commercial or financial relationships that could be construed as a potential conflict of interest. The authors want to thank Caroline Labbé and Amandine Lebreton (Université Laval) for technical assistance for the bioassays.

DATA AVAILABILITY STATEMENT

The data that support the findings of this study are openly available in the NCBI SRA repository at www.ncbi.nlm.nih.gov/sra under the bioproject PRJNA434589.

ORCID

Richard R. Bélanger http://orcid.org/0000-0001-8549-975X

REFERENCES

Abeysekara, N., Matthiesen, R., Cianzio, S. R., Bhattacharyya, M. and Robertson, A.E. (2016) Novel sources of partial resistance against *Phytophthora sojae* in soybean PI 399036. *Crop Science*, 56, 2322–2335.

Arsenault-Labrecque, G., Sonah, H., Lebreton, A., Labbé, C., Marchand, G., Xue, A. *et al.* (2018) Stable predictive markers for *Phytophthora sojae* avirulence genes that impair infection of soybean uncovered by whole genome sequencing of 31 isolates. *BMC Biology*, 16, 80. https://doi.org/10.1186/s12915-018-0549-9

Bartnicki-Garcia, S. (1968) Cell wall chemistry, morphogenesis, and taxonomy of fungi. *Annual Review of Microbiology*, 22, 87–108. https://doi.org/10.1146/annurev.mi.22.100168.000511

Bruns, T.D., & Shefferson, R.P. (2004) Evolutionary studies of ectomycorrhizal fungi: recent advances and future directions. *Canadian Journal of Botany*, 82, 1122–1132. https://doi.org/10.1139/b04-021

Burbank, L.P. and Ortega, B.C. (2018) Novel amplification targets for rapid detection and differentiation of *Xylella fastidiosa* subspecies *fastidiosa* and multiplex in plant and insect tissues. *Journal of Microbiological Methods*, 155, 8–18. https://doi.org/10.1016/j.mimet.2018.11.002

Conti, M., Cinget, B., Vivancos, J., Oudemans, P.V. and Bélanger, R.R. (2019) A molecular assay allows the simultaneous detection of 12 fungi causing fruit rot in cranberry. *Plant Disease*, 103, 2843–2850. https://doi.org/10.1094/PDIS-03-19-0531-RE

Dorrance, A.E. (2018) Management of *Phytophthora sojae* of soybean: a review and future perspectives. *Canadian Journal of Plant Pathology*, 40, 210–219.

Dorrance, A.E., Berry, S.A., Anderson, T.R. and Meharg, C. (2008) Isolation, storage, pathotype characterization, and evaluation of resistance for *Phytophthora sojae* in soybean. *Plant Health Progress*, 10, 1094–1101.

Dorrance, A.E., Jia, H. and Abney, T.S. (2004) Evaluation of soybean differentials for their interaction with Phytophthora sojae. *Plant Health Progress*, 5, 9.

Dorrance, A.E., Kurle, J., Robertson, A.E., Bradley, C.A., Giesler, L., Wise, K. *et al.* (2016) Pathotype diversity of *Phytophthora sojae* in eleven states in the United States. *Plant Disease*, 100, 1429–1437.

Dorrance, A.E., McClure, S.A. and Desilva, A. (2003) Pathogenic diversity of *Phytophthora sojae* in Ohio soybean fields. *Plant Disease*, 87, 139–146.

Dou, D., Kale, S.D., Liu, T., Tang, Q., Wang, X., Arredondo, F.D. *et al.* (2010) Different domains of *Phytophthora sojae* effector *Avr4/6* are recognized by soybean resistance genes *Rps4* and *Rps6*. *Molecular Plant-Microbe Interactions*, 23, 425–435.

Dou, D., Kale, S.D., Wang, X., Chen, Y., Wang, Q., Wang, X. *et al.* (2008) Conserved C-terminal motifs required for avirulence and suppression of cell death by *Phytophthora sojae* effector *Avr1b*. *The Plant Cell*, 20, 1118–1133.

Drenth, A., Whisson, S., Maclean, D., Irwin, J., Obst, N. and Ryley, M. (1996) The evolution of races of *Phytophthora sojae* in Australia. *Phytopathology*, 86, 163–169.

Gijzen, M., Ishmael, C. and Shrestha, S.D. (2014) Epigenetic control of effectors in plant pathogens. *Frontiers in Plant Science*, 5, 638. https://doi.org/10.3389/fpls.2014.00638

Guttman, D.S., Mchardy, A.C. and Schulze-Lefert, P. (2014) Microbial genome-enabled insights into plant-microorganism interactions. *Nature Reviews Genetics*, 15, 797. https://doi.org/10.1038/nrg3748

Haudenshield, J.S., Song, J.Y. and Hartman, G.L. (2017) A novel, multiplexed, probe-based quantitative PCR assay for the soybean root- and stem-rot pathogen, *Phytophthora sojae*, utilizes its transposable element. *PLoS ONE*, 12, e0176567. https://doi.org/10.1371/journal.pone.0176567

Jones, J.D.G. and Dangl, J.L. (2006) The plant immune system. *Nature*, 444, 323–329. https://doi.org/10.1038/nature05286

Kaitany, R.C., Hart, L. and Safir, G. (2001) Virulence composition of *Phytophthora sojae* in Michigan. *Plant Disease*, 85, 1103–1106.

Kaufmann, M.J. and Gerdemann, J. (1958) Root and stem rot of soybean caused by *Phytophthora sojae* n. sp. *Phytopathology*, 48, 201–208.

Keeling, B.L. (1984) A new physiologic race of *Phytophthora megasperma* f. sp. *glycinea*. *Plant Disease*, 68, 626–627.

Kostov, K., Verstappen, E., Bergervoet, J., De Weerdt, M., Schoen, C., Slavov, S. *et al.* (2016) Multiplex detection and identification of *Phytophthora* spp. using target-specific primer extension and Luminex xTAG technology. *Plant Pathology*, 65, 1008–1021.

Layton, A., Athow, K. and Laviolette, F. (1986) New physiologic race of *Phytophthora megasperma* f. sp. *glycinea*. *Plant Disease*, 70, 500–501.

Lebreton, A., Labbé, C., De Ronne, M., Xue, A. G., Marchand, G. and Bélanger, R.R. (2018) Development of a simple hydroponic assay to study vertical and horizontal resistance of soybean and pathotypes of *Phytophthora sojae*. *Plant Disease*, 102, 114–123.

Marin-Felix, Y., Hernández-Restrepo, M., Wingfield, M.J., Akulov, A., Carnegie, A.J., Cheewangkoon, R. *et al.* (2019) Genera of phytopathogenic fungi: GOPHY 2. *Studies in Mycology*, 92, 47–133. https://doi.org/10.1016/j.simyco.2018.04.002

Michalecka, M., Bryk, H., Poniatowska, A. and Puławska, J. (2016) Identification of *Neofabraea* species causing bull's eye rot of apple in Poland and their direct detection in apple fruit using multiplex PCR. *Plant Pathology*, 65, 643–654.

Moine, L.M., Labbé, C., Louis-Seize, G., Seifert, K. A. and Bélanger, R.R. (2014) Identification and detection of *Fusarium striatum* as a new record of pathogen to greenhouse tomato in northeastern America. *Plant Disease*, 98, 292–298.

Petit-Houdenot, Y. and Fudal, I. (2017) Complex interactions between fungal avirulence genes and their corresponding plant resistance genes and consequences for disease resistance management. *Frontiers in Plant Science*, 8, 1072. https://doi.org/10.3389/fpls.2017.01072

Qutob, D., Chapman, B.P. and Gijzen, M. (2013) Transgenerational gene silencing causes gain of virulence in a plant pathogen. *Nature Communications*, 4, 1349. https://doi.org/10.1038/ncomms2354

Qutob, D., Tedman-Jones, J., Dong, S., Kuflu, K., Pham, H., Wang, Y. *et al.* (2009) Copy number variation and transcriptional polymorphisms of *Phytophthora sojae* RXLR effector genes *Avr1a* and *Avr3a*. *PLoS ONE*, 4, e5066. https://doi.org/10.1371/journal.pone.0005066

Raja, H.A., Miller, A.N., Pearce, C.J. and Oberlies, N.H. (2017) Fungal identification using molecular tools: a primer for the natural products research community. *Journal of Natural Products*, 80, 756–770. https://doi.org/10.1021/acs.jnatprod.6b01085

Rasoolizadeh, A., Labbé, C., Sonah, H., Deshmukh, R.K., Belzile, F., Menzies, J.G. *et al.* (2018) Silicon protects soybean plants against *Phytophthora sojae* by interfering with effector-receptor expression. *BMC Plant Biology*, 18, 97. https://doi.org/10.1186/s12870-018-1312-7

Reich, J., Alexander, T. and Chatterton, S. (2016) A multiplex PCR assay for the detection and quantification of *Sclerotinia sclerotiorum* and *Botrytis cinerea*. *Letters in Applied Microbiology*, 62, 379–385.

Rollins, L., Coats, K., Elliott, M. and Chastagner, G. (2016) Comparison of five detection and quantification methods for *Phytophthora ramorum* in stream and irrigation water. *Plant Disease*, 100, 1202–1211.

Shan, W.X., Cao, M., Leung, D. and Tyler, B.M. (2004) The *Avr1b* locus of *Phytophthora sojae* encodes an elicitor and a regulator required for avirulence on soybean plants carrying resistance gene *Rps1b*. *Molecular Plant-Microbe Interactions*, 17, 394–403.

Silva, A., Savi, D., Gomes, F., Gos, F., Silva, G. and Glienke, C. (2017) Identification of *Colletotrichum* species associated with postbloom fruit drop in Brazil through GAPDH sequencing analysis and multiplex PCR. *European Journal of Plant Pathology*, 147, 731–748. https://doi.org/10.1007/s10658-016-1038-z

Slaminko, T., Bowen, C.R. and Hartman, G. (2010) Multi-year evaluation of commercial soybean cultivars for resistance to *Phytophthora sojae*. *Plant Disease*, 94, 368–371.

Song, T., Kale, S.D., Arredondo, F.D., Shen, D., Su, L., Liu, L. *et al.* (2013) Two RxLR avirulence genes in *Phytophthora sojae* determine soybean *Rps* 1k-mediated disease resistance. *Molecular Plant-Microbe Interactions*, 26, 711–720.

Statistique Canada (2018) *Superficies des Principales Grandes Cultures, Mars 2018, 27 Avril*. Component of Statistics Canada Catalog no. 11-001-X. Ottawa: Statistics Canada. Available at https://www150.statcan.gc.ca/n1/fr/daily-quotidien/180427/dq180427a-fra.pdf?st=UtoXzQxU.

Sugimoto, T., Kato, M., Yoshida, S., Matsumoto, I., Kobayashi, T., Kaga, A. *et al.* (2012) Pathogenic diversity of *Phytophthora sojae* and breeding strategies to develop *Phytophthora*-resistant soybeans. *Breeding Science*, 61, 511–522. https://doi.org/10.1270/jsbbs.61.511

Tyler, B.M. (2007) *Phytophthora sojae*: root rot pathogen of soybean and model oomycete. *Molecular Plant Pathology*, 8, 1–8. https://doi.org/10.1111/j.1364-3703.2006.00373.x

Tyler, B.M. and Gijzen, M. (2014) The *Phytophthora sojae* genome sequence: foundation for a revolution. In R.A. Dean, A. Lichens-Park and C. Kole (Eds.) *Genomics of Plant-Associated Fungi and Oomycetes: Dicot Pathogens*. Berlin, Heidelberg: Springer, pp. 133–157.

Wang, Q., Han, C., Ferreira, A.O., Yu, X., Ye, W., Tripathy, S. *et al.* (2011) Transcriptional programming and functional interactions within the *Phytophthora sojae* RXLR effector repertoire. *The Plant Cell*, 23, 2064–2086.

Xue, A.G., Marchand, G., Chen, Y., Zhang, S., Cober, E.R. and Tenuta, A. (2015) Races of *Phytophthora sojae* in Ontario, Canada, 2010–2012. *Canadian Journal of Plant Pathology*, 37, 376–383.

Yang, J., Wang, X., Guo, B., Huang, J., Ye, W., Dong, S. *et al.* (2019) Polymorphism in natural alleles of the avirulence gene *Avr1c* is associated with the host adaptation of *Phytophthora sojae*. *Phytopathology Research*, 1, 28.

SUPPORTING INFORMATION

Additional supporting information may be found online in the Supporting Information section.

Figure S1 Sequence alignment of *Avr1b* for *Phytophthora sojae* isolates P6497, P7064, P7074, and P7076. Results show that the allele-specific primer (green arrow) anneals only to P6497 and P7064, thereby predicting a phenotype of avirulence for P6497 and P7064, and a phenotype of virulence for P7074 and 7076

Figure S2 Phylogenetic trees showing the diversity of *Phytophthora sojae* isolates in the United States, Canada, and China for A *Rps1k* and B *Rps6* genes. Virulence and avirulence alleles are circled and identified

Figure S3 Susceptibility scoring of soybean plantlets inoculated with *Phytophthora sojae* isolates A 2012-82 and B 2012-156 complementing the phenotyping assay of Figure 4. Interactions are considered incompatible when values (indicated with *) are significantly different from the *rps* gene (susceptible control) according to Dunnett's test ($p < .01$)

How to cite this article: Dussault-Benoit C, Arsenault-Labrecque G, Sonah H, Belzile F, Bélanger RR. Discriminant haplotypes of avirulence genes of *Phytophthora sojae* lead to a molecular assay to predict phenotypes. *Molecular Plant Pathology*. 2020;21:318–329. https://doi.org/10.1111/mpp.12898

Arsenault-Labrecque, G., Santhanam, P., Asselin, Y., Cinget, B., Lebreton, A., Labbé, C., ... & Bélanger, R. R. (2022). RXLR effector gene *Avr3a* from *Phytophthora sojae* is recognized by *Rps8* in soybean. *Molecular Plant Pathology*, *23*(5), 693-706.

Received: 11 June 2021 | Revised: 15 January 2022 | Accepted: 17 January 2022

DOI: 10.1111/mpp.13190

Molecular Plant Pathology WILEY

ORIGINAL ARTICLE

RXLR effector gene *Avr3a* from *Phytophthora sojae* is recognized by *Rps8* in soybean

Geneviève Arsenault-Labrecque[1] | Parthasarathy Santhanam[1] | Yanick Asselin[1] | Benjamin Cinget[1] | Amandine Lebreton[1] | Caroline Labbé[1] | François Belzile[1] | Mark Gijzen[2] | Richard R. Bélanger[1]

[1]Department of Phytology, Université Laval, Québec, Québec, Canada

[2]Agriculture and Agri-Food Canada, London, Ontario, Canada

Correspondence
Richard R. Bélanger, Department of Phytology, Université Laval, Québec, QC, Canada.
Email: Richard.belanger@fsaa.ulaval.ca

Funding information
Genome Canada; Canada Research Chairs; Génome Québec

Abstract

The use of resistance genes in elite soybean cultivars is one of the most widely used methods to manage *Phytophthora sojae*. This method relies on effector-triggered immunity, where a Resistant to *P. sojae* (*Rps*) gene product from the plant recognizes a specific effector from the pathogen, encoded by an avirulence (*Avr*) gene. Many *Avr* genes from *P. sojae* have been identified in the last decade, allowing a better exploitation of this type of resistance. The objective of the present study was to identify the *Avr* gene triggering immunity derived from the soybean resistance gene *Rps8*. The analysis of a segregating F_2 progeny coupled with a genotyping-by-sequencing approach led to the identification of a putative *Avr8* locus. The investigation of this locus using whole-genome sequencing data from 31 isolates of *P. sojae* identified *Avr3a* as the likely candidate for *Avr8*. Long-read sequencing also revealed that *P. sojae* isolates can carry up to five copies of the *Avr3a* gene, compared to the four previously reported. Haplotype and transcriptional analyses showed that amino acid changes and absence of *Avr3a* transcripts from *P. sojae* isolates caused changes in virulence towards *Rps8*. Functional analyses using CRISPR/Cas9 knockout and constitutive expression demonstrated that *Rps8* interacted with *Avr3a*. We also showed that a specific allele of *Avr3a* is recognized by *Rps3a* but not *Rps8*. While *Rps3a* and *Rps8* have been previously described as closely linked, this is the first report of a clear distinction hitherto undefined between these two resistance genes.

KEYWORDS
Avr gene, CRISPR/Cas9, effectors, oomycete, Phytophthora root rot, plant–pathogen interaction *Rps* gene

1 | INTRODUCTION

The oomycete *Phytophthora sojae* is a soilborne pathogen causing Phytophthora root and stem rot (PRR), one of the major threats to the ever-expanding soybean crop. In poorly drained fields with a history of the disease, yield losses can reach 100% when susceptible cultivars are planted (Dorrance, 2018). Over the last two decades, the sum of economic losses attributed to PRR in the United States has been higher than $5000 per hectare, making it among the most important diseases affecting soybean in the country (Bandara et al.,

2020). Worldwide, the disease is causing annual yield damages of up to $2 billion (Tyler, 2007). To manage the pathogen, seed treatments, improved drainage, and host resistance are being used.

Host resistance has long been recognized as a very effective way to manage the disease as numerous sources of quantitative and qualitative host resistance have been identified (Dorrance, 2018). Quantitative disease resistance, also called partial resistance, is conferred by different quantitative trait loci (de Ronne et al., 2020). This type of resistance is known to be particularly effective when used in combination with qualitative resistance, named race-specific resistance, or vertical resistance, which is conditioned by single dominant genes called Resistant to *P. sojae* (*Rps*) (Dorrance et al., 2003). This type of resistance, giving an immune type of response, is the most widely used as it can confer complete resistance against PRR. Controlled by a single gene, it is also easier to select phenotypes during breeding and facilitates their introgression into elite cultivars. Soybean is indeed a rich source of race-specific resistance as nearly 30 *Rps* genes have been identified and mapped to nine chromosomes since the 1950s (Zhong et al., 2020). From this catalogue of genes, six have been successfully introgressed into commercial soybean varieties, namely *Rps1a*, *Rps1b*, *Rps1c*, *Rps1k*, *Rps3a*, and *Rps6* (Abeysekara et al., 2016; Sugimoto et al., 2012).

The resistance conferred by an *Rps* gene relies on the traditional gene-for-gene concept where a relationship exists between host resistance genes and pathogen virulence factors (Flor, 1971). Under this concept, *Rps* genes in the host encode or are predicted to encode specific nucleotide-binding, leucine-rich repeat immune receptors that can recognize specific effectors that typically contain N-terminal RXLR (Arg-any amino acid-Leu-Arg) and EER (Glu-Glu-Arg) motifs produced by avirulence (*Avr*) genes in the pathogen. The recognition of these avirulence factors will lead to effector-triggered immunity in the host plant (Białas et al., 2018; Dodds & Rathjen, 2010). Conversely, the pathogen can avoid recognition conferred by *Rps* genes through various mutations, insertions, deletions, or altered expression of its corresponding *Avr* genes (Tyler & Gijzen, 2014).

This dynamic interplay between effectors and receptors has led to the evolution of more than 200 different pathotypes of *P. sojae*, as more *Rps* genes have been deployed commercially (Stewart et al., 2014). To better exploit the efficacy of each *Rps* gene in elite soybean cultivars, it is then crucial to have a good understanding of each corresponding *Avr* gene and its haplotypic diversity. To date, several *P. sojae Avr* genes have been identified, including *Avr1a*, *Avr1b*, *Avr1c*, *Avr1d*, *Avr1k*, *Avr3a/5*, *Avr3b*, *Avr3c*, and *Avr4/6* (Dong et al., 2009; Dong, Yin, et al., 2011; Dong, Yu, et al., 2011; Dou et al., 2010; Na et al., 2013, 2014; Qutob et al., 2009; Shan et al., 2004; Song et al., 2013). Recently, it was also found that for seven of these *Avr* genes recognized by the seven most common *Rps* genes, genomic signatures can be used as accurate predictors of phenotypes (Arsenault-Labrecque et al., 2018). Subsequently, a molecular assay that reveals the avirulence allele of these seven *Avr* genes was developed in order to diagnose with precision the pathotypes of *P. sojae* isolates (Dussault-Benoit et al., 2020).

While these recent developments will enable growers to better fight PRR, the constant adaptation of *P. sojae* makes the average durability of *Rps* genes within commercial soybean varieties to be approximately 8–20 years (Grau et al., 2004; Schmitthenner, 1985). This leads to the constant need of deploying new *Rps* genes and thereby subsequent identification of associated *Avr* genes from *P. sojae*. One of these resistance genes is *Rps8*, which maps on chromosome 13, close to the *Rps3* locus (Burnham et al., 2003; Dorrance et al., 2016; Gordon et al., 2006; Sandhu et al., 2005). As a matter of fact, *Rps3a* and *Rps8* have yet to be dissociated clearly (Gunadi, 2012) while other reports indicate that *Rps5* could also be linked to *Rps3a* (Dong et al., 2011). *Rps8* is of particular interest as it showed potential for management of *P. sojae*, notably in the United States and Brazil (Costamilan et al., 2012; Dorrance et al., 2016). These two countries account for more than 70% of global soybean production and both struggle with PRR problems.

The objective of this study was to identify *Avr8*, presumably an RXLR effector, from *P. sojae* leading to an immune response from the plants bearing *Rps8*. We first identified the *Avr8* locus via genetic mapping of this locus within a segregating F_2 population of *P. sojae* isolates. These were tested for virulence in a hydroponic assay and genotyped via a genotyping-by-sequencing (GBS) approach. By taking advantage of exhaustive whole-genome sequencing (WGS) data for a collection of *P. sojae* from a previous study (Arsenault-Labrecque et al., 2018), it was possible to identify a single gene at the *Avr8* locus, namely *Avr3a*, that interacts with *Rps8*. The functional interaction of the product of the *Avr3a* gene with *Rps8* was first confirmed via genome editing with CRISPR/Cas9 and showed a clear compatibility between plants carrying *Rps8* and isolates lacking the *Avr3a* gene. In parallel, constitutive expression experiments validated the interaction between *Rps8* and *Avr3a* as its expression triggered an incompatible interaction with plants carrying *Rps8*. Nanopore long-read sequencing also highlighted the presence of a fifth copy of *Avr3a* from isolates carrying the $Avr3a^{45C}$ allele, which is the one recognized by *Rps8*.

2 | RESULTS

2.1 | Localization of the *Avr8* region

From the crosses of *P. sojae* isolates 45C (avirulent on *Rps8*) and 7B (virulent on *Rps8*), three F_1 hybrids were obtained, and the phenotypic assay revealed that they were all avirulent on *Rps8* (Figure 1). Self-fertilization of each of these F_1 hybrids led to a total of 83 F_2 progenies. Based on the hydroponic phenotyping assay, 35 F_2 progenies were determined to be avirulent on *Rps8* while 22 were virulent. The remaining 26 F_2 isolates showed intermediate responses towards *Rps8* and/or the susceptible control plants.

The 83 F_2 progenies were genotyped using a GBS approach. A total of 110.8 million reads (50–220 bp in length) for an average of 1.34 million reads per isolate were obtained, and 97.7% of these reads were successfully mapped to the *P. sojae* reference genome

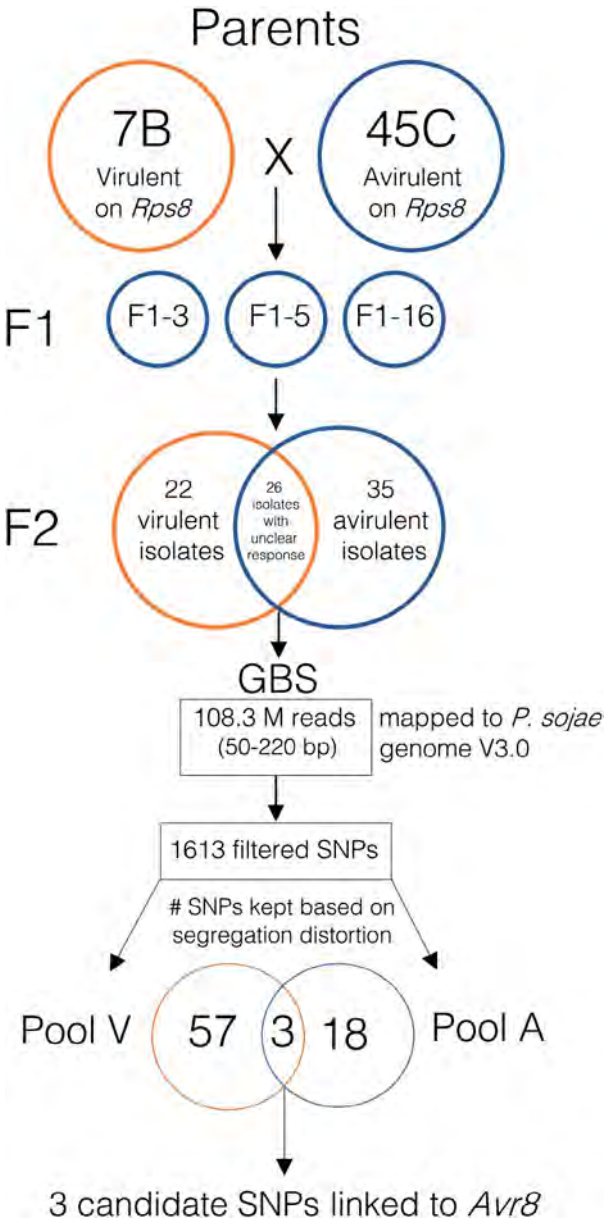

FIGURE 1 Genetic mapping of the *Avr8* locus in *Phytophthora sojae* in a segregating F_2 population. Single-nucleotide polymorphisms (SNPs) showing a marked allelic contrast between virulent and avirulent isolate were deemed to mark the *Avr8* locus

(v. 3.0). After retaining positions with a coverage depth equal to or higher than 10, these reads covered approximately 2.5% of the whole genome and 29,053 single-nucleotide polymorphisms (SNPs) were successfully called from these data (with minor allele frequency >0.008). Using SnpEff, it was found that 35% of those SNPs were in coding regions and 51% in the immediate vicinity of a coding region (1000 bp upstream or downstream of a coding region), with the remaining 14% located in intergenic regions. Among SNPs present in the coding regions, 63% induced nonsynonymous mutations. After filtering and imputation of missing data, a set of 1613 SNPs was retained (Figure 1).

Two pools of individuals were created based on their phenotypic reaction on *Rps8*: a virulent (V) pool and an avirulent (A) pool. For each SNP, the frequency of each allele was estimated in the entire F_2 population, as well as in pools V and A. For each SNP in each pool, χ^2 tests were performed to assess segregation distortion from the entire F_2 population. When a SNP locus presented a significant segregation bias in both pools and the genotype of the favoured allele matched the parent with the corresponding phenotype, it was considered as potentially linked to *Avr8*. In pool V, a total of 60 SNPs inherited from the virulent parent presented a segregation bias while 21 SNPs in pool A, inherited from the avirulent parent, had a significant segregation distortion. From these selected SNPs, three consecutive SNPs were present in both pools and exhibited *p* values and genotype distributions that met all expected criteria for an avirulence locus. The allele frequencies of the candidate alleles for each SNP in each pool are presented in Table 1 and the genotype of each F_2 isolate for each of these variants is shown in Figure 2a.

The region circumscribed by the candidate SNPs is a gene-rich region with a total of 34 genes, from which five have been previously characterized as either *Avr* genes (*Avr3a-1* and *Avr3a-2*) or effectors based on the presence of RXLR motifs (*Avh37*, *Avh36*, and *Avh38*).

2.2 | RXLR effector candidates for *Avr8*

From the catalogue of variants called using WGS data for 31 isolates of *P. sojae*, including parents 7B and 45C, variants located in the *Avr8* locus and for which the virulent parental isolate 7B carried the alternative allele were extracted. A total of 252 SNPs and indels smaller than 50 bp, two deletions of more than 50 bp, and one copy number variation were found in this region (Table S1).

Using SnpEff, it was revealed that 75% of these variants were nonsynonymous and could potentially affect 28 out of 34 genes (of which four are predicted to encode RXLR effectors as presented in Figure 2b) by being located within the gene coding region or within 1000 bp upstream or downstream of these genes. Of these nonsynonymous variants, 60 were located directly in the coding regions of 15 genes, including the predicted RXLR effector gene *Avh37* (four variants) and two copies of the *Avr3a* gene (*Avr3a-1* and *Avr3a-2*; 16 variants). Five variants out of these 60 were also predicted to have a potentially high impact on the proteins coded by five different genes, including *Avh37* (frameshift insertion) and *Avr3a-1* and *Avr3a-2* (loss of stop codon for both genes). Furthermore, the copy number variation region detected in the parents included both copies of *Avr3a-1*

TABLE 1 Candidate single-nucleotide polymorphisms (SNPs) linked to *Avr8* in *Phytophthora sojae*

SNP	Position	Allele frequency pool V[a]	Allele frequency pool A
1	PHYSOscaffold_9:589,423	0.76[b]	0.89
2	PHYSOscaffold_9:604,324	0.76	0.89
3	PHYSOscaffold_9:691,142	0.81	0.87

[a] V: 7B (virulent parent); A: 45C (avirulent parent).

[b] Frequency of the favoured allele at the SNP loci showing the greatest degree of segregation distortion (χ^2 test, $p < 0.05$ in both pools).

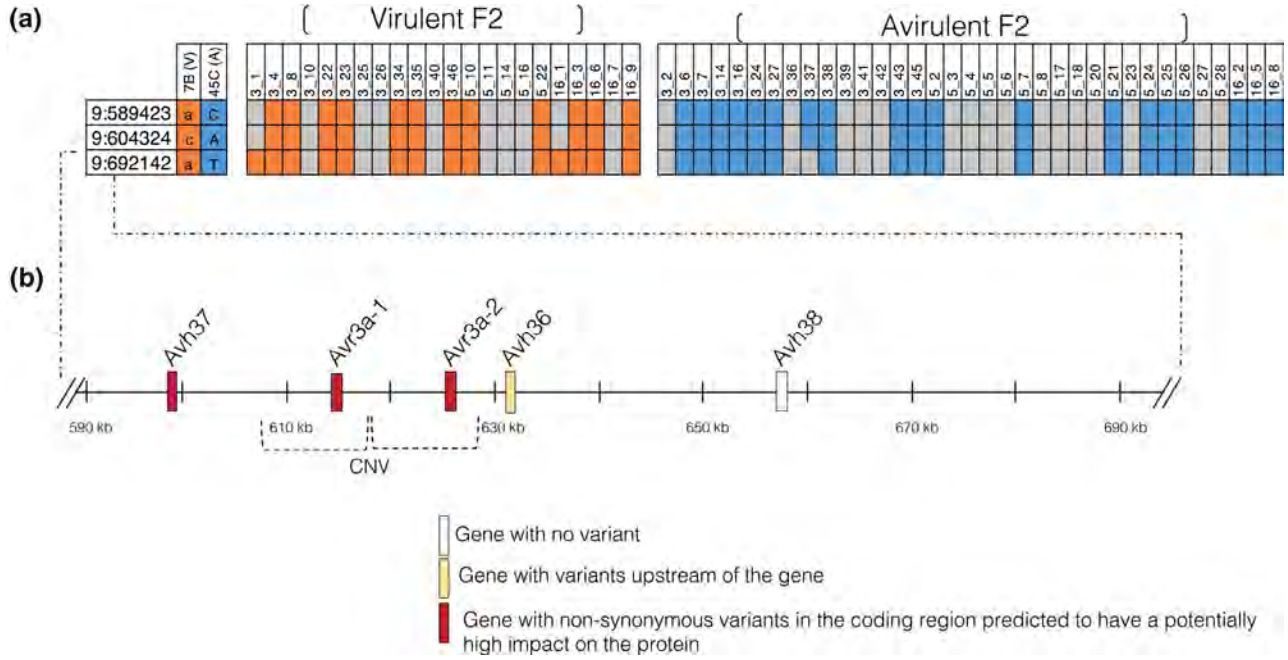

FIGURE 2 *Avr8* locus of *Phytophthora sojae* defined in this study. (a) Genotypes of F_2 isolates for single-nucleotide polymorphisms (SNPs) linked to *Avr8*. Orange and blue boxes represent homozygous genotypes and grey boxes represent heterozygous genotypes. (b) Overview of the potential impact of variants inherited from the virulent parent 7B on genes encoding RXLR effectors located in the *Avr8* region

TABLE 2 Summary of the variants affecting gene translation and encoding predicted RXLR effectors in the *Avr8* locus of *Phytophthora sojae*

Predicted RXLR effector	Position on PHYSOscaffold_9	Polymorphisms from virulent parent 7B
Avh37	598,793–598,248	• 7 variants upstream of the gene including 2 insertions of 6 and 25 bp • 2 missense mutations • 1 in-frame insertion • 1 frameshift insertion
Avr3a	615,105–615,440 (*Avr3a-1*) 625,907–626,242 (*Avr3a-2*)	• 9 variants upstream of the gene including 1 deletion of 276 bp and 3 insertions of 10, 11, and 26 bp • 14 missense variants • 1 in-frame insertion • Loss of stop codon • Copy number variation
Avh36	631,330–631,530	• 2 variants upstream of the gene
Avh38	657,499–657,924	• No variant

and *Avr3a-2* represented in the reference genome of *P. sojae*, which are two exact copies of the same gene. The two deletions of 276 bp detected in the virulent parent were also located 1.1 kb upstream of *Avr3a-1* and *Avr3a-2*. A summary of the impact of the variants on RXLR effector genes at the *Avr8* locus is presented in Figure 2b and variants associated with genes encoding RXLR effectors present at the *Avr8* locus are shown in Table 2. These results led us to consider *Avh37* and *Avr3a* as the most promising candidates for *Avr8*.

Based on the polymorphisms presented in Table 2, predicted amino acid sequences of the different alleles of the two candidate genes *Avh37* and *Avr3a* are shown in Figure 3. For both genes, amino acid changes were found in the N-terminal portion, as well as in the C-terminal portion. In the N-terminal portion, amino acid changes altered the EER motif of the virulent alleles for both genes. Two amino acid changes were also located in the signal peptide for *Avr3a*. The frameshift insertion in the C-terminal portion of $Avh37^{7B}$ led to two proteins of different length as the stop codon from the 45C allele was lost. For *Avr3a*, the stop codon present in the 45C allele was also lost due to a SNP.

2.3 | Transcript analysis of candidate genes

Expression levels of candidate genes *Avh37* and *Avr3a* in five different isolates of *P. sojae* were compared to determine whether transcript abundance could be associated with virulence phenotypes; results are shown in Table 3 (original image from gel electrophoresis

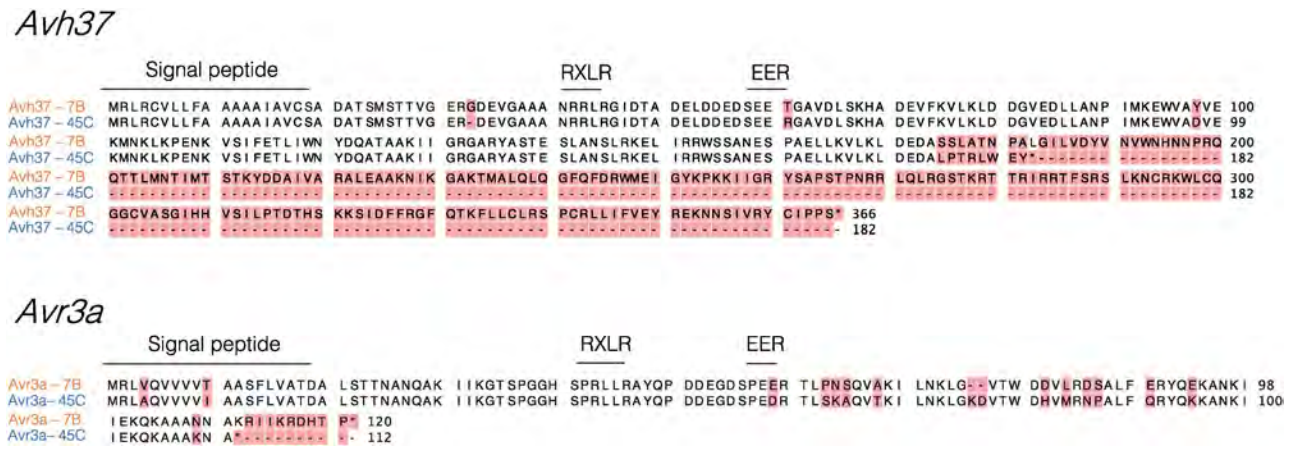

FIGURE 3 Predicted amino acid sequences of *Phytophthora sojae Avr8* candidate genes, based on alleles from parent 7B (virulent on *Rps8*) and 45C (avirulent on *Rps8*). Signal peptides and RXLR and EER motifs are shown, and polymorphic residues among the two different alleles are highlighted with a red background for *Avh37* and *Avr3a* genes

TABLE 3 Reverse transcription PCR analysis of gene expression of candidate genes *Avh37* and *Avr3a* in *Phytophthora sojae* isolates showing contrasting phenotypes on soybean plants carrying *Rps8*

		Avh37		*Avr3a*	
Isolate	**Virulence *Rps8*[a]**	**Sequence[b]**	**mRNA[c]**	**Sequence**	**mRNA**
F2-3-7	A	45C	+	45C	+
45C	A	45C	+	45C	+
8-5-7	A	45C	±	45C	+
Race 7	V	7B	+	7B	–
2012_70	V	7B	+	7B	–

[a] A: avirulent; V: virulent.

[b] Two different sequences, according to the sequence from the representative strains 7B (virulent parent) and 45C (avirulent parent).

[c] (+), mRNA detected; (–), mRNA not detected. Transcriptional analysis was performed by reverse transcription PCR on mRNA isolated from infected root tissues 5 dpi.

is presented in Figure S1). For *Avh37*, the transcript was present in every isolate studied regardless of the phenotype on *Rps8* or the allele of the gene carried by these isolates. For *Avr3a*, transcriptional analysis showed that expression of the gene occurred in the three isolates avirulent on *Rps8* and that possessed the *Avr3a* allele from the avirulent parent 45C. On the other hand, *Avr3a* mRNA was not detected in the two virulent isolates tested and carrying the allele of isolate 7B, which is virulent on *Rps8*.

2.4 | Interaction of effectors encoded by candidate genes with *Rps8*

To test the interaction of Avr proteins encoded by candidate genes *Avh37*^{45C} and *Avr3a*^{45C} with the soybean *Rps8* gene product, two different *P. sojae* transformations were performed. To see if the absence of transcript from each candidate gene caused gain of virulence in the presence of *Rps8*, CRISPR/Cas-9-mediated genome editing was used to knock out the two candidate genes independently in the *P. sojae* isolates showing avirulence on *Rps8*. Constitutive expression of the candidate genes in a *P. sojae* isolate virulent on *Rps8* was also performed to determine if its expression would trigger a defence response from plants carrying *Rps8*. Regarding the CRISPR/Cas9 transformation, 36 transformants were screened and sequenced and one stable transformant was obtained for *Avr3a*, while 48 transformants were screened and sequenced but no stable transformants were generated for *Avh37*. For the constitutive expression, two stable transformants were obtained for *Avr3a* and three for *Avh37*. Phenotyping assays were conducted for each of these transformants.

The stable transformant obtained from CRISPR/Cas9 transformation targeting the *Avr3a*^{45C} gene presented a single-nucleotide deletion causing a mutation in the dEER (Asp-Glu-Glu-Arg) motif of the protein and leading to a truncated protein before the predicted effector domain containing the W-like motif near the C-terminal end (see Figure S2). Phenotyping results of the wild-type isolate 45C (45C WT) and the *Avr3a*^{45C} knockout isolate (45C:KO-*Avr3a*^{45C}) are shown in Figure 4 and susceptibility scores can be found in Figure S3. As expected, the WT isolate 45C was avirulent in the presence of *Rps8*. By contrast, inoculation with the *Avr3a*^{45C} knockout isolate led to a phenotype of virulence on plants carrying *Rps8*. As shown in Figure 4, plants containing *Rps8* showed resistance in both the aerial

and root parts when inoculated with the WT isolate 45C, compared to the susceptible control plants Haro (1-7)1. For their part, plants containing *Rps8* showed a compatible reaction when inoculated with the *Avr3a*^{45C} knockout isolate, thus indicating that the lack of *Avr3a*^{45C} gene resulted in a gain of virulence in the presence of *Rps8*.

With respect to the constitutive expression of *Avr3a*^{45C}, transcript analysis confirmed its expression in transformed isolates 7C OE-*Avr3a*-1, -2, and -3, while it went undetected in WT isolate 7B (Figure S4). Phenotyping results of the WT isolate 7B and the two transformants expressing *Avr3a*^{45C} are shown in Figure 5 (susceptibility scores are found in Figure S3). The WT isolate 7B was virulent in the presence of *Rps8* on control plants Haro (1-7)1, as anticipated. In contrast, transformed isolates expressing *Avr3a*^{45C} were avirulent on plants containing *Rps8*, demonstrating that constitutive expression of *Avr3a*^{45C} in *P. sojae* isolate 7B causes gain of avirulence in the presence of *Rps8*.

For candidate gene *Avh37*, transcript analysis was performed on WT isolate 7B (virulent in the presence of *Rps8*) and the three stable transformants obtained (7B OE-*Avh37*-1, -2, and -3) from constitutive expression of *Avh37*^{45C}. This analysis showed expression of the gene in transformed isolates and none in the WT isolate 7B (Figure S4). Phenotyping results of the WT isolate 7B and the three transformants expressing *Avh37* are shown in Figure 6 (susceptibility scores are found in Figure S3). As expected, the WT isolate 7B was virulent in the presence of *Rps8* and on susceptible control plants Haro(1-7)1. Similar virulent responses were observed on plants inoculated with the transformants, showing that overexpression of *Avh37* did not cause an incompatible interaction with plants containing *Rps8*.

2.5 | New definition of the *Avr3a* locus

To obtain a better definition of the *Avr3a* locus, Nanopore long-read sequencing was performed for parental isolates 45C and 7B. To observe the inheritance pattern of the *Avr3a* region in the progeny, two F_2 isolates (8-3-6, avirulent on *Rps8*, and 8-3-34, virulent on *Rps8*) were also sequenced. From the parental isolate 45C, a read was obtained with a length of 79,521 kb that carried five identical copies of the *Avr3a* gene. Each copy was embedded in a segment of 10.8 kb with four other genes, and this segment was repeated five times, as a result of tandem duplication (Figure 6). Reads from Illumina and Nanopore sequencing of isolate 45C were used to construct a new consensus sequence of the whole region (File S1). This sequence was used to align contigs obtained from de novo assembly of Nanopore reads of the F_2 isolate 8-3-6 (avirulent on *Rps8*). This alignment showed that five identical copies of the *Avr3a* gene were also present in the avirulent F_2 progeny. To define the *Avr3a* region in parental and F_2 isolates virulent on *Rps8* (7B and 8-3-34), de novo assembly and alignment of contigs on the 45C new consensus

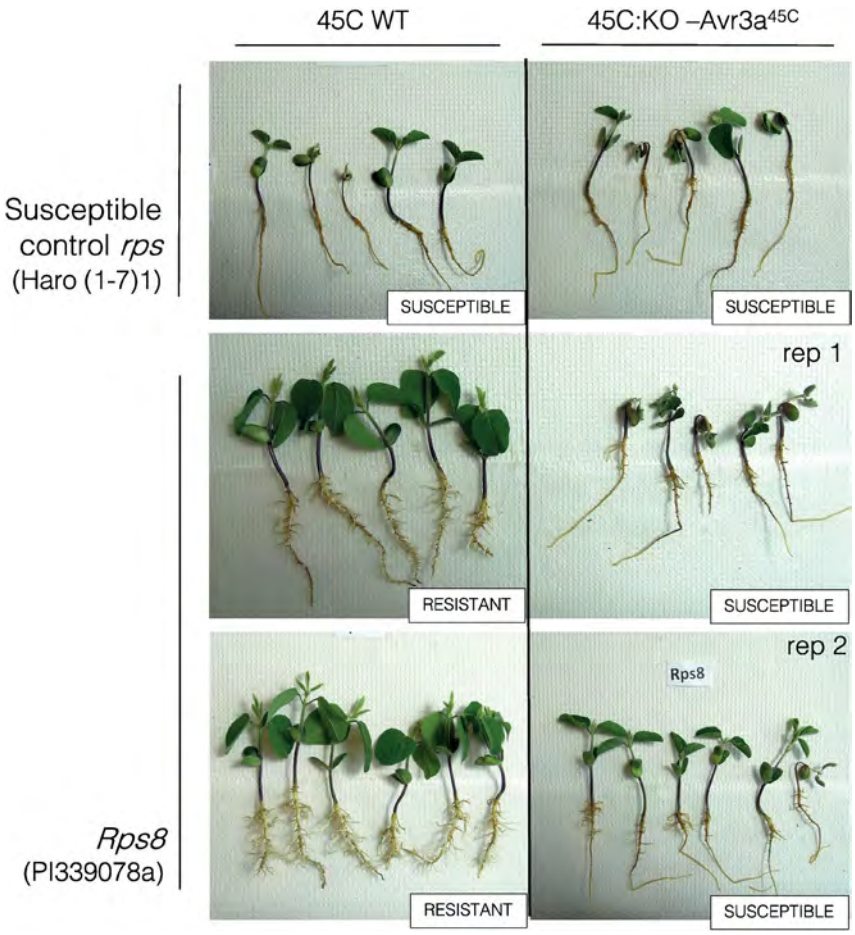

FIGURE 4 Virulence phenotypes of *Phytophthora sojae* wild-type (45C) and *Avr3a* knockout (KO) strains

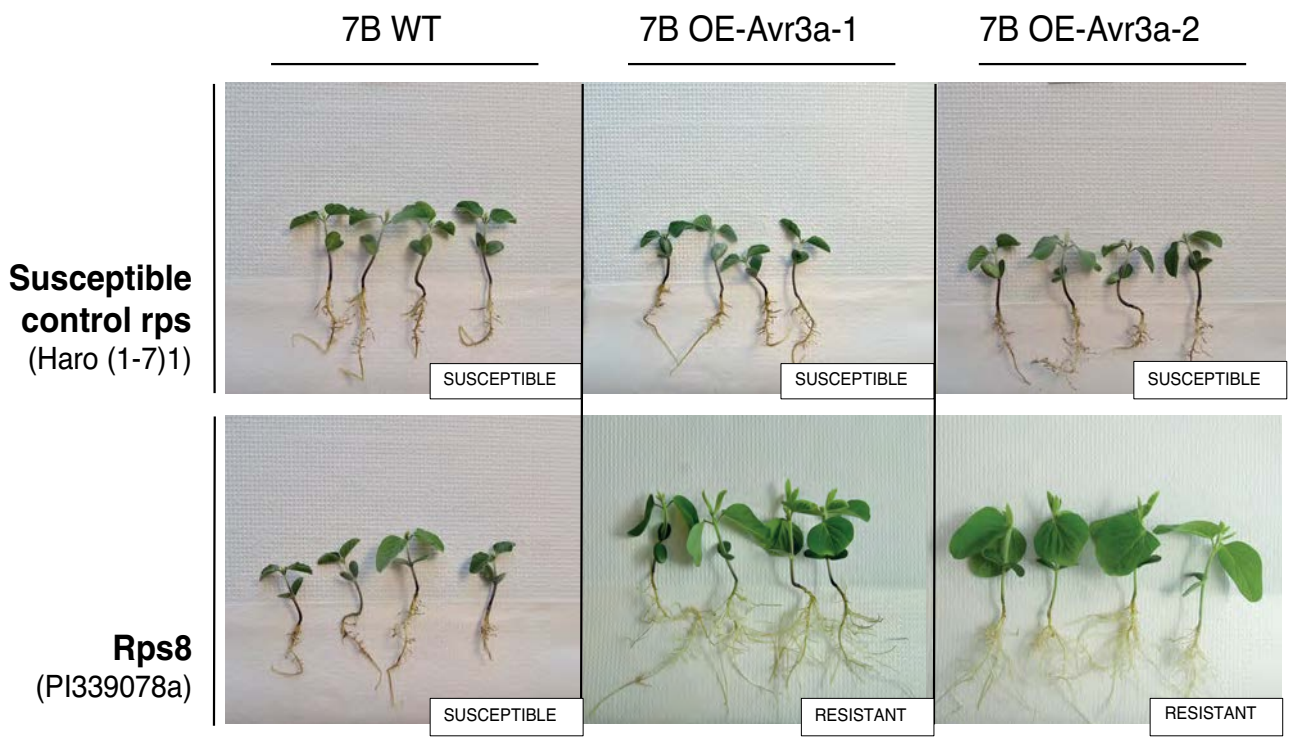

FIGURE 5 Virulence phenotypes of *Phytophthora sojae* wild-type (7B WT) and *Avr3a*^{45C} overexpression (OE) strains

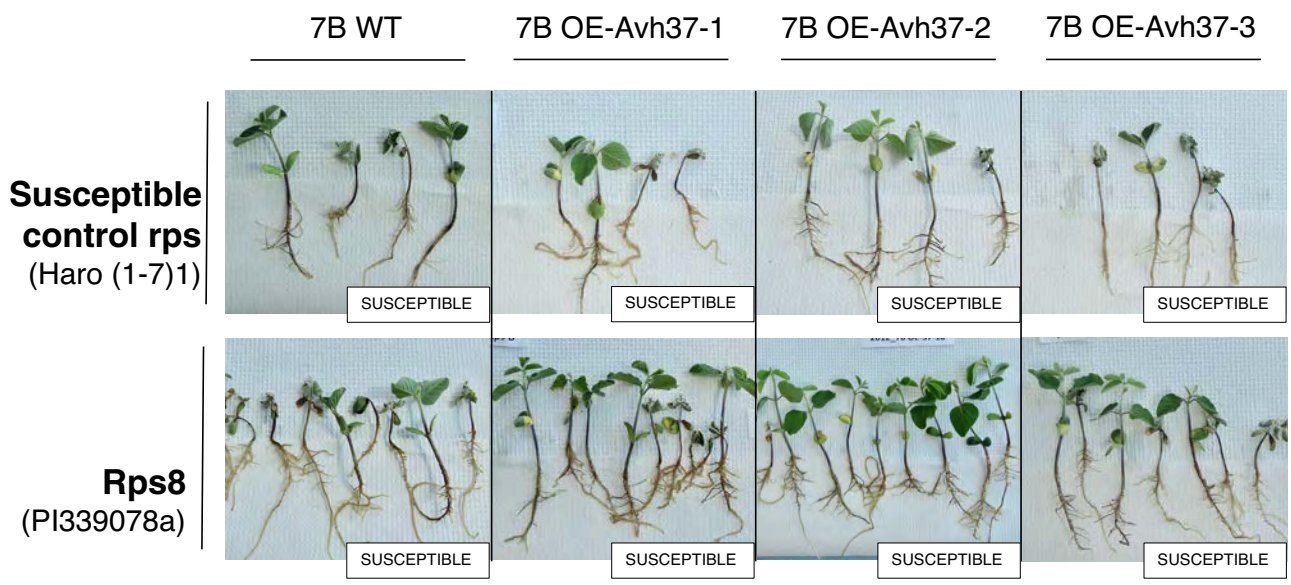

FIGURE 6 Virulence phenotypes of *Phytophthora sojae* wild-type (7B WT) and *Avh37*^{45C} overexpression (OE) strains

sequences were performed, which demonstrated a clear deletion of four copies of the 10.8-kb repetitive unit in both strains (Figure 6).

3 | DISCUSSION

The use of *Rps* genes in elite soybean cultivars has proven to be an effective source of resistance against *P. sojae* in the last decades. However, the capacity of the pathogen to avoid recognition by *Rps* genes through various mutations of its corresponding *Avr* genes has led to the constant need of renewed sources of resistance. In turn, these require an in-depth knowledge of the different mechanisms by which the pathogen succeeds in circumventing this resistance to maintain its virulence. The last two decades have been prolific in terms of the discovery of *P. sojae Avr* genes (Tyler & Gijzen, 2014) and the present study fits in this continuum with the identification of the *Avr3a* gene as encoding the effector interacting with *Rps8* from soybean. The presence of a fifth copy of this gene in a strain avirulent on *Rps8* also led to the definition of a new haplotype for this gene. This was made possible by using novel approaches such as an

improved GBS technique (Sonah et al., 2013), a recently developed and accurate phenotypic assay (Lebreton et al., 2018), the CRISPR/Cas9 system for transformation of *P. sojae* (Fang et al., 2017), and the use of Nanopore long-read sequencing.

The homothallic nature of *P. sojae* offers the advantage of facilitating the generation of F_2 populations to follow the inheritance of virulence phenotypes. Many studies, including this one, have relied on this method for the identification of *P. sojae Avr* genes (Dong et al., 2009; Dong, Yin, et al., 2011; Dong, Yu, et al., 2011; Dou et al., 2010; Na et al., 2013, 2014; Qutob et al., 2009; Shan et al., 2004; Song et al., 2013). Downstream analysis of the F_2 population requires a great set of high-quality genotypic data to capture the precise genetic regions linked to the targeted phenotype. The existence of a repertoire of predicted and annotated RXLR effectors from *P. sojae* prompted the preselection of candidate effectors to accelerate the identification of some *Avr* genes (Dong et al., 2009; Dong, Yin, et al., 2011; Na et al., 2013). However, this strategy carries the risk of omitting potential effectors, as has been the case in initial attempts to identify *Avr1c* (Na et al., 2014). The advent of next-generation sequencing (NGS) has given access to high-throughput sequencing technologies that facilitate the search for *Avr* genes at the whole-genome level. In our work, we further benefited from NGS technology by using an improved GBS method that yields high SNP coverage. This method uses restriction enzymes to reduce genome complexity and leads to extensive marker coverage across the entire genome (Elshire et al., 2011). The SNPs obtained from our sequencing data were indeed located in gene-rich regions as 86% of the SNPs were found in coding regions or within 1000 bp of those regions. Previous studies in a variety of organisms simplified library preparation by pooling DNA samples based on phenotype prior to sequencing, in order to accelerate gene mapping (Abe et al., 2012; Austin et al., 2011; Na et al., 2014; Takagi et al., 2013). Given that the GBS approach enables a high level of multiplexing (Sonah et al., 2013), we were able to generate individual sequencing data for all 83 F_2 isolates and pool genotype data afterwards. This allowed us to select candidate SNPs both on the basis of expected allelic frequencies in each pool and on the precise genotype expected from every F_2 individual according to their phenotype. This brought a new level of precision to identify a locus of interest linked to the phenotype of avirulence on an *Rps* gene. This strategy including GBS sequencing and pooling of F_2 isolates postsequencing led to the definition of the *Avr8* locus, which is a segment of 102.7 kb on PHYSOscaffold_9 where three RXLR effector genes are located among a total of 34 genes.

Once the locus for *Avr8* was defined, WGS data of 31 *P. sojae* isolates with a wide diversity of pathotypes allowed us to generate an exhaustive catalogue of SNPs and structural variations occurring in the region of interest. Because all *P. sojae Avr* genes identified to date are predicted to code for RXLR effector proteins, emphasis was placed on four genes encoding RXLR effectors found at the *Avr8* locus. Incidentally, for two of them, *Avr3a* and *Avh37*, many polymorphisms, including SNPs and structural variations, were present in the coding and promoter regions of the genes, making them prime candidates for *Avr8*.

Regarding the first candidate, *Avr3a*, the allele carried by the virulent parent, $Avr3a^{7B}$, possesses multiple amino acid changes that could impact the recognition of the protein by *Rps8*. Furthermore, no transcripts were detected from isolates carrying this allele. The multiple indels found in the promoter region of the gene, coupled with deletion of copies of the gene in virulent isolates carrying allele $Avr3a^{7B}$, could interfere with transcription, as has been hypothesized in previous work on *Avr3a* (Dong, Yu, et al., 2011; Shrestha et al., 2016). Therefore, the multiple polymorphisms associated with *Avr3a* and the differences in transcript abundance observed between isolates virulent and avirulent on *Rps8* prompted us to consider this gene as a good candidate for *Avr8*.

Regarding the second candidate, the allele associated with the virulent parent, $Avh37^{7B}$, contains an amino acid change that alters the dEER motif. This could possibly impact the translocation of the effector into the host cell, making it unrecognizable by *Rps8*. The frameshift insertion causing the loss of the stop codon leads to a sequence twice as long as the sequence of $Avh37^{45C}$, the allele present in the avirulent parent. Results from the transcript analysis showed that the gene was expressed in all isolates regardless of the phenotype on *Rps8*. For most of the *Avr* genes identified to date, a lower level of expression of the transcript or total loss of transcript are correlated with the phenotype of virulence. On the other hand, amino acid changes can also be sufficient to confer a gain of virulence (Dong et al., 2009; Dong, Yu, et al., 2011; Dou et al., 2010). For this reason and considering the possibility that the mutation in the dEER motif prevents recognition by *Rps8*, *Avh37* was further investigated to test its interaction with *Rps8*.

To determine the functionality of our candidate genes, the CRISPR/Cas9-mediated genome editing method was first prioritized. Knockout of *Avr3a* in transformed isolate 45C:KO-$Avr3a^{45C}$ demonstrated an evident gain of virulence in the presence of *Rps8*. Because the isolate 45C used for the knockout of *Avr3a* still expresses $Avh37^{45C}$, we concluded that *Rps8* plants interacted with only one gene product, *Avr3a*. Results of the overexpression of $Avr3a^{45C}$ in a *P. sojae* isolate virulent on *Rps8* and not expressing this gene also support the interaction between *Avr3a* and *Rps8* as the transformed isolates triggered resistance on plants carrying *Rps8*. Owing to our inability to obtain an $Avh37^{45C}$ knockout transformant via CRISPR/Cas9, we relied on overexpression of $Avh37^{45C}$ in a *P. sojae* isolate virulent on *Rps8* that does not normally express this gene to test the possible interaction with *Rps8*. The three transformed isolates expressing $Avh37^{45C}$ were as virulent on plants carrying *Rps8* as the WT isolate, supporting that *Avh37* does not induce resistance in plants carrying *Rps8*. These results confirmed that *Avr3a* alone yielded an incompatible interaction with *Rps8*.

The *Avr3a* gene encodes a well-studied avirulence factor that has been extensively characterized in the past (Dong, Yu, et al., 2011; Qutob et al., 2009, 2013; Shrestha et al., 2016). In an attempt to get the highest resolution of the *Avr3a* region organization in our *P. sojae* population, we used Nanopore long-read sequencing. The *Avr3a* region is indeed characterized by repetitive elements occurring in tandem arrays of clustered genes, making sequence assembly

problematic, especially with short reads. Previous studies reported that the copy number of *Avr3a* varied from one to four, depending on the *P. sojae* isolate (Arsenault-Labrecque et al., 2018; Qutob et al., 2009). Our long-read sequencing data demonstrate that *P. sojae* can carry up to five copies of the *Avr3a* gene, as is the case in the parental isolate 45C Figure 7. Contigs obtained with reads of F_2 isolates 8-3-6 (avirulent on *Rps8*) also support that these five copies are inherited by the F_2 progeny. The fifth copy of the *Avr3a* gene defines a new haplotype for this *Avr* gene and emphasizes the role of this effector in pathogenicity, prior to its recognition by different resistance genes.

In our study, parental isolates used to identify *Avr8* were as virulent against *Rps8* as they were against *Rps3a*. Furthermore, 34 of the 35 isolates phenotyped in this study gave a similar response when tested against *Rps8* and *Rps3a* (see Table S2). Isolates with a phenotype of avirulence on *Rps3a*/*Rps8* possessed allele *Avr3a*^{45C} while isolates virulent on *Rps3a* and *Rps8* possessed allele *Avr3a*^{7B}. From previous studies (Dong, Yu, et al., 2011; Qutob et al., 2009), these alleles correspond, respectively, to allele *Avr3a*^{P6497}, the allele recognized by *Rps3a* when expressed, and *Avr3a*^{P7064}, which is not expressed and associated to a phenotype of virulence on *Rps3a*. Only one isolate in our collection, ACR20, presented a differential reaction towards *Rps3a* and *Rps8*. Interestingly, that isolate carries a third allele of *Avr3a*, previously described as *Avr3a*^{ACR12} (Table S2). This allele is expressed during infection but differs by two amino acids from *Avr3a*^{45C} (K64P and A65S), a change that could possibly explain the differential responses of *Rps3a* and *Rps8* towards its gene product (Figure S4). It would indeed be plausible that *Rps3a* is able to recognize *Avr3a*^{ACR12} while *Rps8* is not, as represented in Figure 8. The *Rps8* resistance gene was previously located on chromosome 13, as was *Rps3a*, and an allelism study suggested that *Rps8* and *Rps3a* are linked within this chromosome at ≥11.0 cM apart (Gordon et al., 2006; Gunadi, 2012). It has also been hypothesized that these two genes recognize the same *P. sojae* effectors or are closely related resistance genes because of the similar disease reaction pattern between *Rps3a* and *Rps8* from the 75 *P. sojae* isolates used in a previous study (Gunadi, 2012). The report in the present study of a third allele of *Avr3a* recognized differentially by *Rps3a* and *Rps8* supports that the two genes are clearly distinct and recognize different alleles of the same effector.

The fact that *Rps8* is able to recognize the product of the same *Avr* gene as *Rps3a* might explain in part the mitigated efficiency of *Rps8* towards *P. sojae* populations observed in the United States, even before its commercial deployment. In a survey from 2006, seven different pathotypes were observed among the *P. sojae* populations in Missouri and almost all isolates designated as races (pathotypes) 15, 17, 24, or 26. All four were highly virulent on soybeans carrying *Rps8* (Smith et al., 2006). Incidentally, these four isolates were distinct from the others by being also virulent on *Rps3a*. In a recent survey assessing the pathotype diversity of 873 *P. sojae* isolates from 11 states in the United States, *Rps8* presented higher efficiency as only 1.5% of all isolates were virulent on *Rps8* (Dorrance et al., 2016). Again, 85% of these isolates virulent on *Rps8* were also virulent on *Rps3a*. Interestingly, approximately 15% of the isolates from this study were virulent on *Rps3a* but not on *Rps8*, a phenotype that has not been encountered in our study. It would be interesting to retrieve those isolates that originate mostly from Illinois and to confirm their phenotypes and genotypes in order to investigate if an additional allele of *Avr3a* is recognized by *Rps8* but not *Rps3a*.

A previous study also demonstrated that *Avr3a* interacted with *Rps5* and that *Avr3a* and *Avr5* were allelic (Dong, Yu, et al., 2011).

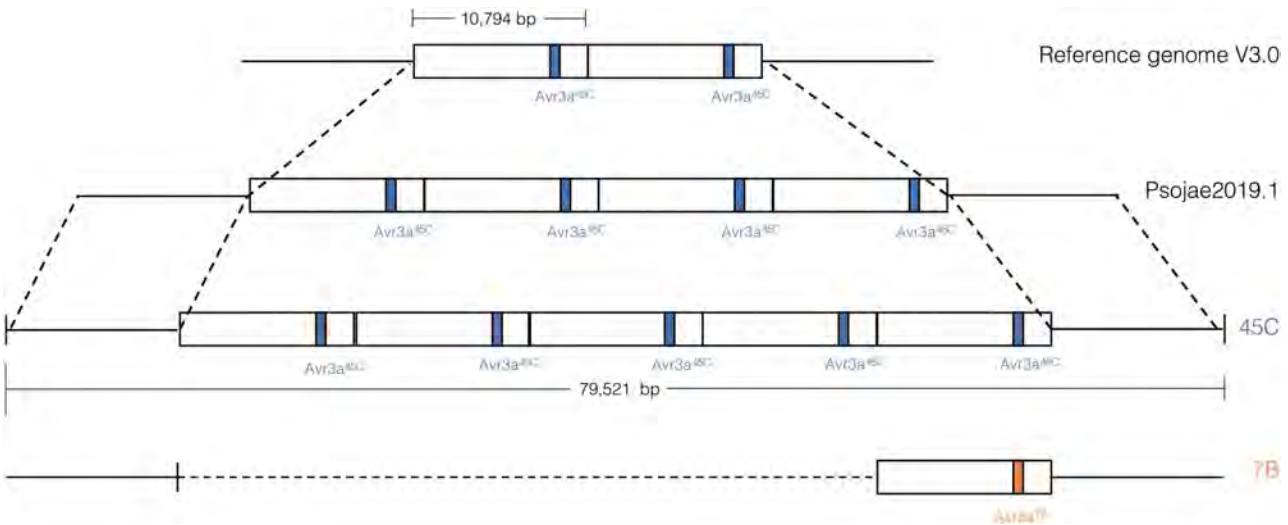

FIGURE 7 Representation of the copy number variation occurring in the *Avr3a* locus among *Phytophthora sojae* isolates. The red boxes represent the *Avr3a* gene. The *Avr3a* gene is embedded in a repetitive unit of 10,794 kb in every sequence. In the reference genome v. 3.0, based on Sanger sequencing of isolate P6497, two copies of the *Avr3a*^{45C} are represented, while four copies are present in the assembly Psojae2019.1 based on the Nanopore sequencing of P6497. Nanopore sequencing of parental isolates revealed a fifth copy of *Avr3a*^{45C} for isolate 45C (avirulent on *Rps8*) while isolate 7B (virulent on *Rps8*) carries only one copy of *Avr3a*^{7B}. The consensus sequence for 45C is based on a single read of 79,521 bp encompassing the whole region carrying the five copies of *Avr3a* and its flanking regions. Those flanking regions are identical among the different sequences represented here

Surprisingly, when comparing the interaction of *Rps8* plants with the three different alleles of *Avr3a*, nothing could distinguish the response from *Rps8* and the responses from *Rps5* in this previous study (Table 4). The *Rps5* phenotype was first described in 1981 and has since been mapped on chromosome 18 and linked with *Rps4* and *Rps6* (Buzzell & Anderson, 1981; Sun et al., 2014). In another study that aimed to identify simple-sequence repeat (SSR) markers linked to *Rps1* to *Rps6*, linkages were found for all but *Rps5*, due to a skewed genotypic segregation in the *Rps5/rps5* population (Demirbas et al., 2001). This complicates the understanding of the association among the *Rps3a*, *Rps5*, and *Rps8* genes. As opposed to *Rps3a*, *Rps5* does not seem to be genetically linked to *Rps8* despite its similar response to *Avr3a*. To distinguish the interaction of *Avr3a* with *Rps5* and *Rps8*, one would require *P. sojae* isolates that present distinctive phenotypes against each of the genes and investigate the genotypic differences between the isolates. That said, such distinct isolates are currently undefined to our knowledge.

The present study is the first to exploit the CRISPR/Cas9-mediated genome editing method developed for *P. sojae* in order to knock out an *Avr* gene and confirm its interaction with an *Rps* gene (Fang et al., 2017). Previously, such knockouts were impossible to obtain with *P. sojae* because of the presence of nonhomologous end-joining (Judelson, 1997; Tyler & Gijzen, 2014). Knockdown of *P. sojae* genes to identify avirulence factors has been mostly accomplished by gene silencing. However, this knockdown method leads to residual transcription and expression of the targeted gene that can leave intermediate responses from the plant (Fang & Tyler, 2016). By taking advantage of methods derived from NGS and CRISPR/Cas9-mediated genome editing, this study identified *Avr3a* as the *Avr* gene recognized by *Rps8*, a resistance gene providing a new source of resistance for elite soybean cultivars (Abeysekara et al., 2016). In addition, overexpression of *Avr3a* in *P. sojae* transformants supported the fact that *Avr3a* led to an avirulent response when interacting with *Rps8*. Furthermore, long-read sequencing brought a new insight for the *Avr3a* gene, with the discovery of a fifth copy of the gene in isolates avirulent on *Rps3a* and *Rps8*. A precise definition of the different haplotypes associated with the virulence of *P. sojae* towards *Rps8* will therefore make it possible to better manage the disease, especially in the context of the recent development of molecular tools (Dussault-Benoit et al., 2020) that allow a tailored use of *Rps* genes based on a precise and rapid determination of pathotypes in soybean fields.

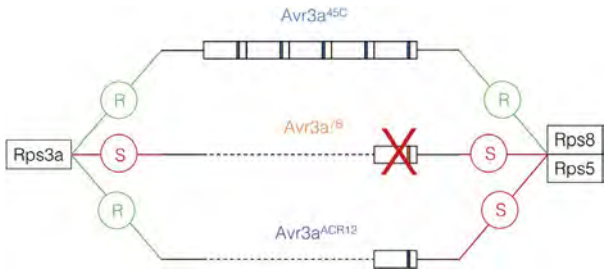

FIGURE 8 Schematic representation of the interaction of the different *Avr3a* alleles of *Phytophthora sojae* with soybean plants carrying *Rps3a* and *Rps8*. The letter in the circle represents the response from the plants carrying the corresponding *Rps* gene. R, resistant; S, susceptible. *P. sojae* isolates carrying the $Avr3a^{45C}$ allele possess multiple identical copies of the *Avr3a* gene while isolates carrying allele $Avr3a^{7B}$ or $Avr3a^{ACR12}$ carry only one copy. No transcripts of the *Avr3a* gene are expressed for isolates carrying $Avr3a^{7B}$

4 | EXPERIMENTAL PROCEDURES

4.1 | *P. sojae* isolates and plant materials

Detailed information about the 35 *P. sojae* isolates used in this study is listed in Table S2. Isolates were grown and maintained on V8 gellan gum medium at 28°C. For long-term storage, pieces of mycelium grown on V8 agar for 2 weeks were transferred in 3 ml sterile deionized water in plastic sterile tubes. Tubes were kept at room temperature in the dark. Each isolate was characterized for the presence of *Avr* genes using a hydroponic assay in which zoospores are inoculated directly into the hydroponic nutrient solution (Lebreton et al., 2018). For each isolate, four plants from accessions Williams L83-570 (*Rps3a*) and PI399073a (*Rps8*) and a susceptible control cultivar not carrying the appropriate *Rps* gene were tested. Phenotypic responses for resistance or susceptibility were recorded at 10 days postinoculation (dpi) and based on comparative responses of control resistant and susceptible cultivars.

TABLE 4 Virulence characteristics of *Phytophthora sojae* isolates on *Rps3a*, *Rps5*, and *Rps8* and haplotype analysis

Isolate	Virulence *Rps3a*[a]	Virulence *Rps5*[b]	Virulence *Rps8*[a]	*Avr3a* allele	mRNA *Avr3a*[c]
P6497	A	A	A	45C/P6497	+
P7064	V	V	V	7B/P7064	–
P7074	V	V	V	7B/P7064	–
ACR20	A	V	V	ACR12	+

[a] Virulence phenotypes observed in this study and in Dong, Yu, et al. (2011).

[b] Virulence phenotypes obtained in Dong, Yu, et al. (2011).

[c] Positive (+) or negative (–) for expression of *Avr3a* transcripts, as determined by reverse transcription PCR (Dong, Yu, et al., 2011).

4.2 | Crossing of *P. sojae* isolates

To follow the inheritance of virulence towards *Rps8*, two *P. sojae* isolates from our collection, 45C (avirulent on *Rps8*) and 7B (virulent on *Rps8*), were crossed to obtain F_1 and F_2 progenies. Pieces of mycelium from long-term storage were transferred on 20% V8 gellan gum (0.4%). The Petri dishes were placed in an incubator at 28°C. After 1 week of growth, mycelia from the two isolates were mixed together with a syringe and transferred on Petri plates containing crossing medium (2.5% clarified V8, 1.2% gellan gum supplemented with 10 μg/ml β-sitosterol). The plates were left in the dark at room temperature. After 3 weeks, two plates were sliced using a sterile blade and blended together in a prechilled blender for 2 min with 50 ml of fridge-cold sterile water. The mix was filtrated through four layers of sterile cheesecloth to remove agar and mycelium and the filtrate was transferred to a 50-ml sterile conical tube. The mixture was kept on ice for 24 h to kill the residual mycelium. The filtrate was then centrifuged at $956 \times g$ for 3 min and the supernatant was removed. The pellet of oospores was washed three times with sterile water and centrifugation cycles. Oospores were transferred on water agar supplemented with penicillin at a concentration of 500 oospores per Petri dish and spread with a sterile loop. After three or four days, each germinating oospore was transferred individually using a 20-gauge needle and grown on 20% V8 agar medium for subsequent DNA extraction.

4.3 | F_1 hybrid selection and F_2 generation

DNA of each culture grown from pure isolated oospores was extracted using an adapted cetyltrimethylammonium bromide (CTAB) and chloroform/isoamyl alcohol extraction method followed by isopropanol precipitation. To determine F_1 hybrid progeny from crosses of 45C × 7B, codominant DNA markers polymorphic between the parents were used to determine whether the individuals resulted from self-fertilization or from outcrossing events between the parental isolates (F_1). The polymorphism used to distinguish alleles from both parents was a deletion; isolate 7B has a deletion of 35 bp in the amplicon region while isolate 45C does not. Selected F_1 hybrid isolates were then cultured individually on crossing medium in the dark at room temperature for self-fertilization and generation of F_2 individuals. Oospores produced from F_1 individuals were isolated using the method described above and grown on 20% (vol/vol) V8 agar medium. All F_1 and F_2 individuals were phenotyped for their compatibility interaction with *Rps8* using the hydroponic assay developed by Lebreton et al. (2018) and cultivars PI399073a (*Rps8*) and susceptible control Haro (1-7)1 (*rps*).

4.4 | Segregant analysis of F_2 populations

To find a region that co-segregated with the phenotype of avirulence on *Rps8* and to identify potential candidate genes for *Avr8*, the F_2 progenies were genotyped using a GBS approach. DNA from F_2 individuals was extracted using the CTAB and chloroform/isoamyl alcohol method followed by isopropanol precipitation. DNA was quantified using a Qubit 4 fluorometer (Thermo Fisher Scientific) and concentrations were normalized to 10 ng/μl for library preparation. Sequencing libraries were prepared using the *Ape*K1 restriction enzyme following the protocol from Elshire et al. (2011), with minor modifications as described by Sonah et al. (2013). Single-end sequencing of multiplex GBS libraries was performed on an Ion Proton sequencer (Thermo Fisher Scientific) at the Institut de Biologie Intégrative et des Systèmes (IBIS) of Université Laval, Quebec, Canada. Read processing, mapping to the *P. sojae* reference genome v. 3.0 (Tyler et al., 2006), variant calling, and genotyping were performed using the Fast-GBS pipeline (Torkamaneh et al., 2017), using default parameters except for the depth of coverage (minimum of 10 supporting reads before a variant candidate was considered, instead of two). Variants were filtered using VCFtools (Danecek et al., 2011) with the following parameters: biallelic SNPs conserved only, maximum missing data (MaxMD) = 80%, and minimum minor allele frequency (MinMAF) = 0.2. Missing data were imputed using Beagle (Browning & Browning, 2016).

Polymorphisms detected were used to identify loci where segregation followed the phenotype of avirulence on *Rps8*. From the variants obtained after filtering and imputation, only the variants for which the parental alleles were mutually polymorphic and homozygous were kept and based on the parental genotypes, alleles were coded as originating from a specific parent. Variant data for each F_2 individual were pooled together based on the phenotype of virulence or avirulence on *Rps8*. Allelic frequencies based on the genotype called were estimated for the entire population and for each pool using VCFtools (Danecek et al., 2011). For each SNP in each pool, χ^2 tests were performed to assess segregation distortion for the entire population and segregation bias was declared to be significant at $p < 0.05$. It was expected to find heterozygous genotypes in both pools while homozygous genotypes for each individual had to be associated to the allele from the parent carrying the same phenotype towards *Rps8*. Following subsequent oospore formation from F_2 individuals during inoculum preparation, some heterozygous genotypes were found to acquire a stable phenotype in either the virulent or avirulent group. This was reflected in some specific individuals because this study performed individual analysis of each F_2 progeny rather than pooled analysis as done in previous studies (MacGregor et al., 2002; Na et al., 2014; Qutob et al., 2009).

4.5 | Selection of candidate genes from WGS data

To find potential candidate genes in the region of *Avr8*, a collection of 31 isolates previously sequenced on an Illumina Hi-Seq (68×; Arsenault-Labrecque et al., 2018) and from which the parents were selected was used to generate polymorphisms in the region of *Avr8*. Reads from this sequencing were aligned to *P. sojae* genome reference v. 3.0 using the Burrows–Wheeler transform alignment

software package v. 0.7.13 (Li, 2013). Calling of SNPs and small indels was done using the Genome Analysis Toolkit, a variant-calling pipeline based on its own best practices (DePristo et al., 2011). Larger indels and structural variations were generated using two different callers, Lumpy (Layer et al., 2014) and Manta (Chen et al., 2016). Finally, the copy number variation was detected with CNVnator (Abyzov et al., 2011). Because we expected that the causal variants leading to a phenotype of virulence toward *Rps8* would come from the virulent parent (7B) solely and we know that the isolate used to produce the reference genome (P6497) is avirulent on *Rps8*, we only kept variants from which the virulent parent isolate 7B (*avr8*) carried the alternative allele and the parent isolate 45C (*Avr8*) carried the reference allele.

4.6 | RNA isolation and RT-PCR

RNA isolation was performed on 7-day-old *P. sojae*-infected soybean roots using TRIzol reagent followed by purification using the RNeasy Mini kit (Qiagen). RNA samples were treated with DNase I enzyme to avoid DNA contamination and 2 μg of each sample was used for the conversion to single-stranded cDNA using random primers and the multiscribe reverse transcriptase from the High-Capacity cDNA Reverse Transcription Kit (ThermoFisher Scientific). Primers for the reverse transcription PCR were designed using the PrimerQuest tool.

4.7 | Plasmid construction

To generate *Avr3a*^{45C} knockouts using CRISPR/Cas9, single-guide RNAs (sgRNAs) were designed using EuPaGDT (Peng & Tarleton, 2015). The resulting sgRNAs were searched against the *P. sojae* genome using BLAST (Altschul et al., 1990) to check for potential off-target sites. Based on sequence alignment, sgRNA1 and sgRNA2 were selected, targeting the *Avr3a*^{45C} coding sequence at 90 and 139 nucleotides, respectively, from the start codon. The double-stranded DNA fragment containing the left overlapping region, sgRNA1 or sgRNA2, coding sequences for HH ribozyme, and the right overlapping region was synthesized as a gBLOCK (Integrated DNA Technologies Inc.). The gBlock was assembled in *Nhe*I- and *Bsa*I-digested plasmid pYF515 (Fang et al., 2017) using HiFi assembly (New England Biolabs). All Cas9-sgRNA expression plasmids were sequence-verified and named pRBCas9-Avr3a-1 and pRBCas9-Avr3a-2.

For constitutive expression of *Avr3a*^{45C} and *Avh37*^{45C}, the coding sequences were cloned separately into the vector pUC-57. The *Avr3a*^{45C} and *Avh37*^{45C} coding sequences were amplified from *P. sojae* isolate 45C and the Ham34 promoter was amplified from the plasmid pYF515 using specific primers. The Ham34 promoter and the coding sequences of the two candidate genes (*Avr3a*^{45C} and *Avh37*^{45C}) were assembled in pRB-*Avr6* digested with *Kpn*I and *Avr*II using HiFi NEB assembly (New England Biolabs). Plasmids were sequence-verified and named pRB-OE-*Avr3a* and pRB-OE-*Avh37*.

4.8 | Transformation of *P. sojae*

Knockout and constitutive expression vectors were introduced in *P. sojae* avirulent isolate 45C and virulent isolate 7B, respectively, using polyethylene glycol-mediated transformation following a previously published protocol (Fang et al., 2017). Briefly, mycelium was grown in nutrient pea broth at 28°C in the dark. After 5–7 days, mycelium was harvested and digested using the enzyme mix to release protoplasts. Polyethylene glycol-mediated protoplast transformation was used to introduce knockout vectors (pRBCas9-*Avr3a*-1 and pRBCas9-*Avr3a*-2) and constitutive expression vectors (pRB-OE-*Avr3a* and pRB-OE-*Avh37*). Transformants growing on regenerative medium containing 50 μg of G418 (Thermo Fisher Scientific) were selected and subcultured on V8 gellan gum medium supplemented with G418. To detect the presence of indels in *Avr3a*, genomic DNA was isolated from the stable transformants and the entire open reading frame of *Avr3a* was amplified and sequenced. For the constitutive expression of the *Avr3a*^{45C} gene, primers M13R and M13F were used to amplify the expression cassette (promoter-gene-terminator) from the transformants' genomic DNA.

4.9 | Phenotyping of *P. sojae* transformants

The virulence profile (phenotype) of selected *P. sojae* transformants towards *Rps8* was evaluated with the hydroponic system described previously (Lebreton et al., 2018) using cultivars PI399073a (*Rps8*) and Williams L83-570 (*Rps3a*) and the susceptible control Haro (1-7)1 (*rps*). The virulence phenotype towards *Rps3a* was also evaluated using Williams L83-570 (*Rps3a*) and the susceptible control Williams (*rps rps*). Plants were scored based on a 1 to 5 scale developed by Lebreton et al. (2018), where 1 = none to limited root symptoms and 5 = mortality and advanced root necrosis. A statistical comparison (Dunnett's test) was performed to determine the phenotype of each of the isolates. When values were statistically similar to the ones obtained with cv. Haro(1-7)1 (*rps*), the isolate was considered virulent, and when values were statistically lower, the isolate was considered avirulent.

4.10 | Nanopore sequencing and data analysis

High-molecular weight DNA was extracted from *P. sojae* isolates grown in liquid culture for 7 days with an adapted CTAB and chloroform/isoamyl alcohol method that uses a lower incubation temperature and reduced centrifugation speed to avoid DNA shearing. DNA purity was assessed with a NanoDrop spectrophotometer and quantification was performed with a Qubit 4 fluorometer. DNA libraries were prepared according to the protocol of Oxford Nanopore Technologies using the adaptor ligation kit (SQK-LSK109). Sequencing was performed on a SpotON R9.4 flow cell using a MinION device. Sequences were base-called with Guppy v. 3.2.4. Adapters were trimmed with Porechop (https://github.com/rrwick/

Porechop) and reads were filtered for quality (Q > 7) with NanoFilt (De Coster et al., 2018). Nanopore metrics can be found in Table S3. Subsequent bioinformatic analyses comprising mapping, de novo assembly, and alignments were accomplished using the CLC Genomics Workbench v. 20 (Qiagen).

ACKNOWLEDGEMENTS

We would like to thank the following partners for their financial support to R.R.B.: Genome Canada, Génome Québec, and the Canada Research Chairs Program. We would also like to thank Professor Luciano Gomes Fietto for the technical help with *P. sojae* transformation.

DATA AVAILABILITY STATEMENT

The data that support the findings of this study are available in the supplementary material of this article.

ORCID

Richard R. Bélanger https://orcid.org/0000-0001-8549-975X

REFERENCES

Abe, A., Kosugi, S., Yoshida, K., Natsume, S., Takagi, H., Kanzaki, H. et al. (2012) Genome sequencing reveals agronomically important loci in rice using MutMap. *Nature Biotechnology*, 30, 174.

Abeysekara, N.S., Matthiesen, R.L., Cianzio, S.R., Bhattacharyya, M.K. & Robertson, A.E. (2016) Novel sources of partial resistance against *Phytophthora sojae* in soybean PI 399036. *Crop Science*, 56, 2322–2335.

Abyzov, A., Urban, A.E., Snyder, M. & Gerstein, M. (2011) CNVnator: an approach to discover, genotype, and characterize typical and atypical CNVs from family and population genome sequencing. *Genome Research*, 21, 974–984.

Altschul, S.F., Gish, W., Miller, W., Myers, E.W. & Lipman, D.J. (1990) Basic local alignment search tool. *Journal of Molecular Biology*, 215, 403–410.

Arsenault-Labrecque, G., Sonah, H., Lebreton, A., Labbé, C., Marchand, G., Xue, A. et al. (2018) Stable predictive markers for *Phytophthora sojae* avirulence genes that impair infection of soybean uncovered by whole genome sequencing of 31 isolates. *BMC Biology*, 16, 80.

Austin, R.S., Vidaurre, D., Stamatiou, G., Breit, R., Provart, N.J., Bonetta, D. et al. (2011) Next-generation mapping of Arabidopsis genes. *The Plant Journal*, 67, 715–725.

Bandara, A.Y., Weerasooriya, D.K., Bradley, C.A., Allen, T.W. & Esker, P.D. (2020) Dissecting the economic impact of soybean diseases in the United States over two decades. *PLoS One*, 15, e0231141.

Białas, A., Zess, E.K., De la Concepcion, J.C., Franceschetti, M., Pennington, H.G., Yoshida, K. et al. (2018) Lessons in effector and NLR biology of plant–microbe systems. *Molecular Plant-Microbe Interactions*, 31, 34–45.

Browning, B.L. & Browning, S.R. (2016) Genotype imputation with millions of reference samples. *The American Journal of Human Genetics*, 98, 116–126.

Burnham, K., Dorrance, A., Francis, D., Fioritto, R. & St. Martin, S. (2003) *Rps8*, a new locus in soybean for resistance to *Phytophthora sojae*. *Crop Science*, 43, 101–105.

Buzzell, R. & Anderson, T. (1981) Research notes: another major gene for resistance to *Phytophthora megasperma* var. *sojae* in soybeans. *Soybean Genetics Newsletter*, 8, 10.

Chen, X., Schulz-Trieglaff, O., Shaw, R., Barnes, B., Schlesinger, F., Källberg, M. et al. (2016) Manta: rapid detection of structural variants and indels for germline and cancer sequencing applications. *Bioinformatics*, 32, 1220–1222.

Costamilan, L.M., Clebsch, C.C., Soares, R.M., Seixas, C.D.S., Godoy, C.V. & Dorrance, A.E. (2012) Pathogenic diversity of *Phytophthora sojae* pathotypes from Brazil. *European Journal of Plant Pathology*, 135, 845–853.

Danecek, P., Auton, A., Abecasis, G., Albers, C.A., Banks, E., DePristo, M.A. et al. (2011) The variant call format and VCFtools. *Bioinformatics*, 27, 2156–2158.

De Coster, W., D'Hert, S., Schultz, D.T., Cruts, M. & Van Broeckhoven, C. (2018) NanoPack: visualizing and processing long-read sequencing data. *Bioinformatics*, 34, 2666–2669.

Demirbas, A., Rector, B.G., Lohnes, D.G., Fioritto, R.J., Graef, G.L., Cregan, P.B. et al. (2001) Simple sequence repeat markers linked to the soybean *Rps* genes for *Phytophthora* resistance. *Crop Science*, 41, 1220–1227.

DePristo, M.A., Banks, E., Poplin, R., Garimella, K.V., Maguire, J.R., Hartl, C. et al. (2011) A framework for variation discovery and genotyping using next-generation DNA sequencing data. *Nature Genetics*, 43, 491–498.

Dodds, P.N. & Rathjen, J.P. (2010) Plant immunity: towards an integrated view of plant–pathogen interactions. *Nature Reviews Genetics*, 11, 539–548.

Dong, S., Qutob, D., Tedman-Jones, J., Kuflu, K., Wang, Y., Tyler, B.M. et al. (2009) The *Phytophthora sojae* avirulence locus *Avr3c* encodes a multi-copy RXLR effector with sequence polymorphisms among pathogen strains. *PLoS One*, 4, e5556.

Dong, S., Yin, W., Kong, G., Yang, X., Qutob, D., Chen, Q. et al. (2011) *Phytophthora sojae* avirulence effector Avr3b is a secreted NADH and ADP-ribose pyrophosphorylase that modulates plant immunity. *PLoS Pathogens*, 7, e1002353.

Dong, S., Yu, D., Cui, L., Qutob, D., Tedman-Jones, J., Kale, S.D. et al. (2011) Sequence variants of the *Phytophthora sojae* RXLR effector Avr3a/5 are differentially recognized by *Rps*3a and *Rps*5 in soybean. *PLoS One*, 6, e20172.

Dorrance, A.E. (2018) Management of *Phytophthora sojae* of soybean: a review and future perspectives. *Canadian Journal of Plant Pathology*, 40, 210–219.

Dorrance, A.E., Kurle, J., Robertson, A.E., Bradley, C.A., Giesler, L., Wise, K. et al. (2016) Pathotype diversity of *Phytophthora sojae* in eleven states in the United States. *Plant Disease*, 100, 1429–1437.

Dorrance, A.E., McClure, S.A. & deSilva, A. (2003) Pathogenic diversity of *Phytophthora sojae* in Ohio soybean fields. *Plant Disease*, 87, 139–146.

Dou, D., Kale, S.D., Liu, T., Tang, Q., Wang, X., Arredondo, F.D. et al. (2010) Different domains of *Phytophthora sojae* effector Avr4/6 are recognized by soybean resistance genes *Rps4* and *Rps6*. *Molecular Plant-Microbe Interactions*, 23, 425–435.

Dussault-Benoit, C., Arsenault-Labrecque, G., Sonah, H., Belzile, F. & Bélanger, R.R. (2020) Discriminant haplotypes of avirulence genes of *Phytophthora sojae* lead to a molecular assay to predict phenotypes. *Molecular Plant Pathology*, 21, 318–329.

Elshire, R.J., Glaubitz, J.C., Sun, Q.I., Poland, J.A., Kawamoto, K., Buckler, E.S. et al. (2011) A robust, simple genotyping-by-sequencing (GBS) approach for high diversity species. *PLoS One*, 6, e19379.

Fang, Y., Cui, L., Gu, B., Arredondo, F. & Tyler, B.M. (2017) Efficient genome editing in the oomycete *Phytophthora sojae* using CRISPR/Cas9. *Current Protocols in Microbiology*, 44, 21A.1.1–21A.1.26.

Fang, Y. & Tyler, B.M. (2016) Efficient disruption and replacement of an effector gene in the oomycete *Phytophthora sojae* using CRISPR/Cas9. *Molecular Plant Pathology*, 17, 127–139.

Flor, H.H. (1971) Current status of the gene-for-gene concept. *Annual Review of Phytopathology*, 9, 275–296.

Gordon, S.G., St. Martin, S.K. & Dorrance, A.E. (2006) *Rps8* maps to a resistance gene rich region on soybean molecular linkage group F. *Crop Science*, 46, 168–173.

Grau, C.R., Dorrance, A.E., Bond, J. & Russin, J.S. (2004) Fungal diseases. In: Shibles, R.M., Harper, J.E., Wilson, R.F. & Shoemaker, R.C. (Eds.) *Soybeans: improvement, production, and uses, Vol. 16*. Madison: American Society of Agronomy, pp. 679–763.

Gunadi, A. (2012) *Characterization of Rps8 and Rps3 resistance genes to Phytophthora sojae through genetic fine mapping and physical mapping of soybean chromosome 13*. PhD thesis, Ohio State University.

Judelson, H.S. (1997) The genetics and biology of *Phytophthora infestans*: modern approaches to a historical challenge. *Fungal Genetics and Biology*, 22, 65–76.

Layer, R.M., Chiang, C., Quinlan, A.R. & Hall, I.M. (2014) LUMPY: a probabilistic framework for structural variant discovery. *Genome Biology*, 15, R84.

Lebreton, A., Labbe, M.C., de Ronne, M.M., Xue, D.A., Marchand, M.G. & Bélanger, D.R.R. (2018) Development of a simple hydroponic assay to study vertical and horizontal resistance of soybean and pathotypes of *Phytophthora sojae*. *Plant Disease*, 102, 114–123.

Li, H. (2013) Aligning sequence reads, clone sequences and assembly contigs with BWA-MEM. *arXiv* 1303.3997 [q-bio.gn] [preprint].

MacGregor, T., Bhattacharyya, M., Tyler, B., Bhat, R., Schmitthenner, A.F. & Gijzen, M. (2002) Genetic and physical mapping of *Avr1a* in *Phytophthora sojae*. *Genetics*, 160, 949–959.

Na, R., Yu, D., Chapman, B.P., Zhang, Y., Kuflu, K., Austin, R. et al. (2014) Genome re-sequencing and functional analysis places the *Phytophthora sojae* avirulence genes *Avr1c* and *Avr1a* in a tandem repeat at a single locus. *PLoS One*, 9, e89738.

Na, R., Yu, D., Qutob, D., Zhao, J. & Gijzen, M. (2013) Deletion of the *Phytophthora sojae* avirulence gene *Avr1d* causes gain of virulence on *Rps1d*. *Molecular Plant-Microbe Interactions*, 26, 969–976.

Peng, D. & Tarleton, R. (2015) EuPaGDT: a web tool tailored to design CRISPR guide RNAs for eukaryotic pathogens. *Microbial Genomics*, 1, e000033.

Qutob, D., Chapman, B.P. & Gijzen, M. (2013) Transgenerational gene silencing causes gain of virulence in a plant pathogen. *Nature Communications*, 4, 1349.

Qutob, D., Tedman-Jones, J., Dong, S., Kuflu, K., Pham, H., Wang, Y. et al. (2009) Copy number variation and transcriptional polymorphisms of *Phytophthora sojae* RXLR effector genes *Avr1a* and *Avr3a*. *PLoS One*, 4, e5066.

de Ronne, M., Labbé, C., Lebreton, A., Sonah, H., Deshmukh, R., Jean, M. et al. (2020) Integrated QTL mapping, gene expression and nucleotide variation analyses to investigate complex quantitative traits: a case study with the soybean–*Phytophthora sojae* interaction. *Plant Biotechnology Journal*, 18, 1492.

Sandhu, D., Schallock, K., Rivera-Velez, N., Lundeen, P., Cianzio, S. & Bhattacharyya, M. (2005) Soybean *Phytophthora* resistance gene *Rps8* maps closely to the *Rps3* region. *Journal of Heredity*, 96, 536–541.

Schmitthenner, A.F. (1985) Problems and progress in control of Phytophthora root rot of soybean. *Plant Disease*, 69, 362–368.

Shan, W., Cao, M., Leung, D. & Tyler, B.M. (2004) The *Avr1b* locus of *Phytophthora sojae* encodes an elicitor and a regulator required for avirulence on soybean plants carrying resistance gene *Rps1b*. *Molecular Plant-Microbe Interactions*, 17, 394–403.

Shrestha, S.D., Chapman, P., Zhang, Y. & Gijzen, M. (2016) Strain specific factors control effector gene silencing in *Phytophthora sojae*. *PLoS One*, 11, e0150530.

Smith, D., Abney, T. & Shannon, J. (2006) *Virulence in Phytophthora sojae isolates to soybeans with Rps8 resistance*. Jackson, TN: Proc. Southern Disease Workers, p. 3.

Sonah, H., Bastien, M., Iquira, E., Tardivel, A., Légaré, G., Boyle, B. et al. (2013) An improved genotyping by sequencing (GBS) approach offering increased versatility and efficiency of SNP discovery and genotyping. *PLoS One*, 8, e54603.

Song, T., Kale, S.D., Arredondo, F.D., Shen, D., Su, L., Liu, L. et al. (2013) Two RxLR avirulence genes in *Phytophthora sojae* determine soybean *Rps1k*-mediated disease resistance. *Molecular Plant-Microbe Interactions*, 26, 711–720.

Stewart, S., Abeysekara, N. & Robertson, A.E. (2014) Pathotype and genetic shifts in a population of *Phytophthora sojae* under soybean cultivar rotation. *Plant Disease*, 98, 614–624.

Sugimoto, T., Kato, M., Yoshida, S., Matsumoto, I., Kobayashi, T., Kaga, A. et al. (2012) Pathogenic diversity of *Phytophthora sojae* and breeding strategies to develop *Phytophthora*-resistant soybeans. *Breeding Science*, 61, 511–522.

Sun, J., Li, L., Zhao, J., Huang, J., Yan, Q., Xing, H. et al. (2014) Genetic analysis and fine mapping of *RpsJS*, a novel resistance gene to *Phytophthora sojae* in soybean [*Glycine max* (L.) Merr.]. *Theoretical and Applied Genetics*, 127, 913–919.

Takagi, H., Uemura, A., Yaegashi, H., Tamiru, M., Abe, A., Mitsuoka, C. et al. (2013) MutMap-Gap: whole-genome resequencing of mutant F2 progeny bulk combined with de novo assembly of gap regions identifies the rice blast resistance gene *Pii*. *New Phytologist*, 200, 276–283.

Torkamaneh, D., Laroche, J., Bastien, M., Abed, A. & Belzile, F. (2017) Fast-GBS: a new pipeline for the efficient and highly accurate calling of SNPs from genotyping-by-sequencing data. *BMC Bioinformatics*, 18, 5.

Tyler, B.M. (2007) *Phytophthora sojae*: root rot pathogen of soybean and model oomycete. *Molecular Plant Pathology*, 8, 1–8.

Tyler, B.M. & Gijzen, M. (2014) The *Phytophthora sojae* genome sequence: foundation for a revolution. In: Dean, R., Lichens-Park, A. & Kole, C. (Eds.) *Genomics of plant-associated fungi and oomycetes: dicot pathogens*. Berlin, Heidelberg: Springer, pp. 133–157.

Tyler, B.M., Tripathy, S., Zhang, X., Dehal, P., Jiang, R.H.Y., Aerts, A. et al. (2006) *Phytophthora* genome sequences uncover evolutionary origins and mechanisms of pathogenesis. *Science*, 313, 1261–1266.

Zhong, C., Sun, S., Zhang, X., Duan, C. & Zhu, Z. (2020) Fine mapping, candidate gene identification and co-segregating marker development for the Phytophthora root rot resistance gene *RpsYD25*. *Frontiers in Genetics*, 11, 799.

SUPPORTING INFORMATION

Additional supporting information may be found in the online version of the article at the publisher's website.

How to cite this article: Arsenault-Labrecque, G., Santhanam, P., Asselin, Y., Cinget, B., Lebreton, A., Labbé, C., et al (2022) RXLR effector gene *Avr3a* from *Phytophthora sojae* is recognized by *Rps8* in soybean. *Molecular Plant Pathology*, 23, 693–706. https://doi.org/10.1111/mpp.13190

Annexe III. Ensemble des résultats de pathotypage, par phénotypage et génotypage, ayant servi à mesurer la validation des marqueurs génétiques utilisés dans l'outil moléculaire PCR multiplexe. Les phénotypes entre parenthèses indiquent un manque de discrimination du test; le résultat obtenu en génotypage est alors utilisé pour confirmer le pathotype.

ID Université Laval	Original ID	Harvest year	Origin	Pathotype (1a,1b,1c,1d,1k,2,3a,3b,3c,4,5,6,7,8)	Pathotype 1a,1b,1c,1d,1k,3a,6	Genotype PCR 1a,1b,1c,1d,1k,3a,6
UL_Ps_00002	2010-2	2010	ON	1a,1c,(3c),7	1a,1c	1c,1d
UL_Ps_00015	2010-22	2010	ON	1a,2,(3c),4,5,6,7	1a,6	1a,6
UL_Ps_00020	2010-27	2010	ON	1a,(1b),1c,(1k),2,3b,3c,4,5,6,7	1a,(1b),1c,(1k),6	1a,1c,6
UL_Ps_00023	2010-30	2010	ON	1a,(1c),(2),(3b),3c,4,5,6,7	1a,(1c),6	1a,1c,6
UL_Ps_00055	2010-62	2010	ON	1a,1b,1c,1k,2,3c,4,5,6,7	1a,1b,1c,1k,6	1a,1b,1k,6
UL_Ps_00082	2011-18b	2011	ON	1a,1b,1c,(1d),1k,2,3b,3c,5,7	1a,1b,1c,(1d),1k	1a,1b,1c,1d,1k
UL_Ps_00111	2011-42	2011	ON	1a,(1c),(2),(3b),3c,4,(5),6,7	1a,(1c),6	1a,6
UL_Ps_00119	2011-50	2011	ON	1a,1b,1k,2,(3b),(3c),5,7	1a,1b,1k	1a
UL_Ps_00125	2011-56	2011	ON	1a,1b,1k,5,7	1a,1b,1k	1a,1b,1c,1d,1k
UL_Ps_00154	2011-85	2011	ON	1a,6	1a,6	1a,6
UL_Ps_00185	2012-6	2012	ON	1a,1c,(1d),(2),7	1a,1c,(1d)	1a,1c,1d
UL_Ps_00192	2012-11	2012	ON	1a,1c,(2),(3b),5,7	1a,1c	1a,1c
UL_Ps_00206	2012-25	2012	ON	1a,1c,(2),7	1a,1c	1a,1c
UL_Ps_00210	2012-29	2012	ON	1a,1b,(1c),(1d),1k,2,(3a),(3b),3c,(5),7	1a,1b,(1c),(1d),1k,(3a)	1a
UL_Ps_00211	2012-30	2012	ON	(1a),(1b),(1c),(1k),(2),7	(1a),(1b),(1c),(1k)	
UL_Ps_00214	2012-33	2012	ON	1a,(1c),2,3a,3c,4,(5),6,7,8	1a,(1c),3a,6	1a,3a,6
UL_Ps_00215	2012-34	2012	ON	1a,(1d),2,3a,3c,4,5,6,7	1a,(1d),3a,6	1a,3a,6
UL_Ps_00216	2012-35	2012	ON	1a,1b,1c,1d,1k,2,3c,5,7	1a,1b,1c,1d,1k	1a,1b,1c,1d,1k
UL_Ps_00219	2012-38	2012	ON	1a,1b,(1c),1k,2,(3b),(3c),5,(6),7	1a,1b,(1c),1k,(6)	1a
UL_Ps_00224	2012-44	2012	ON	1a,(1b),(1c),(1k),2,3c,(5),7	1a,(1b),(1c),(1k)	1a
UL_Ps_00231	2012-50	2012	ON	1a,2,3a,3c,4,5,6,7	1a,3a,6	1a,3a,6
UL_Ps_00241	2012-60	2012	ON	Perte de virulence	Perte de virulence	1a,1c
UL_Ps_00242	2012-61a	2012	ON	1a,1c,(2),3c,4,(5),6,7	1a,1c,6	1a,6
UL_Ps_00253	2012-70	2012	ON	1a,(2),3a,(3b),3c,4,5,6,7,8	1a,3a,6	1a,3a,6

Janvier 2023

ANNEXE III

ID Université Laval	Original ID	Harvest year	Origin	Pathotype (1a,1b,1c,1d,1k,2,3a,3b,3c,4,5,6,7,8)	Pathotype 1a,1b,1c,1d,1k,3a,6	Genotype PCR 1a,1b,1c,1d,1k,3a,6
UL_Ps_00255	2012-72	2012	ON	1a,(7)	1a	1a
UL_Ps_00271	2012-88	2012	ON	1a,(1b),1d,(1k),2,(3b),3c,5,7	1a,(1b),1c,1d,(1k)	1a,1c,1d
UL_Ps_00282	2012-99	2012	ON	1a,5,7	1a	1a,1c,1d
UL_Ps_00292	2012-109	2012	ON	1a,(1c),(2),(3c),7	1a,(1c)	1a
UL_Ps_00296	2012-113	2012	ON	1a,(1c),2,(3a),(3b),3c,4,(5),6,7,(8)	1a,(1c),(3a),6	1a,1c,3a,6
UL_Ps_00312	2012-129	2012	ON	1a,(1b),2,(3b),3c,4,5,6,7	1a,(1b),6	1a,6
UL_Ps_00365	2010-81	2010	ON	(1b),(1c),2,(3b),5,7	(1c)	1c
UL_Ps_00369	2010-85	2010	ON	(1a),1b,(1c),1k,2,7	(1a),1b,(1c),1k	
UL_Ps_00465	2017-	2017	USA (Dorrance)	1a,1b,(1k),2,(3b),3c,4,5,6,7	1a,1b,(1k),6	
UL_Ps_00475	PH18-2-1	2018	MB	1a,1b,1c,(1d),1k,2,3b,5	1a,1b,1c,(1d),1k	1a,1b,1c,1d,1k
UL_Ps_00477	PH18-2-3	2018	MB	1a,1b,1c,(1d),1k,2,3b,5	1a,1b,1c,(1d),1k	1a,1b,1c,1d,1k
UL_Ps_00556	2018_QC_10_B	2018	QC	1a,1b,1c,(1d),1k,2,3b,5,7	1a,1b,1c,(1d),1k	1b,1c,1k
UL_Ps_00581	2018_QC_29_C	2018	QC	1a,1c,(1k),2,3b,3c,4,5,6,7	1a,1c,(1k),6	1a,1c,6
UL_Ps_00587	2018_MB_13	2018	MB	1a,1b,1c,1k,2,(3b),(3c),(4),5,(6),7	1a,1b,1c,1k,(6)	1a,1b,1c,1k
UL_Ps_00603	1036-005	2018-2019	ON	1a,1b,1c,1k,2,5,7	1a,1b,1c,1k	1a
UL_Ps_00604	1077-002	2018-2019	ON	1a,1b,1c,1d,1k,2,3b,5,7	1a,1b,1c,1d,1k	1a,1c,1d
UL_Ps_00745	UL_Ps_00745	2019	QC	1a,2,3a,3b,3c,4,5,6,7,8	1a,3a,6	1a,3a,6
UL_Ps_00753	UL_Ps_00753	2019	QC	1a,(1d),2,3a,3b,3c,4,5,6,7,8	1a,(1d),3a,6	1a,3a,6
UL_Ps_00756	UL_Ps_00756	2019	QC	1a,(1d),2,3a,3b,3c,4,5,6,7,8	1a,(1d),3a,6	1a,3a,6
UL_Ps_00758	UL_Ps_00758	2019	QC	1a,(1c),(1d),2,3b.3c,4,5,6,7	1a,(1c),(1d),6	1a,1c,6
UL_Ps_00759	UL_Ps_00759	2019	QC	1a,2,(3b),3c,4,5,6,7	1a,6	1a,6
UL_Ps_00764	UL_Ps_00764	2019	QC	1a,(1b),1c,1d,(1k),2,3b,3c,4,5,6,7	1a,(1b)1c,1d,(1k),6	1a,1c,1d,6
UL_Ps_00767	UL_Ps_00767	2019	QC	1a,(1c),(1d),2,(3b),3c,(4),5,(6),7	1a,(1c),(1d),(6)	1a,1c,6
UL_Ps_00771	UL_Ps_00771	2019	QC	1b,1k,2,(3b),7	1b,1k	
UL_Ps_00778	UL_Ps_00778	2019	QC	1a,2,3c,4,5,6,7	1a,6	1a,1c

Janvier 2023

ID Université Laval	Original ID	Harvest year	Origin	Pathotype (1a,1b,1c,1d,1k,2,3a,3b,3c,4,5,6,7,8)	Pathotype 1a,1b,1c,1d,1k,3a,6	Genotype PCR 1a,1b,1c,1d,1k,3a,6
UL_Ps_00782	MB11	2019	MB	1a,1c,1d,(1k),2,3b,7	1a,1c,1d,(1k)	1a,1c,1d
UL_Ps_00783	MB12	2019	MB	1a,1b,1c,1k,(2),5,(7)	1a,1b,1c,1k	1a,1b,1c,1d,1k
UL_Ps_00784	MB15	2019	MB	1a,(1d),2,7	1a,(1d)	1a,1c,1d
UL_Ps_00785	MB16	2019	MB	1a,1b,1c,(1d),1k,2,(3b),5,7	1a,1b,1c,(1d),1k	1a,1c
UL_Ps_00786	MB41	2019	MB	1a,1b,1c,1d,1k,2,3b,5,7	1a,1b,1c,1d,1k	1a,1b,1c,1d,1k
UL_Ps_00787	MB46	2019	MB	1a,1b,(1c),1d,1k,2,(3b),4,7	1a,1b,(1c),1d,1k	1a,1b,1c,1d,1k
UL_Ps_00788	MB49	2019	MB	1a,1b,1c,1d,1k,2,(3a),(3b),5,7	1a,1b,1c,1d,1k,(3a)	1a,1b,1c,1d,1k
UL_Ps_00789	MB51	2019	MB	1a,1d,2,(3b),7	1a,1d	1a,1c,1d
UL_Ps_00790	MB52	2019	MB	1a,1c,(1d),(1k),2,3b,7	1a,1c,(1d),(1k)	1a,1c,1d
UL_Ps_00791	MB53	2019	MB	1a,1b,1c,1d,1k,2,5,7	1a,1b,1c,1d,1k	1a,1b,1c,1d,1k
UL_Ps_00792	MB54	2019	MB	1a,1b,1c,1k,2,3b,5	1a,1b,1c,1k	1a,1b,1c,1d,1k
UL_Ps_00793	MB65	2019	MB	1a,1c,1d,(1k),(2),5,7	1a,1c,1d,(1k)	1a,1c,1d
UL_Ps_00794	MB57	2019	MB	1a,1c,1d,1k,2,(3b),7	1a,1c,1d,1k	1a,1c,1d
UL_Ps_00795	MB59	2019	MB	1a,1c,1d,(1k),2,(3b),(5),7	1a,1c,1d,(1k)	1a,1c,1d,1k
UL_Ps_00796	MB60	2019	MB	1a,1c,1d,(1k),2,(3b),(5),7	1a,1c,1d,(1k)	1a,1c,1d
UL_Ps_00797	MB64	2019	MB	1a,1b,1c,1k,2,(3b),5,(7)	1a,1b,1c,1k	1a,1b,1c,1d,1k
UL_Ps_00798	MB66	2019	MB	1a,1b,1c,1d,1k,2,5,7	1a,1b,1c,1d,1k	1a,1b,1c,1d,1k
UL_Ps_00799	MB68	2019	MB	1a,1b,1c,(1d),1k,2,3b,5,(7)	1a,1b,1c,(1d),1k	1a,1b,1c,1d,1k
UL_Ps_00800	MBH+M	2019	MB	1a,1c,1d,2,(3b),7	1a,1c,1d	1a,1c,1d
UL_Ps_00801	SK04	2019	SK	1a,1b,1c,1d,1k,2,(3a),(3b),5,7	1a,1b,1c,1d,1k,)3a	1a,1c,1d
UL_Ps_00802	PE01	2019	PEI	1a,1b,1c,1d,1k,2,(3b),5,7	1a,1b,1c,1d,1k	1a,1b,1c,1d,1k
UL_Ps_00803	SYN58-2020	2020	QC	1a,(1c),2,(3b),7	1a,(1c)	1a,1c,1d
UL_Ps_00804	SYN59-2020	2020	QC	1a,(1d),2,3b,7	1a,(1d)	1c,1d
UL_Ps_00805	SYN89.a-2020	2020	MB	1a,(1c),(1d),2,7	1a,(1c),(1d)	1a,1c,1d
UL_Ps_00806	SYN89.b-2020	2020	MB	1a,(1c),(1d),2,(7)	1a,(1c),(1d)	1a,1c,1d
UL_Ps_00807	SYN100-2020	2020	MB	1a,(1b),(1c),(1d),(1k),2,(3b),5,7	1a,(1b),(1c),(1d),(1k)	1a,1b,1c,1d,1k

Janvier 2023

ID Université Laval	Original ID	Harvest year	Origin	Pathotype (1a,1b,1c,1d,1k,2,3a,3b,3c,4,5,6,7,8)	Pathotype 1a,1b,1c,1d,1k,3a,6	Genotype PCR 1a,1b,1c,1d,1k,3a,6
UL_PS_00814	SYN72-2020	2020	ON	1a,(1c),(1d),7	1a,(1d)	1a,1c,1d
UL_PS_00815	SYN80-2020	2020	ON	1a,1c,2,3a,3b,3c,4,6,7,8	1a,1c,3a,6	1a,3a,6
UL_PS_00816	SYN85-2020	2020	MB	1a,1c,1d,2,(3a),(3b),7	1a,1c,1d,(3a)	1a,1c,1d
UL_PS_00817	SYN88-2020	2020	MB	1a,1c,(1d),2,(5),7	1a,1c,(1d)	1a,1c,1d
UL_PS_00818	#1site3-2020	2020	QC	1a,1c,1d,2,7	1a,1c,1d	1a,1c,1d
UL_PS_00819	#1site11-2020	2020	QC	1a,1c,(1d),2,3b,7	1a,1c,(1d)	1a,1c,1d
UL_PS_00820	#3site11-2020	2020	QC	1a,1b,1c,1d,1k,2,3b,5,7	1a,1b,1c,1d,1k	1a,1b,1c,1d,1k
UL_PS_00822	#1site20-2020	2020	QC	1a,1b,1c,1d,1k,2,(3a),3b,5,7	1a,1b,1c,1d,1k,(3a)	1a,1b,1c,1d,1k
UL_PS_00823	#1site30-2020	2020	QC	1a,(1b),(1c),(1k),2,(3b),3c,4,5,6,7	1a,(1b),(1c),(1k),6	1a,1b
UL_PS_00824	#2site31-2020	2020	QC	1a,(1b),1c,2,7	1a,(1b),1c	1a,1c
UL_PS_00825	#1site39-2020	2020	QC	1a,1c,2,7	1a,1c	1a,1c
UL_PS_00826	#3site39-2020	2020	QC	1a,1c,2,7	1a,1c	1a,1c
UL_PS_00840	#2site22	2020	QC	1a,1c,(1k),2,3b,5,7	1a,1c,(1k)	1a,1c
UL_PS_00841	#3site36	2020	QC	1a,1b,1c,1k,2,3b,5,7	1a,1b,1c,1k	1a,1c
UL_PS_00842	#1site21	2020	QC	1a,1c,2,3a,(3b),3c,4,5,6,7,8	1a,1c,3a,6	1a,1c,3a,6
UL_PS_00844	#2site30	2020	QC	1a,(1b),1c,1d,(1k),2,3b,5,7	1a,(1b),1c,1d,(1k)	1a,1c,1d
UL_PS_00845	#2site15	2020	QC	1a,1b,1c,1d,1k,2,(3b),5,7	1a,1b,1c,1d,1k	1a,1c,1d
UL_PS_00846	#3site31	2020	QC	1a,1c,2,5,7	1a,1c	1a,1c
UL_PS_00847	#2site23	2020	QC	1a,(1b),1c,2,(3a),(3b),(4),5,(6),7	1a,(1b),1c,(3a),(6)	1a,1c
UL_PS_00848	#2site17	2020	QC	1a,1b,1c,(1d),1k,2,(3b),5,7	1a,1b,1c,(1d),1k	1a,1b,1c,1d,1k
UL_PS_00849	#1site21	2020	QC	1a,1c,(1d),2,3a,(3b),3c,4,5,6,7,8	1a,1c,(1d),3a,6	1a,1c,3a,6
UL_PS_00850	#1site29	2020	QC	1a,(1b),1c,(1d),(1k),2,3a,3b,3c,5,7,8	1a,(1b),1c,(1d),(1k),3a	1a,3a
UL_PS_00851	#2site26	2020	QC	1a,1b,1c,1d,1k,2,3b,5,7	1a,1b,1c,1d,1k	1a,1b,1c,1d,1k
UL_PS_00852	#1site35	2020	QC	1a,(1b),1c,(1d),(1k),2,(3b),3c,5,7	1a,(1b),1c,(1d),(1k)	1a,1c,1d
UL_PS_00854	#3site19	2020	QC	1a,(1c),2,(3b),5,7	1a,(1c)	1a,1c
UL_PS_00856	#3site30	2020	QC	1a,1c,2,(3b),5,7	1a,1c	1a,1c,1d

ANNEXE III

ID Université Laval	Original ID	Harvest year	Origin	Pathotype (1a,1b,1c,1d,1k,2,3a,3b,3c,4,5,6,7,8)	Pathotype 1a,1b,1c,1d,1k,3a,6	Genotype PCR 1a,1b,1c,1d,1k,3a,6
UL_PS_00858	#2site33	2020	QC	(1a),(1b),1c,2,(3a),5,7	(1a),(1b),1c,(3a)	1c
UL_PS_00859	#1site22	2020	QC	1a,(1b),1c,(1d),(1k),2,(3b),5,7	1a,(1b),1c,(1d),(1k)	1a,1c,1d,3a,6
UL_PS_00860	#1site26	2020	QC	1a,1b,1c,1d,1k,2,3b,5,7	1a,1b,1c,1d,1k	1a,1b,1c,1d,1k
UL_PS_00861	#3site22	2020	QC	1a,1c,(1k),2,(3b),5,7	1a,1c,(1k)	1a,1d,3a,6
UL_PS_00862	#4site38	2020	QC	1a,1c,2,(3b),5,7	1a,1c	1a,1c
UL_PS_00864	#3site18	2020	QC	1a,(1b),(1k),2,3a,3c,4,5,6,7,8	1a,(1b),(1k)3a,6	1a,3a,6
UL_PS_00865	MB13	2020	MB	(1a),1b,(1c),(1d),1k,2,(3b),5,7	(1a),1b,(1c),(1d),1k	1a,1b,1c,1d,1k
UL_PS_00866	#1site1	2021	QC	1a,2,(3b),3c,4,(5),6,7	1a,6	1a,1c,6
UL_PS_00867	#2site23	2021	QC	1a,1b,1c,1k,2,3b,5,7	1a,1b,1c,1k	1a,1b,1c,1k
UL_PS_00869	#1site22	2021	QC	1a,1b,(1d),1k,2,(3a),5,7	1a,1b,(1d),1k,(3a)	1a,1d
UL_PS_00871	#3site4	2021	QC	1a,(1b),1c,1d,(1k),2,(3a),(3b),5,7	1a,(1b),1c,1d,(1k),(3a)	1a,1c,1d
UL_PS_00872	#2site6(plant)	2021	QC	1a,1b,1c,1k,2,5	1a,1b,1c,1k	1a,1b,1c,1d,1k
UL_PS_00873	mb28	2020	MB	1a,1b,(1c),(1d),1k,2,3b,(5),7	1a,1b,(1c),(1d),1k	1a,1b,1c,1d,1k
UL_PS_00874	#3site27	2021	QC	1a,(1b),(1k),2,3a,(3c),(4),5,(6),7,8	1a,(1b),(1k),3a,(6)	1a,1c,3a
UL_PS_00875	#3site23	2021	QC	1a,2,3a,3c,4,5,6,7,8	1a,3a,6	1a,3a,6
UL_PS_00877	#1site19	2021	QC	(1a),1b,1c,(1d),1k,2,7	(1a),1b,1c,(1d),1k	1a,1b,1c,1d,1k
UL_PS_00878	#2site13	2021	QC	1a,1b,(1k),2,5,7	1a,1b,(1k)	1a,1b,1k
UL_PS_00879	#3site32	2021	QC	1a,1c,(1d),2,3c,4,5,6,7	1a,1c,(1d),6	1a,1c
UL_PS_00880	#1site6(plant)	2021	QC	1b,1c,(1k),2,(3b),5	1b,1c,(1k)	1a,1b,1c,1d,1k
UL_PS_00882	#7SITE39	2021	QC	1a,1b,1c,(1k),2,(3b),5,7	1a,1b,1c,(1k)	1a,1b,1c,1k
UL_PS_00883	#3site37	2021	QC	1a,1c,2,(3a),3b,5,7	1a,1c,(3a)	1a,3a,6
UL_PS_00885	#2site38	2021	QC	1a,1b,1c,1k,2,7	1a,1b,1c,1k	1a,1b,1c,1k
UL_PS_00886	#1site8	2021	QC	(1a),(1b),(1c),(1d),(1k),2,(3a),(5),7	(1a),(1b),(1c),(1d),(1k),(3a)	1a,1b,1c,1d,1k
UL_PS_00887	#2site31	2021	QC	1a,1b,1c,(1d),1k,2,(3b),(5),7	1a,1b,1c,(1d),1k	1a,1b,1c,1k
UL_PS_00890	#3site28b	2021	QC	1a,1b,1c,1d,1k,2,(3b),5,7	1a,1b,1c,1d,1k	1a,1b,1c,1d,1k
UL_PS_00918	#1site2	2021	QC	1a,1b,1c,1d,1k,2,3a,3b,5,7	1a,1b,1c,1d,1k,3a	1a,1b,1c,1d,1k,3a,6

Janvier 2023

ANNEXE III

ID Université Laval	Original ID	Harvest year	Origin	Pathotype (1a,1b,1c,1d,1k,2,3a,3b,3c,4,5,6,7,8)	Pathotype 1a,1b,1c,1d,1k,3a,6	Genotype PCR 1a,1b,1c,1d,1k,3a,6
UL_PS_00936	TechnovaMiko	2021	QC	(1a),(1b),(1c),(1d),(1k),(2),(3a),(3b),(3c),(4),(5),(6),(7),(8)	(1a),(1b),(1c),(1d),(1k),(3a),(6)	avirulent
UL_PS_00939	#3site35	2021	QC	1a,(1b),1c,1d,(1k),2,(3a),3b,5,7	1a,(1b),1c,1d,(1k),(3a)	1a,1c,1d,3a
UL_PS_00940	#1site25	2021	QC	1a,(1b),1c,(1k),2,(3a),5,7,(8)	1a,(1b),1c,(1k),(3a)	1a,1c,1d,3a,6

Annexe IV. Figure illustrant le type de résultats obtenus par phénotypage hydroponique. A. bioessai discriminant où il est simple d'identifier le pathotype de la souche; B et C bioessais non-discriminants car les résultats obtenus sont difficiles à interpréter soit, par excès de virulence (B) ou encore par manque de virulence (C).

Discriminant

Non-discriminant; trop de virulence générale

Non-discriminant; manque de virulence générale

ANNEXE V

Protocole de la méthodologie « Speed Baiting »

Janvier 2023

SPEED BAITING

Protocole préparé par Caroline Labbé, Vanessa Tremblay et Amandine Lebreton
Laboratoire de Richard Bélanger, Université Laval
Septembre 2022

AVANT-PROPOS

Le protocole de « *speed-baiting* » a été développé au laboratoire de Richard Bélanger en vue d'accélérer le protocole de « *baiting* » (appât) régulièrement utilisé pour isoler *Phytophthora sojae* du sol.

Le protocole de « *baiting* » consiste à semer des graines de soya dans des pots contenant des échantillons de sol provenant du champ. Il faut entre trois et quatre semaines à partir du semis, avant d'isoler le *P. sojae* des échantillons de plantules. Bien que cette méthode ait fait preuve d'efficacité dans le contexte où l'on veut obtenir des isolats virulents de *P. sojae* et, par la suite, en déterminer le pathotype par bio-essai en hydroponique, il s'ensuit que cette méthode est relativement lente et ne permet pas d'obtenir le pathotype de façon rapide bien que fiable.

La méthode qui a été retenue pour déterminer le pathotype de *P. sojae* provenant d'un sol, est le test de génotypage par analyse PCR. Brièvement, on utilise l'ADN du champignon et, grâce à des amorces spécifiques aux gènes d'avirulence, il est possible de déterminer le pathotype de l'isolat sans utiliser le bio-essai en hydroponique. Toutefois, il fallait encore utiliser les souches isolées par *baiting* pour y arriver, méthode comme dit précédemment, longue et fastidieuse.

On a donc testé l'extraction d'ADN directement à partir de sols afin de voir s'il était possible d'utiliser les amorces PCR développées au laboratoire (brevet) et d'amplifier les gènes d'avirulence de *P. sojae* ciblés. Cette approche s'est révélée infructueuse, peu importe les protocoles/kits utilisés, car la présence d'inhibiteurs de PCR dans les extraits nous empêchait de faire l'analyse génotypique par PCR. De plus, la quantité de sol extraite lors de ces essais n'était aucunement représentative de la fréquence de la présence de l'agent pathogène dans le sol.

Suite à ces travaux, la problématique était double, méthode sûre mais très lente (*baiting*) ou méthode rapide mais totalement inefficace…

Nous avons finalement mis au point une méthode intermédiaire que nous avons appelé « *speed-baiting* ».

Cette méthode consiste à utiliser des bouts de feuilles et de racines de plants de soya que l'on fait flotter à la surface d'un sol saturé en eau comme appâts, afin de favoriser la présence de *P. sojae*. Lors d'essais préliminaires, ces appâts étaient récoltés, et l'ADN en était extrait en vue d'un test PCR avec des amorces universelles pour *P. sojae.*
Après de multiples essais, il est apparu que les meilleurs temps d'incubation pour lesquels on obtenait une bonne fréquence de détection de *P. sojae* étaient de 24h et 7 jours.
Cette méthode a été testée au début de l'été 2022 et a été utilisée pour le pathotypage par génotypage sur les échantillons d'AYOS technologies tout au long de la saison été 2022.

ÉTAPE 1. Réception des échantillons de sol

1.1 Référencement

Les échantillons de sol sont reçus et traités dès leur arrivée. En premier lieu, les échantillons se voient attribuer un ID unique référencé sur un document de traçage où l'on indique la date de réception, la provenance, le no de champ/échantillon, ainsi que l'ID unique. De plus, dans ce document, il y a pour chaque échantillon, les différentes étapes de traitement : de l'arrivée jusqu'au pathotype.

1.2 Entreposage dans chambre froide 6˚C en attendant la première étape de « speed-baiting »

Chambre froide 6˚C

Boîte de rangement identifiée

ÉTAPE 2. Speed-baiting

2.1 Identification des contenants (verres à bière) de plastique et des tubes d'extraction 2 ml avec l'ID UL.

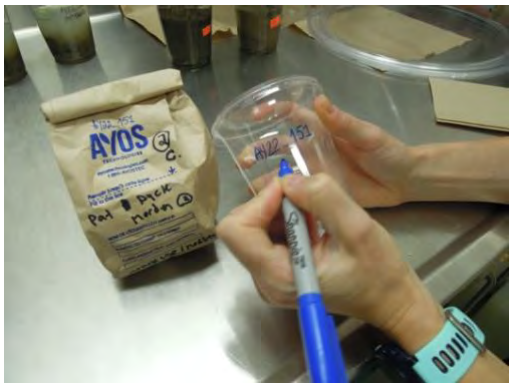

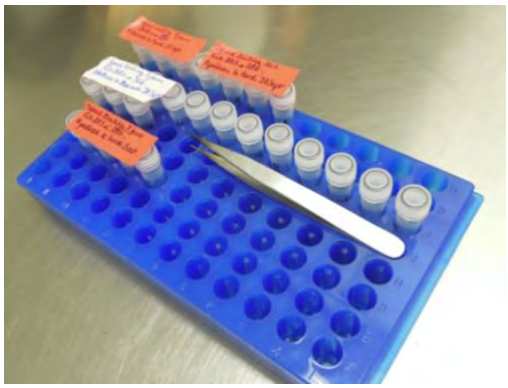

2.2 Transfert des sols dans leur verre correspondant, entre la moitié et les deux tiers du récipient.

2.3 Ajouter de l'eau du robinet de façon à ce que le sol soit complètement saturé en eau avec un excès de 1-2 cm.

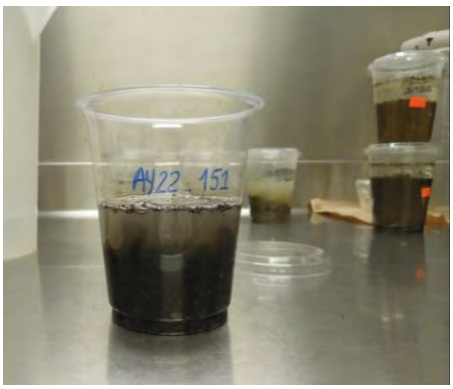

2.4 Préparation des appâts « *baits* ».

Avoir au préalable, semé et transféré des plantules de soya dans un bassin hydroponique gardé en chambre de croissance au moins deux semaines avant le début du speed-baiting.

Pour chaque échantillon de sol, découper 8-10 morceaux de feuille d'environ 8 x 8 mm ainsi que 4-8 bouts de racines de 2 cm.

2.5 Transfert des appâts dans le sol saturé en eau et transfert en chambre de croissance

Déposer à la surface de l'eau un minimum de 8 appâts foliaires et 4 appâts racinaires de façon qu'ils flottent à la surface.

Couvrir ensuite le pot avant de le transférer en chambre de croissance

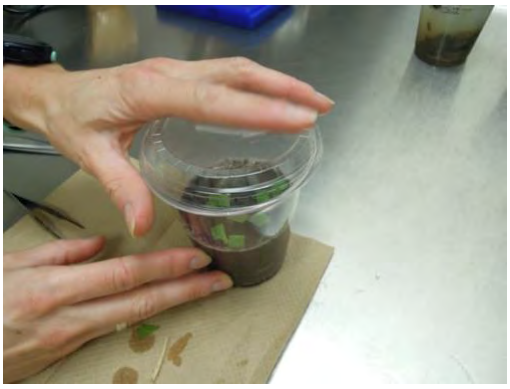

Conditions de la chambre de croissance

Photopériode : 14 heures
T˚C jour : 26˚C
T˚C nuit : 14˚C
HR% : 40 %
Intensité lumineuse : 245-300 µMOL

ÉTAPE 3. Récolte des échantillons

À raison de 4 morceaux de feuilles et 2 morceaux de racines, les appâts sont récoltés aux temps 24h (a) et 7 jours (b) soit, environ la moitié des appâts pour chacun des temps.

Les appâts sont déposés sur du papier absorbant afin d'en retirer l'excédent d'eau et les impuretés du sol.
Ils sont ensuite transférés dans les tubes d'extraction préalablement identifiés et contenant 2 billes de céramique/tube.

Échantillons prêts à récolter (temps 24h ou 7j)

N.B. Les pinces sont désinfectées à la flamme entre chaque échantillon de sol traité.

Les tubes récoltés sont mis à -80˚C en vue de la lyophilisation.

ANNEXE VI

Protocole d’extraction d’ADN à partir d’échantillons provenant du Speed-Baiting

Janvier 2023

EXTRACTION D'ADN
« SPEED-BAITING »

Protocole préparé par Caroline Labbé et Amandine Lebreton
Laboratoire de Richard Bélanger, Université Laval
Septembre 2022

ÉTAPE 1. Lyophilisation des échantillons de feuilles/racines (speed-baiting)

Les échantillons de feuilles/racines sont mis à lyophiliser pour 24 heures.

N.B. La lyophilisation est utilisée pour maximiser les étapes de broyage pour l'extraction d'ADN afin d'obtenir de meilleurs rendements.
L'extraction sur du matériel frais n'ayant pas été vraiment testée, l'étape de lyophilisation reste fortement recommandée pour ce protocole

ÉTAPE 2. Extraction d'ADN

Liste des consommables :

1. Étiquettes résistantes à la congélation (facultatif); (VRW; 76271-522)
2. CTAB (compagnies variées)
3. TRIS (compagnies variées)
4. EDTA disodique dihydrate (compagnies variées)
5. Polyvinylpyrrolidone K30 (MW ≈50.000) (Thermo Fisher #AC227545000)
6. NaOH (compagnies variées)
7. Chloroforme :iso-amyl alcool 24 :1 (compagnies variées)
8. Isopropanol
9. Éthanol
10. Tubes à centrifugation 1.5 ml (compagnies variées)
11. Tips 10, 200 et 1000 µl

Liste des équipements :

1. Congélateur -80˚C (de préférence)
2. Lyophilisateur
3. Set de pipettes 10, 200 et 1000 µl
4. pH-mètre
5. Broyeur à billes style BeadRuptor de Omni avec adapteur pour les tubes de 2 ml
6. Centrifugeuse avec rotor approprié pour tubes de 1.5 à 2 ml
7. Bain chauffant
8. Nanodrop (ou autre équipement pour vérifier la qualité de l'ADN)

Préparation des solutions stock et tampons

À préparer à l'avance :

Préparation du CTAB 10%

- Peser 50g de CTAB
- Compléter le volume à 500 ml avec de l'eau distillée
- Dissoudre au micro-ondes et terminer avec le barreau magnétique.

**Entreposer à 37˚C sinon le CTAB va précipiter dans le mélange*
***Cette dilution 10% de CTAB dans l'eau peut se garder indéfiniment à 37˚C*

Préparation du Tris-HCl 1M pH8 : 500 ml

- Peser 60.6 g de Tris (MW : 121.14)
- Ajouter de l'eau distillée à environ 400 ml
- Ajouter du HCl concentré* jusqu'à pH 8

*(*faire cette étape sous la hotte car il y a dégagement de vapeur d'acide*)

- Une fois le pH atteint, compléter le volume à 500 ml avec de l'eau distillée
- Autoclavage : facultatif

Entreposer à la température de la pièce.

Préparation de l'EDTA 0.5 M pH 8.0 : 100ml

- Peser 18,61 g d'EDTA disodique dihydraté (MW : 372.24);
- Ajouter 80 ml d'eau distillée déminéralisée.
- Mettre sur agitateur magnétique et ajouter 2 g de pastilles de NaOH; si les pastilles de NaOH sont fondues et que le pH 8 n'est pas atteint, rajouter parcimonieusement du NaOH.

(* *l'EDTA va se dissoudre complètement lorsque le pH atteindra 8.0*)

- Lorsque dissolution complète du NaOH et pH 8 atteint, ajuster le volume final à 100 ml en utilisant de l'eau distillée.
- Stériliser à l'autoclave 20 minutes à 121C : Facultatif

Entreposer à la température de la pièce.

Préparation de NaCl 5 M : 500 ml

- Peser 146g de NaCl (MW 58.44)
- Compléter le volume à 500 ml avec de l'eau distillée

Entreposer à la température de la pièce.

À préparer le jour même :
N.B. Tampons et solutions requis pour environ 24 échantillons

Tampon CTAB pour plantes : 50 ml
*racines ou autre matériel végétal
** IMPORTANT *: à préparer le jour de l'extraction.*
*** Assez pour un peu plus de 24 échantillons*

- CTAB 10% 10 ml (concentration finale : 2%)
- Tris-HCl 1M pH8 5 ml (concentration finale : 100 mM)
- NaCl 5M 14 ml (concentration finale : 1.4 M)
- EDTA 0.5M pH8 2 ml (concentration finale : 20 mM)
- PVP 0.5 g (concentration finale : 1%)
- ddH_2O Compléter le volume final à 100 ml

Elution buffer (TE) : 50 ml* peut être conservé et réutilisé

- Tris-HCl 1M pH8 0.25 ml (concentration finale : 10 mM)
- EDTA 0.5M pH8 0.1 ml (concentration finale : 1 mM)
- Compléter le volume à 50 ml avec de l'eau déminéralisée, distillée.
- Filtrer sur 0.22 µm ou autoclaver

Chloroforme : alcool iso-amyl 24 :1 : 25 ml

- 24 ml chloroforme
- 1 ml alcool iso-amyl
  Bien mélanger et fermer le contenant de façon étanche pour ne pas perdre le chloroforme par évaporation. Conserver au frigo.

Ethanol 70% : 50 ml

- Mesurer 15 ml d'eau dans un tube conique de 50 ml
- Ajouter de l'éthanol anhydre jusqu'à la barre des 50 ml
- Mettre au congélateur jusqu'à utilisation

Isopropanol froid : 50 ml

- Mettre 50 ml d'isopropanol dans un tube conique de 50 ml au congélateur jusqu'à utilisation.

Procédure/protocole

N.B. Préparer la quantité de tampon requise pour la journée; le tampon ne se conserve pas, et autres solutions requises pour l'extraction (voir pages précédentes).

1_Mettre les tubes 2 ml contenant les échantillons de « speed baiting » lyophilisés, ainsi que 2 billes de porcelaine par tube, sur le broyeur à billes (BeadRuptor) : ☐

2_Réduire les échantillons en poudre selon les paramètres suivants :

Vitesse : 5 m/sec
Temps : 2 x 35 secondes
Pause : 30 secondes

☐

3_Ajouter 600 µl de tampon CTAB pour plantes dans chaque tube et replacer les tubes sur le broyeur Omni-Bead Ruptor® aux conditions suivantes :

Vitesse : 5 m/sec
Temps : 2 x 30 secondes
Pause : 30 secondes

☐

4_Après le broyage, transférer au bain-marie @ 65˚C pendant 30 minutes ☐

5_Faire un « spin-down » des échantillons ☐

6_Ajouter 450 µl de tampon CTAB pour plantes à chaque échantillon ☐

7_Mélanger en inversant les tubes une dizaine de fois ☐

8_Centrifuger @ 14000*g* pendant 5 minutes ☐

9_Prélever 700 µl de surnageant et transférer dans des microtubes à centrifugation 1.5 ml stériles préalablement identifiés ☐

10_Ajouter un volume égal (700 µl) du mélange chloroforme : isoamyl alcool (24 :1) ☐

11_Mélanger au vortex brièvement et centrifuger 5 minutes @ 14000*g* ☐

12_Après centrifugation, transférer environ 600 µl de la phase supérieure dans un nouveau microtube à centrifugation 1.5 ml stérile préalablement identifié (avec une étiquette si possible). Attention de ne pas prendre la phase inférieure de l'extrait en pipettant ☐

13_ Ajouter ensuite 0.7 volume d'isopropanol froid (420 µl d'isopropanol pour 600 µl de l'extrait); mélanger bien en inversant les tubes une dizaine de fois. ☐

14_Incuber au froid au congélateur (-20˚C pendant 15 minutes) ☐

15_Centrifuger les échantillons à 14000*g* pendant 15 minutes. Retirer le surnageant (isopropanol) en décantant tout doucement en faisant bien attention de garder le culot d'ADN intact ☐

16_Ajouter délicatement 500 µl d'ETOH 70% glacé sur la paroi du tube qui est opposée au culot *(en effet, il est primordial à cette étape de ne pas détacher le culot du fond du tube car on risque de le perdre à l'étape de décantation suivante)* ☐

17_Centrifuger @14000 *g* pendant 2 minutes et retirer l'éthanol par décantation ☐

Si culot brunâtre, refaire les étapes 14 et 15

18_Aprés avoir jeter l'éthanol par décantation, déposer les tubes tête en bas sur papier absorbant pour que l'éthanol résiduel soit asséché par capillarité. (*Pas plus de 10 minutes)* ☐

19_Suspendre le culot d'ADN dans 50 µl de TE (TRIS-HCl 10 mM; EDTA 1mM; pH 8) ☐

20_Mettre tubes au bain chauffant à 65˚C pendant 5 minutes; ☐

21_Ouvrir les tubes un par un à la sortie du bain et refermer. *Ça permet d'éliminer les résidus d'éthanol de l'ADN et la chaleur permet de dissoudre le culot de façon plus efficace.* ☐

22_Dissoudre l'ADN par « flicking » si nécessaire ☐

23_Faire un spin-down ☐

18_Doser l'ADN au Nanodrop ☐

19_Déposer les échantillons dans des boîtes dédiées et laisser au réfrigérateur (maximum de 1 mois) ☐

ANNEXE VII

Santhanam, P., Labbé, C., Tremblay, V., Bélanger, R.R. 2023. A rapid molecular diagnostic tool to discriminate haplotypes of *Phytophthora sojae* avirulence genes using high-resolution melting analysis.

Janvier 2023

A rapid molecular diagnostic tool to discriminate haplotypes of *Phytophthora sojae* avirulence genes using high-resolution melting analysis.

Parthasarathy Santhanam[1#], Caroline Labbé[1], Vanessa Tremblay[1] and Richard R. Bélanger[1*]

[1] Département de Phytologie, Université Laval, Québec, QC, Canada.

[#] Current address: Agriculture Agri-Food Canada, Morden, MB, Canada.

[*] Corresponding author: richard.belanger@fsaa.ulaval.ca (Richard R. Bélanger)

Key words: High-resolution melting curve analysis; HRM; *P. sojae*; avirulence; virulence; effectors; disease diagnosis

ABSTRACT

Background

Effectors encoded by avirulence genes (*Avr*) interact with the resistance to *Phytophthora sojae* gene (*Rps*) products to generate incompatible interactions. *Phytophthora sojae* virulence profile is rapidly evolving due to large-scale deployment of *Rps* genes in soybean. For a successful exploitation of *Rps* genes, soybean growers must use cultivars containing the *Rps* genes corresponding to *Avr* genes present in *P. sojae* isolates in their field. Determination of the virulence profile of *P. sojae* isolates is critical for the selection of soybean cultivars. High resolution melting curve analysis (HRM) can be a cost-effective, sensitive and efficient tool to detect polymorphisms in the avirulence genes of *P. sojae*.

Results

Here, we report the optimization of PCR coupled with HRM assay to differentiate *P. sojae* pathotypes. High resolution melting analysis was performed on 24 *P. sojae* isolates with different pathotypes collected from soybean fields across Canada. The results clearly showed that HRM assay discriminated different virulence genotypes. Moreover, the HRM assay was able to differentiate multiple haplotypes representing small allelic variations. HRM based prediction was validated by phenotyping assays.

Conclusions

The HRM assay is a rapid, cost effective and an efficient tool to predict virulence pathotypes associated with of six different *Avr* (*1b, 1c, 1d, 1k, 3a, 6*) genes from *P. sojae*.

Background

Soybean (*Glycine max* (L.) Merr.) seeds provide protein and oil for animal feed and human consumption. Soybean is the fourth largest field crop in the world and meets 60% of global vegetable oil demand (USDA, 2019). Worldwide production reached 350 million tons in 2018 (FAOStat, 2021) but diseases caused by fungal and oomycete pathogens remain a major limitation for soybean production. Among them, Phytophthora stem and root rot (PRR), caused by the oomycete soilborne pathogen *Phytophthora sojae* (M.J. Kaufmann and J.W. Gerdemann) is particularly devastating because it can attack soybean plants at all growth stages (Dorrance et al., 2007; Tyler., 2007).

An effective way to reduce *P. sojae* damage is by planting soybean cultivars with genes conferring resistance to *Phytophthora sojae* (*Rps*). These genes encode proteins containing nucleotide-binding site and leucine-rich repeat (NLR) motifs. Avirulence (*Avr*) genes of *P. sojae* encode effector proteins that are expressed only during infection, and most of them contain RxLR and DEER domains believed to be required for cytoplasmic translocation. When a soybean *Rps* recognizes the corresponding *Avr* from *P. sojae*, immune responses are triggered resulting in disease resistance (Madina MH et al., 2023).

Overexploitation of single *Rps* genes in the field exerts a strong selection pressure against the avirulent isolates, which in turn become virulent through genetic modification of *Avr* genes or its regulatory elements (Arsenault-Labrecque et al., 2018). Genetic modifications like insertion, deletion, and substitution in the promoter region or in the coding sequence of *Avr* genes allow the pathogen to evade host recognition and infect the plant. Diversification of *Avr* genes in *P. sojae*

has led to increased virulence profiles and limits the effectiveness of *Rps* genes in soybean (Tremblay et al., 2021). To date, more than 33 *Rps* genes/alleles have been identified in soybean while six of them (*Rps1a*, *1b*, *1c*, *1k*, *3a*, and *6*) have been introgressed into commercial soybean varieties (Dorrance 2018; Jiang et al. 2020).

Most of the *Avr* genes in *P. sojae* are located in repeat-rich regions, have high levels of sequence homology (e.g. *Avr1a* and *Avr1c*), and vary in copy numbers (e.g. *Avr1a*, *Avr3a*), which makes it very difficult to develop sequence-based diagnostic markers. To identify and characterize rapidly evolving *P. sojae* isolates, Arsenault-Labrecque et al. (2018) defined specific haplotypes for seven *Avr* genes (1a, 1b, 1c, 1d, 1k, 3a, and 6) using comparative whole-genome analysis of 31 *P. sojae* isolates. Further validation by hydroponic assay showed each identified haplotype corresponded to a distinct virulence profile (Arsenault-Labrecque et al., 2018). Based on these results, Dussault-Benoit et al., (2019) identified unique sequences and developed a diagnostic multiplex PCR tool to detect the presence of alleles conferring an avirulent phenotype for isolates containing seven *Avr* genes (*1a*, *1b*, *1c*, *1d*, *1k*, *3a*, and *6*).

Quantitative PCR monitors the amount of PCR product in real time by using intercalating dyes (SYBR Green), but these dyes also bind non-specifically to off-target DNA, and primer dimers (Navarro et al. 2015). Melting curve analysis verifies the specificity of a given primer pair by discriminating the amplicon based on the melting point. Intercalating fluorescent dyes exhibits fluorescence only when bound to double stranded DNA; during the melting process, where the double stranded DNA dissociates into single strands, the fluorescence level decreases (Tong and Giffard 2012; Bezdicek et al. 2016). Major limitations of non-saturating dyes like SYBR Green

are that they inhibit polymerase activity at higher concentration and re-bind on free sites during the melting process. However, saturating dyes such as EvaGreen, LcGreen, SYTO9 do not inhibit polymerase even at higher concentrations and hence can be used at saturation (Duyvejonck et al. 2015). With the advancement of precise detection of minute variation in fluorescence, and use of upgraded software and saturation dyes, it is possible to distinguish sequences with a single nucleotide variation. High-resolution melting analysis has been successfully utilized in clinical medicine (Garritano et al., 2009; Bezdicek et al., 2016), in detection and differentiation of viruses (Gelaye et al., 2017), in detection and genotyping of plant pathogenic *Fusarium* spp., (Brandfass et al., 2006; Ganopoulos et al., 2012; Schiwek et al., 2020), in genotyping isolates of apple scab pathogen (Chatzidimopoulos et al., 2019), and recently in identification of mutants generated by CRISPR-Cas9 (Rocafort et al., 2022).

In this study, we have developed a sensitive and robust high-resolution melting assay to discriminate all haplotypes of six different *Avr* genes (*Avr1b*, *1c*, *1d*, *1k*, *3a*, and *6*) in *P. sojae* isolates that confer virulence/avirulence in soybean lines containing the corresponding *Rps* gene. In the context of the *P. sojae*-soybean interaction, these results offer a powerful tool to better manage the disease through an educated selection of *Rps* genes resistant to *P. sojae* haplotypes present in the field.

Materials and methods

Phytophthora sojae isolates and inoculum preparation.

All *P. sojae* isolates used in this study, were sampled across Quebec, Ontario, and Manitoba from commercial and experimental soybean fields (Tremblay et al., 2021). Using a seedling bioassay

procedure, individual *P. sojae* isolates were extracted from soil samples. The single-spore isolates were maintained on V8 agar medium and for long term storage agar pieces were stored in water at room temperature or 4 °C. The inoculum for hydroponic assay were prepared by blending 12-day-old cultures grown on V8 Phytagel medium with 60 ml of sterile water in a commercial blender. The oospore concentration was determined from the mycelial slurry and adjusted to 1×10^6 oospores/ml.

Genomic DNA isolation.

Phytophthora sojae isolates were grown on cellophane paper placed on V8 agar for seven days at 28 °C. Mycelial mats were harvested and transferred to tubes containing two beads. The samples were homogenized (4 m s−1 × 2 cycles of 30 s with a 40-s pause) with an Omni Bead Ruptor 24 (OMNI International) and genomic DNA was extracted using a CTAB method according to Werth et al. (2016). DNA was eluted with 100 µL of elution buffer, quantified using Qubit dsDNA BR assay kit (Invitrogen), normalised to 20 ng/ µL and 2.5 µL were used for HRM analyses.

PCR and High-resolution melting analyses of *Phytophthora sojae Avr* genes

The HRM curve analysis was performed on a magnetic induction cycler (MIC) qPCR instrument (Bio Molecular Systems, Australia) using Precision Melt Supermix (BioRad, #1725112, USA) in a 20-µL reaction with 1x Precision Melt Supermix, each primer at concentration of 300 nM and 50 ng of genomic DNA. At least two technical replicates were performed for each sample. Conditions for PCR were as follows, an initial denaturation step at 95 °C for 3 min, followed by 40 cycles of 95 °C for 10 s, 59 °C for 30 s, 72 °C for 30 s, and final extension step at 72 °C for 5 min with fluorescence reading at the end of each extension step. The qPCR was followed by a

139 melting program where the amplicon was heated 70 °C to 98 °C by ramping up the temperature at
140 0. 2 °C/s with a continuous signal acquisition. The HRM curve data (Supplemental Table X) were
141 analyzed using the in-built HRM analysis software (Bio Molecular Systems, Australia). The raw
142 melting curves were normalized and then converted to difference plots.
143
144 ***Phytophthora sojae*** **pathotype characterization**.
145 To validate the results obtained from HRM assays, all 16 *P. sojae* isolates (4-controls and 12- test)
146 were subjected to hydroponic bioassay developed by Lebreton et al. (2018). Soybean differentials
147 possessing different *Rps* genes ('Haro13' [*Rps1b*], 'Haro14' [*Rps1c*], 'Haro16' [*Rps1d*], 'Haro15'
148 [*Rps1k*], 'Haro3272' [*Rps3a, 7*], and 'Haro6272' [*Rps6, 7*]) were inoculated with *P. sojae* isolates
149 as mentioned in Tremblay et al. (2021). Briefly, soybean seeds were sown in vermiculite and five-
150 days post seeding, plantlets were transferred into the hydroponic system containing the nutrient
151 solution. The hydroponic system was inoculated with 1×10^6 oospores at 24 hr post transfer of
152 seedlings. Each isolate was characterized in two independent experiments with two biological
153 replications. At 14 dpi, plants were scored as resistant or susceptible to the isolate tested.
154
155 **Results**
156 **Variant detection by HRM from known genotypes.**
157 To develop the initial proof of concept, high-resolution melting curve analysis was performed on
158 the amplicon of four different genotypes of *Avr6*: a wild type, a transversion mutation of T to G at
159 the 218th nucleotide from the start codon, a deletion of G at the 214th nucleotide from the start
160 codon and finally, deletion of five nucleotides 214-218 nucleotides from the start codon. As shown
161 in Figure 1, based on the fluorescence melting-curve analysis, each genotype exhibited a unique

and distinct curve pattern compared to the wild type. The differences were easily visualized even if a single nucleotide separated the amplicons.

HRM analysis of six *Avr* genes with known genotypes.

In order to ascertain that HRM was suitable for efficient genotyping of *P. sojae* isolates, the sensitivity of the assay for detection of different types of DNA polymorphisms was tested using six common *Avr* genes in 12 *P. sojae* isolates previously characterized phenotypically and genotypically. These 12 isolates carried either avirulent or virulent alleles for each *Avr* gene (Table 1). In the case of *Avr3a* and *Avr6* with only two haplotypes, a virulent and an avirulent form, melt curve analysis clearly formed two separate curves representing the presence of the avirulence (haplotype A) and virulence (haplotype B) allele in 12 *P. sojae* isolates (Figure 2A and B). As for *Avr1b* and *Avr1k*, which are often present in tandem in isolates, all 12 tested isolates had either two avirulent forms (haplotypes A and B) or one virulent form (haplotype C). High resolution melt analysis not only predicted the pathotypes but also distinguished all three haplotypes with unique curves (Figure 2C and D). In the case of *Avr1d*, previously reported to have three haplotypes (Arsenault-Labrecque et al. 2018), A, B, and C, the results clearly separated the expected avirulent (haplotypes A and B) and virulent forms (haplotype C; Figure 3E). Interestingly, the virulent isolate UL-Ps-82, which had exhibited a few base-pair differences with other virulent isolates in Arsenault-Labrecque et al (2018), exhibited a unique curve from the rest of the isolates consistently (Figure 2C). Sequencing of the amplicon confirmed the reported differences (Supp. Fig. X). The coding sequence of *Avr1c* was by far the most complex with five different haplotypes, two avirulent and three virulent ones, including an 8- to 10-Kb deletion, that could not be amplified. As a result, HRM analysis effectively predicted DNA sequence polymorphisms in *Avr1c* and

produced a unique melt curve for each haplotype (Figure 2F). Expectedly, isolate UL_Ps_296, containing the large deletion and referred to as haplotype E, did not amplify (Supp. Fig. X).

Predicting *Phytophthora sojae* pathotypes from field isolates.

After successfully establishing a perfect correlation between genotypes determined by the HRM method and phenotypes with previously characterized isolates, we applied the HRM method to predict the pathotype of unknown isolates collected in the field. For this purpose, we selected 12 uncharacterized field isolates, that were compared for six *Avr* genes to four control isolates described above. HRM analysis of *Avr3a* and *Avr6* in 12 field isolates exhibited two distinguishing melt curves similar to the control isolates corresponding to either a virulent or avirulent pathotype. Overall, 11/12 were avirulent toward *Avr3a* and 11/12 toward *Avr6* (Figure. 3A and B). For *Avr1b* and *Avr1k*, both are known to contain three haplotypes, A and B (avirulent) and C (virulent). When HRM analysis was performed with the 12 field isolates, they all exhibited distinguishable melt curves identical to the control isolates for each of the pathotypes as well as haplotypes (Figure 3C and D). In the end, six isolates were avirulent, and expectedly, isolates avirulent toward *Avr1b* were also toward *Avr1k*. In the case of *Avr1d* displaying three possible haplotypes, only two haplotypes were found in the isolates tested and all but two carried the virulent allele (Fig 3E). As mentioned previously, *Avr1c* has five different haplotypes of which four are detectable (A-D) owing to a large deletion in the region of the fifth haplotype (E). HRM analysis on the 12 field isolates clearly detected the presence of four haplotypes and curves were similar to curves generated by controls (Figure. 3F). None of the field isolates carried haplotype E.

To validate the HRM-based pathotype prediction, all 12 isolates were phenotyped using the hydroponic assay. As shown in Figure 4A and Supplemental Figure 2, phenotyping results are

presented for all isolates against all six *Rps* genes. In all cases, the phenotypic response in terms of virulence or avirulence matched the predicted pathotyping by the HRM based on the haplotypes. For *Avr1b*, isolate 82 (virulent control), 820, 829, 848, 851,860 and 865 were predicted to be virulent by HRM analysis. When the hydroponics assay was performed on *Rps1b* containing soybean cultivar, n these isolates were virulent and results matched perfectly with the HRM prediction (Fig-4B). Similarly, HRM based assay was able to predict the pathotype of *Avr1c* (Fig-4C), *Avr1d* (Fig-4D), *Avr1k* (Fig-4E), *Avr3a* (Fig-4F), and *Avr6* (Fig-4G) in all 12 field isolates with 100% accuracy.

Discussion

Development of efficient diagnostic tools to detect the presence of *Avr* genes in *Phytophthora sojae* is a prerequisite for the deployment of corresponding *Rps* genes in soybean. Molecular markers have been widely used in the identification, detection and characterisation of plant pathogens. Nucleotide insertion or deletion (InDels) of varying lengths is the most common type of DNA polymorphisms. High resolution melting curve analysis is a post-PCR step where the amplicon is subjected to a small increment in temperature (0.2–0.3 °C/s). When the amplicon melts, the fluorescent dyes are released and the sensor measures the rate of change in fluorescence. Melting characteristics are specific to the amplicon whereby insertion or deletion at a specific site will result in the formation of unique curves during the melting process. PCR amplification and melting analysis are performed in the same instrument in closed-tube conditions, has shorter run time, is highly specific and sensitive where even a single base change can be detected [28,29,30, this study].

Several recent studies have highlighted the growing concerns about *P. sojae* evolving pathotypes that are steadily overcoming commercial *Rps* genes around the world (ref). As a matter of fact, there is a general consensus that *Rps1a* and *1c* have become mostly inefficient while *Rps1k* is rapidly becoming overcome. For these reasons, there is an increasing need to properly and rapidly define the pathotype of *P. sojae* isolates in order to deploy the proper *Rps* genes. Historically, the virulence profile of *P. sojae* has been determined following extraction of isolates from soil or plant samples followed by inoculation on soybean differentials containing the *Rps* genes of interest through hypocotyl inoculation or other bioassays. This approach is fastidious and time-consuming and prone to phenotyping errors (ref). The aim of this study was to develop a simple and rapid HRM assay that would allow to discriminate between virulence and avirulence alleles of *P. sojae* isolates as a rapid and precise predictive tool of their pathotype. Indeed, by rapidly identifying pathotypes of *P. sojae* isolates present in soybean fields, soybean lines containing the proper *Rps* can be recommended. In this work, we report the successful differentiation of *P. sojae* haplotypes of six different *Avr* genes (1b, 1c, 1d, 1k, 3a, 6) by HRM analysis to precisely predict the pathotypes of *P. sojae* isolates.

A number of reports have been exploited HRM-based identification of genetic variants in clinical trials (45-46), and drug resistant isolates (77-79), but the technology applied to plant pathogen detection and characterization is still emerging. High resolution melting analysis has been used mainly used for differentiating *Alternaria* and *Aspergillus* species (Garganese et al., 2018; Xanthopoulou et al., 2019), or for genotyping *Botrytis cinerea*, *Colletotrichum spp*. and *Venturia inaequalis* (Chatzidimopoulos et al., 2014b; Forcelini et al., 2018 and Chatzidimopoulos 2019). In order to determine whether HRM could actually capture the SNP variants of a single gene with a

253 unique melting curve, we first proceeded with a proof of concept by synthesizing and cloning wild
254 type *Avr6* along with multiple SNP variants including a transversion (T to G), a single base deletion
255 (G) and a five-base deletion (GCGAT). The results clearly illustrated the defining power of HRM
256 and supported previous arguments that even a single base change could be distinguished using the
257 technique (28, 29).
258
259 In 2018, Arsenault-Labrecque et al. provided a detailed haplotype map for seven *Avr* genes (1a,
260 1b, 1c, 1d, 1k, 3a, and 6) of *P. sojae* and they were able to assign specific haplotypes to a distinct
261 pathotype. These data provided an invaluable source of sequences to design HRM primers around
262 SNP sites and used HRM assays to assign pathotypes to 12 *P. sojae* isolates with a different range
263 of haplotypes. Our results showed that HRM was able to discriminate not only virulence/
264 avirulence pathotype, but also exhibit unique curves for all tested haplotypes. For instance, isolate
265 PS_82 exhibited a minor shift in the curve when tested for *Avr1d*. Further analyses of multiple
266 alignments of *Avr1d* amplification site revealed that isolate PS?_82 had additional SNPs and HRM
267 was able to precisely capture those variants (see Fig. 2E?). For genotyping *Avr1a* three
268 discriminative primers pairs are required for pathotyping and these primers are designed far from
269 the *Avr1a* coding sequence (Chloe., 2020). As the goal of this study is to discriminate pathotypes
270 using single primer pairs, *Avr1a* was excluded from this study.
271
272 In order to assess if HRM could accurately predict the pathotypes of unknown isolates, the same
273 set of primers was used to test 12 *P. sojae* isolates collected across Quebec, Ontario and Manitoba.
274 In all cases, the primer set consistently amplified all haplotypes of the six genes tested and
275 demonstrated a consistent difference in Tm of the corresponding amplified products from isolates

containing different haplotypes. Throughout the different runs, the control melting curves were consistent and maintained similar melting peaks. Interestingly, the virulence profile as ascertained by the haplotype was perfectly corroborated by the phenotyping results obtained using the hydroponic assay. The InDel markers proved to be functional markers in and around *Avr* genes, the amplification was stable, HRM curves were unique, the genotype was clear, and the pathotype could be efficiently predicted. The HRM technique thus provides a rapid detection platform for pathotype and haplotype detection in *P. sojae* isolates and eliminates the cumbersome steps of phenotyping.

The results from this study were all based on pure *P. sojae* isolates that had been obtained from soil samples. In order to improve the diagnostic procedure even further, additional experiments could be conducted. For instance, future efforts could be devoted to expand these assays to detect *P. sojae* pathotypes directly from plant or baiting samples or even from gDNA isolated directly from soil. Moreover, attempts to multiplex the HRM assay would reduce time and cost, if precision is not altered.

Conclusions

In this study, HRM analysis was utilised to differentiate multiple haplotypes associated with six different *Avr* genes (*1b, 1c, 1d, 1k, 3a, 6*) genes from *P. sojae*. The HRM analysis of the amplicons successfully identified the haplotypes of those genes in all 24 *P. sojae* isolates through distinct curve profiles, allowing us to discriminate pathotypes at molecular level through the HRM curves. HRM can thus serve as a powerful diagnostic tool to identify and distinguish *P. sojae* isolates at the haplotype level.

References

Acknowledgements

The authors would like to thank Amandine Lebreton for technical assistance.

Funding

This work was supported by Genome Canada, Genome Québec, the Canadian Field Crop Research Alliance, the Program Prime-Vert #2 #19-002-2.2-C-ULAV of ministère de l'Agriculture, des Pêcheries et de l'Alimentation (MAPAQ) and the Canada Research Chairs Program to RRB.

Author information

Authors and Affiliations

Département de Phytologie, Université Laval, Québec, QC, Canada.

Parthasarathy Santhanam, Caroline Labbé, Vanessa Tremblay, and Richard R. Bélanger

Contributions

PS, CL, and RRB conceived and designed the experiments. PS performed the experiments. VT and PS isolated gDNA. VT and CL performed phenotyping. PS, CL, VT, and RRB analyzed the data. PS wrote the initial draft. RRB wrote, reviewed, and edited the manuscript.

Corresponding author

Correspondence to Richard R. Bélanger (richard.belanger@fsaa.ulaval.ca)

Ethics declarations

Ethics approval and consent to participate

Not applicable.

Consent for publication

All authors read and approved the final manuscript.

Competing interests

The authors declare that they have no competing interests.

Figure. 1. Optimisation of the high-resolution melting assay. Optimization of HRM was performed using the *Avr6* wild type and variants of *Avr6* alleles, a single nucleotide substitution (1-sub: T218G), single nucleotide deletion (1-del: G214X), and five nucleotides deletion (5-del: 214-218X). **A**. The graph displays temperature normalised melting curves for the tested samples. **B.** The graph shows curves displaying the difference in fluorescence (dFt) of the samples in relation to the wild type (WT). Wild type and sample with polymorphic alleles are colour coded (purple-wild type; black-1-sub; blue-1-del; red-5-del). Each sample was analysed in triplicate or duplicate.

Figure. 2. **High-resolution melting analysis of *P. sojae Avr* genes.** Analysis of six *Avr* genes in 12 *P. sojae* isolates with known genotype and phenotype. Six *Avr* genes (A) *Avr1b*, (B) *Avr1c*, (C) *Avr1d*, (D) *Avr1k*, (E) *Avr3a*, (F) *Avr6* were amplified from 12 *P. sojae* isolates which were genotyped and phenotyped previously. When the melt curves were compared, HRM analysis effectively distinguished avirulent (black) from virulent (red) isolates with distinguished melt curves. Moreover, HRM analysis even discriminated haplotypes containing different set of SNPs (blue, orange). Three replicates were used for each isolate and repeated twice with similar results.

Figure 3: **HRM analysis of *Avr1b, Avr1c*, *Avr1d, Avr1k, Avr3a and Avr6* in 12 *Phytophthora sojae* isolates with unknown genotype and phenotype**. *Avr3a* (**A**), *Avr6* (**B**), *Avr1b* (**C**), *Avr1k* (**D**), *Avr1d* (**E**), and *Avr1c* (**F**) were amplified from four controls and 12 uncharacterised *P. sojae* isolates which were collected and isolated from farmer's field. When the melt curves were compared, HRM analysis effectively distinguished avirulent control (black) from virulent control (red) and field isolates (grey) isolates clearly grouped with either avirulent or virulent melt curve. Three technical replicates were used for each isolate and repeated twice with similar results.

Figure 4: **Phenotyping of Phytophthora sojae isolates.** To validate HRM based pathotype prediction, we root inoculated with four control isolates (UL_082; UL_111; UL_192; UL_253) and 12 field isolates (UL_796; UL_800; UL_817; UL_818; UL_820; UL_826; UL_829; UL_842; UL_848; UL_851; UL_860; UL_865) on soybean differentials containing corresponding *Rps* genes (*Rps1b, Rps1c, Rps1d, Rps1k, Rps3a,* and *Rps6*) in hydroponic system. Two weeks post inoculation disease progression was observed and reaction scored as avirulent (Avr) or virulent

(Vir) according to Lebreton et al. (2018). (representative results are shown in **A,** phenotype results for remaining isolates are shown in **supplemental figure 2**). We found 100 % correlation between the phenotyping and HRM analysis for *Avr1b* (**B**)*, Avr1c* (**C**)*, Avr1d* (**D**)*, Avr1k* (**E**)*, Avr3a* (**F**), and *Avr6* (**G**). Williams and Harosoy were used as *rps* controls. Two plants were tested in each experiment and repeated twice with similar results.

Supplemental Figure. 1. For proof of concept, *Avr6* wild type, *Avr6* with a single nucleotide substitution (T218G), *Avr6* with single nucleotide deletion (G214X), and *Avr6* with five nucleotide deletion (214-218X) was synthesized as gBlock, cloned in pGemt vector and used as template for PCR and high-resolution melt curve analysis was performed. Primer binding sites are marked as solid arrow, size of amplicon is 120 bp.

Supplemental Figure. 2. Phenotyping of *Phytophthora sojae* isolates.

To validate HRM-based pathotype prediction, roots were inoculated with control isolates (UL_192; UL_253) and 12 field isolates (UL_796; UL_800; UL_817; UL_818; UL_820; UL_826; UL_829; UL_842; UL_848; UL_851; UL_860; UL_865) on soybean differentials containing corresponding *Rps* genes (*Rps1b, Rps1c, Rps1d, Rps1k, Rps3a,* and *Rps6*) in hydroponics. Two weeks post inoculation, disease progression was observed and reaction scored as avirulent (Avr) or virulent (Vir) according to Lebreton et al. (2018). Williams and Harosoy were used as *rps* controls. Two plants were tested in each experiment and repeated twice with similar results.

389 **Supplemental Figure. 3.** Multiple alignment of *Avr1b* HRM primer binding sites among 31
390 *Phytophthora sojae* isolates. **A**. Amplifying region is highlighted in blue, deletions are marked as
391 hyphens (-). **B**. Variants in the vicinity of *Avr1b*.

Figure. 1

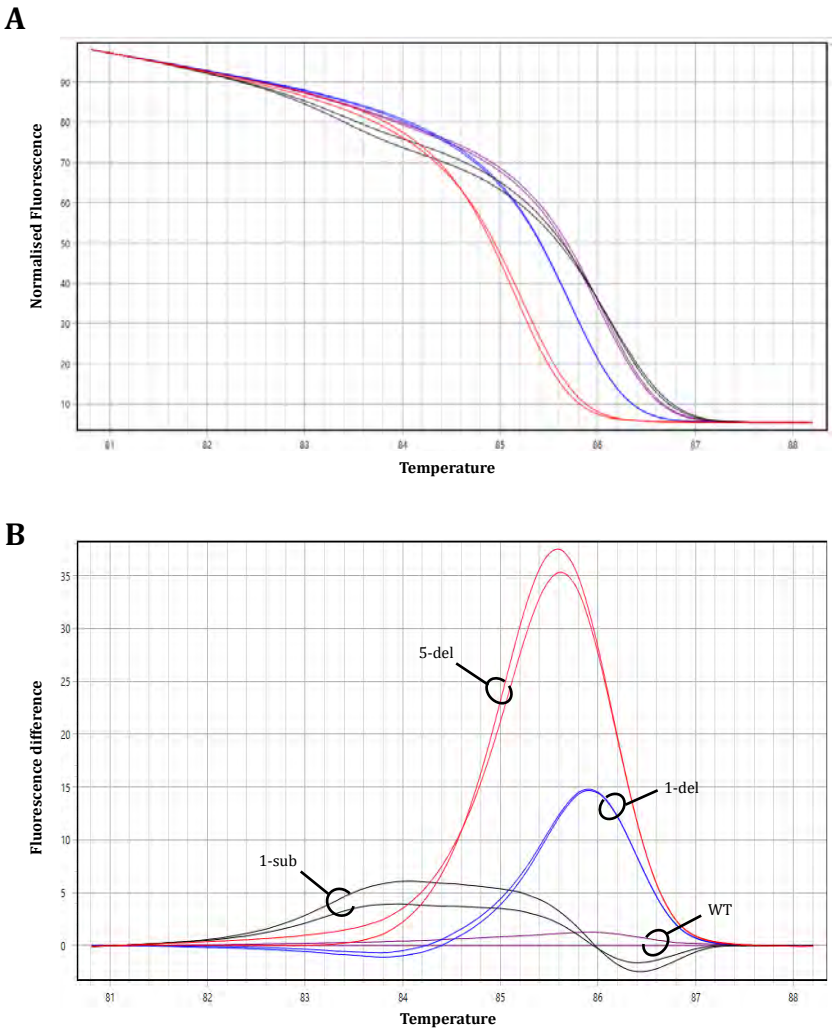
A
Normalised Fluorescence
Temperature
B
Fluorescence difference
5-del
1-del
1-sub
WT
Temperature

Figure. 2

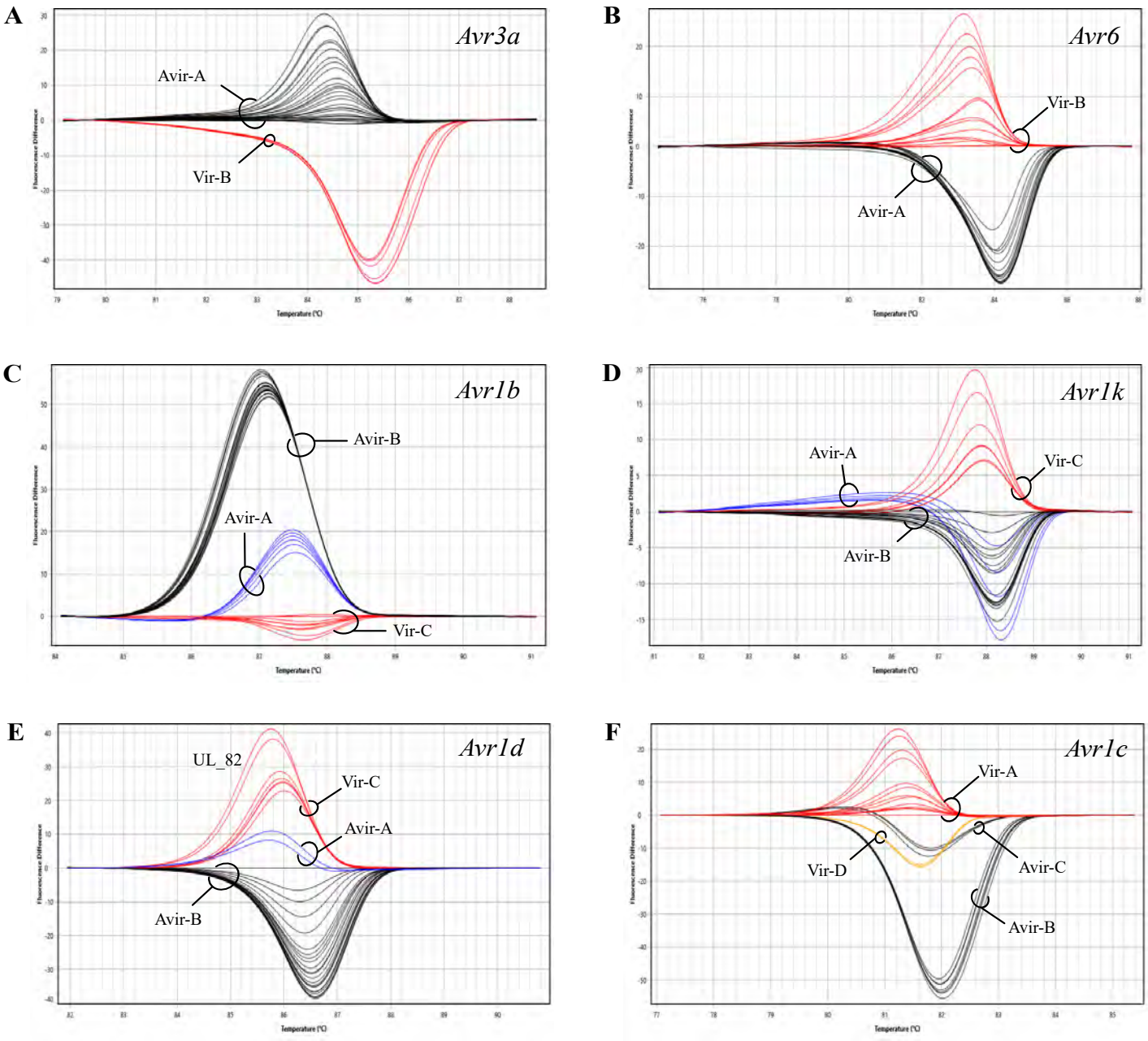
A
Avr3a
Avir-A
Vir-B
B
Avr6
Vir-B
Avir-A
C
Avr1b
Avir-B
Avir-A
Vir-C
D
Avr1k
Avir-A
Vir-C
Avir-B
E
Avr1d
UL_82
Vir-C
Avir-A
Avir-B
F
Avr1c
Vir-A
Vir-D
Avir-C
Avir-B

Figure. 3.

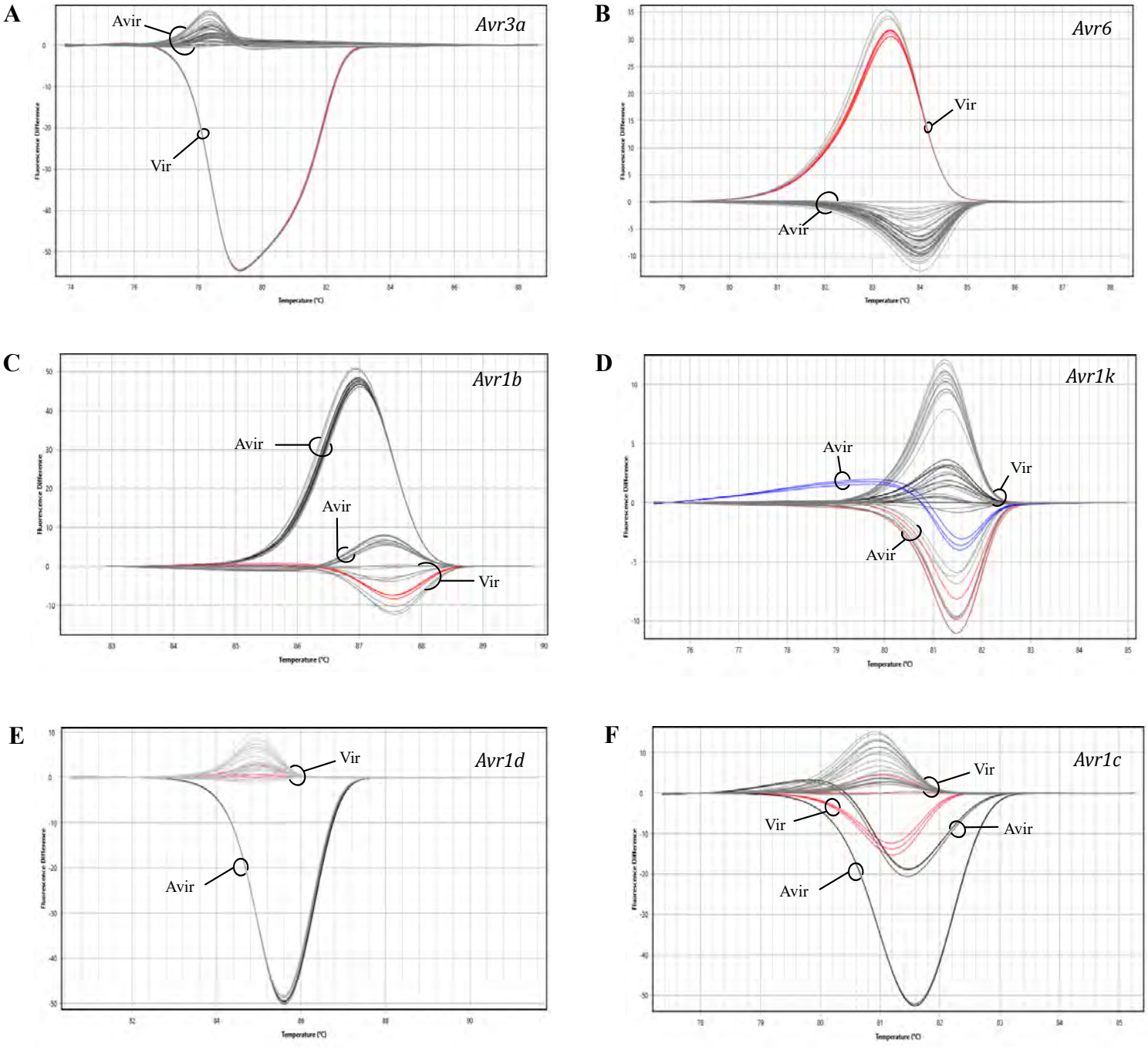
A
Avir
Avr3a
Vir
B
Avr6
Vir
Avir
C
Avr1b
Avir
Avir
Vir
D
Avr1k
Avir
Vir
Avir
E
Vir
Avr1d
Avir
F
Vir
Avr1c
Vir
Avir
Avir
Temperature (°C)

Figure. 4

A

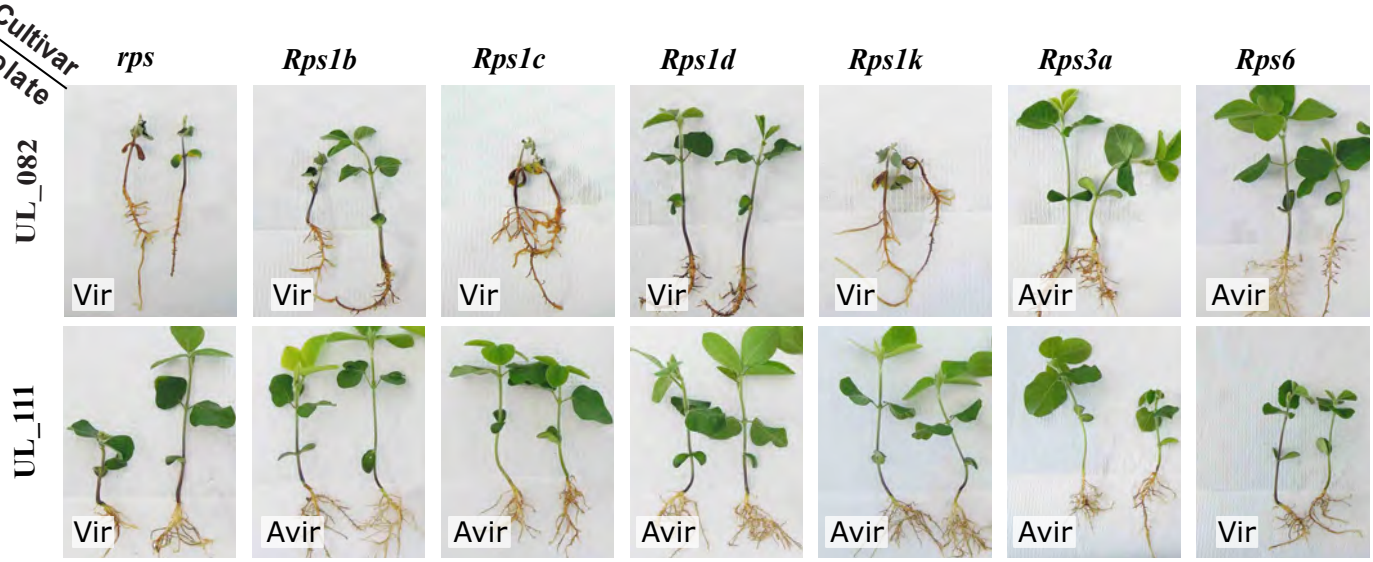

B ***Avr1b***

	Isolates	Genotype by HRM	Phenotype on Rps1b
Control	82	Vir	Vir
	111	Avir	Avir
	192	Avir	Avir
	253	Avir	Avir
isolates tested	796	Avir	Avir
	800	Avir	Avir
	817	Avir	Avir
	818	Avir	Avir
	820	Vir	Vir
	826	Avir	Avir
	829	Vir	Vir
	842	Avir	Avir
	848	Vir	Vir
	851	Vir	Vir
	860	Vir	Vir
	865	Vir	Vir

C ***Avr1c***

	Isolates	Genotype by HRM	Phenotype on Rps1c
Control	82	Vir	Vir
	111	Avir	Avir
	192	Vir	Vir
	253	Avir	Avir
isolates tested	796	Vir	Vir
	800	Vir	Vir
	817	Vir	Vir
	818	Vir	Vir
	820	Vir	Vir
	826	Vir	Vir
	829	Vir	Vir
	842	Vir	Vir
	848	Vir	Vir
	851	Vir	Vir
	860	Vir	Vir
	865	Vir	Vir

D ***Avr1d***

	Isolates	Genotype by HRM	Phenotype on Rps1d
Control	82	Vir	Vir
	111	Avir	Avir
	192	Avir	Avir
	253	Avir	Avir
isolates tested	796	Vir	Vir
	800	Vir	Vir
	817	Vir	Vir
	818	Vir	Vir
	820	Vir	Vir
	826	Avir	Avir
	829	Vir	Vir
	842	Avir	Avir
	848	Vir	Vir
	851	Vir	Vir
	860	Vir	Vir
	865	Vir	Vir

E ***Avr1k***

	Isolates	Genotype by HRM	Phenotype on Rps1k
Control	82	Vir	Vir
	111	Avir	Avir
	192	Avir	Avir
	253	Avir	Avir
isolates tested	796	Avir	Avir
	800	Avir	Avir
	817	Avir	Avir
	818	Avir	Avir
	820	Vir	Vir
	826	Avir	Avir
	829	Vir	Vir
	842	Avir	Avir
	848	Vir	Vir
	851	Vir	Vir
	860	Vir	Vir
	865	Vir	Vir

F ***Avr3a***

	Isolates	Genotype by HRM	Phenotype on Rps3a
Control	82	Avir	Avir
	111	Avir	Avir
	192	Avir	Avir
	253	Vir	Vir
isolates tested	796	Avir	Avir
	800	Avir	Avir
	817	Avir	Avir
	818	Avir	Avir
	820	Avir	Avir
	826	Avir	Avir
	829	Avir	Avir
	842	Vir	Vir
	848	Avir	Avir
	851	Avir	Avir
	860	Avir	Avir
	865	Avir	Avir

G ***Avr6***

	Isolates	Genotype by HRM	Phenotype on Rps6
Control	82	Avir	Avir
	111	Vir	vir
	192	Avir	Avir
	253	Vir	Vir
isolates tested	796	Avir	Avir
	800	Avir	Avir
	817	Avir	Avir
	818	Avir	Avir
	820	Avir	Avir
	826	Avir	Avir
	829	Avir	Avir
	842	Vir	Vir
	848	Avir	Avir
	851	Avir	Avir
	860	Avir	Avir
	865	Avir	Avir

Supplemental Figure. 1

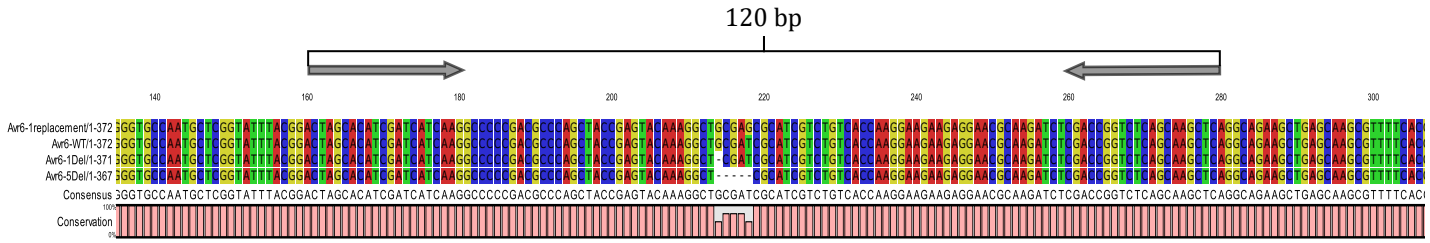

Supplemental Figure. 2

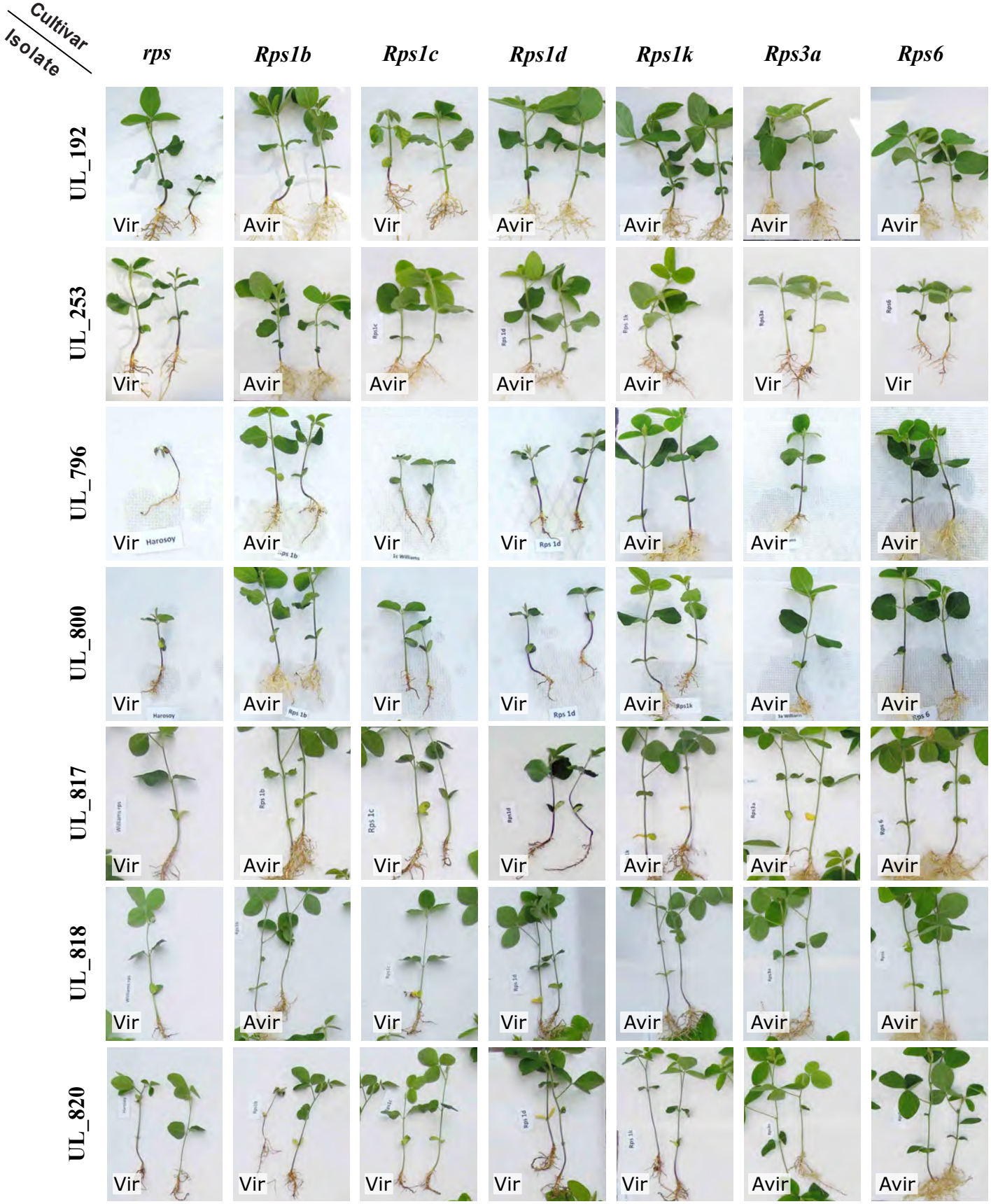

Supplemental Figure. 2 Continued

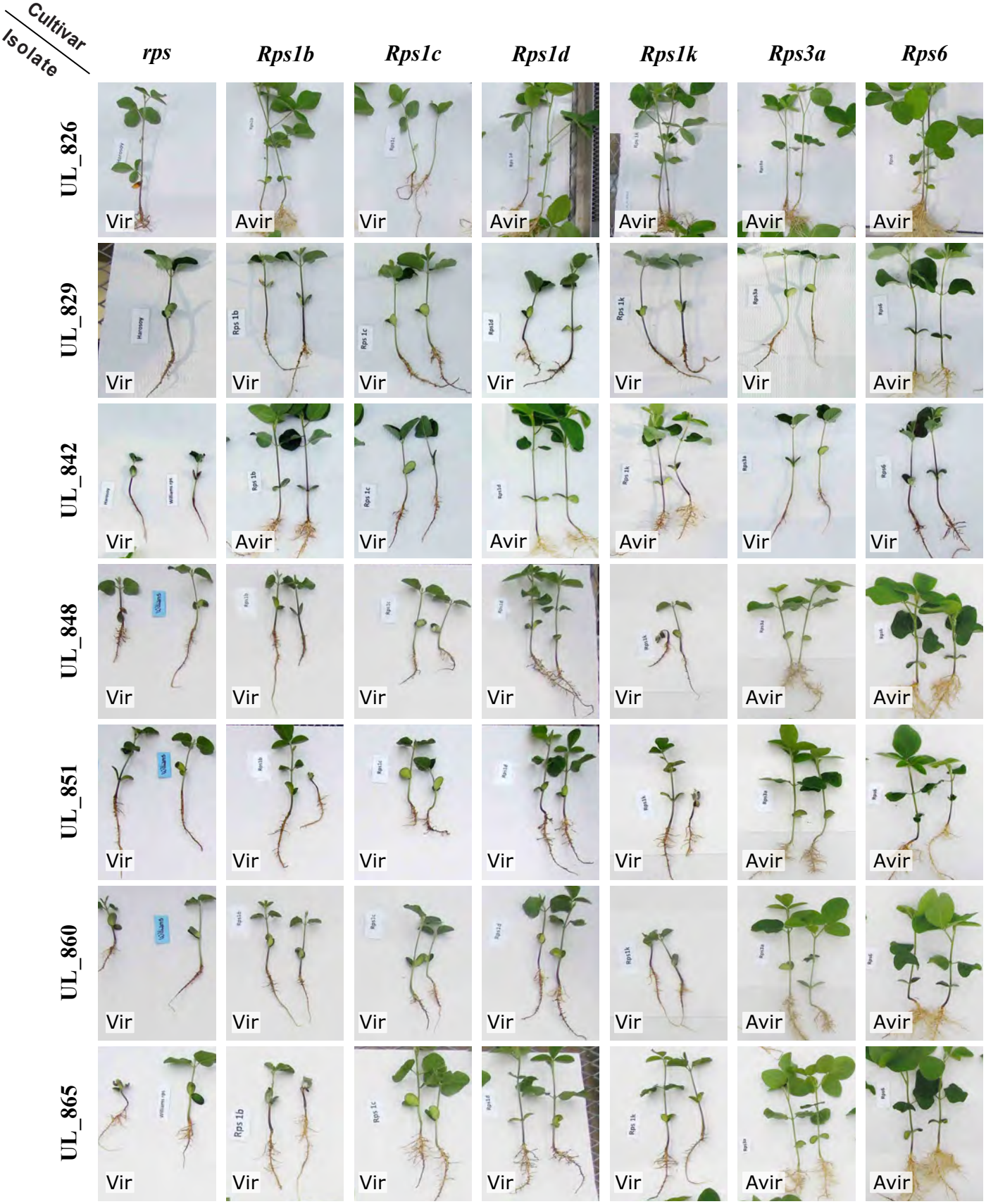

Supplemental Figure. 3

A

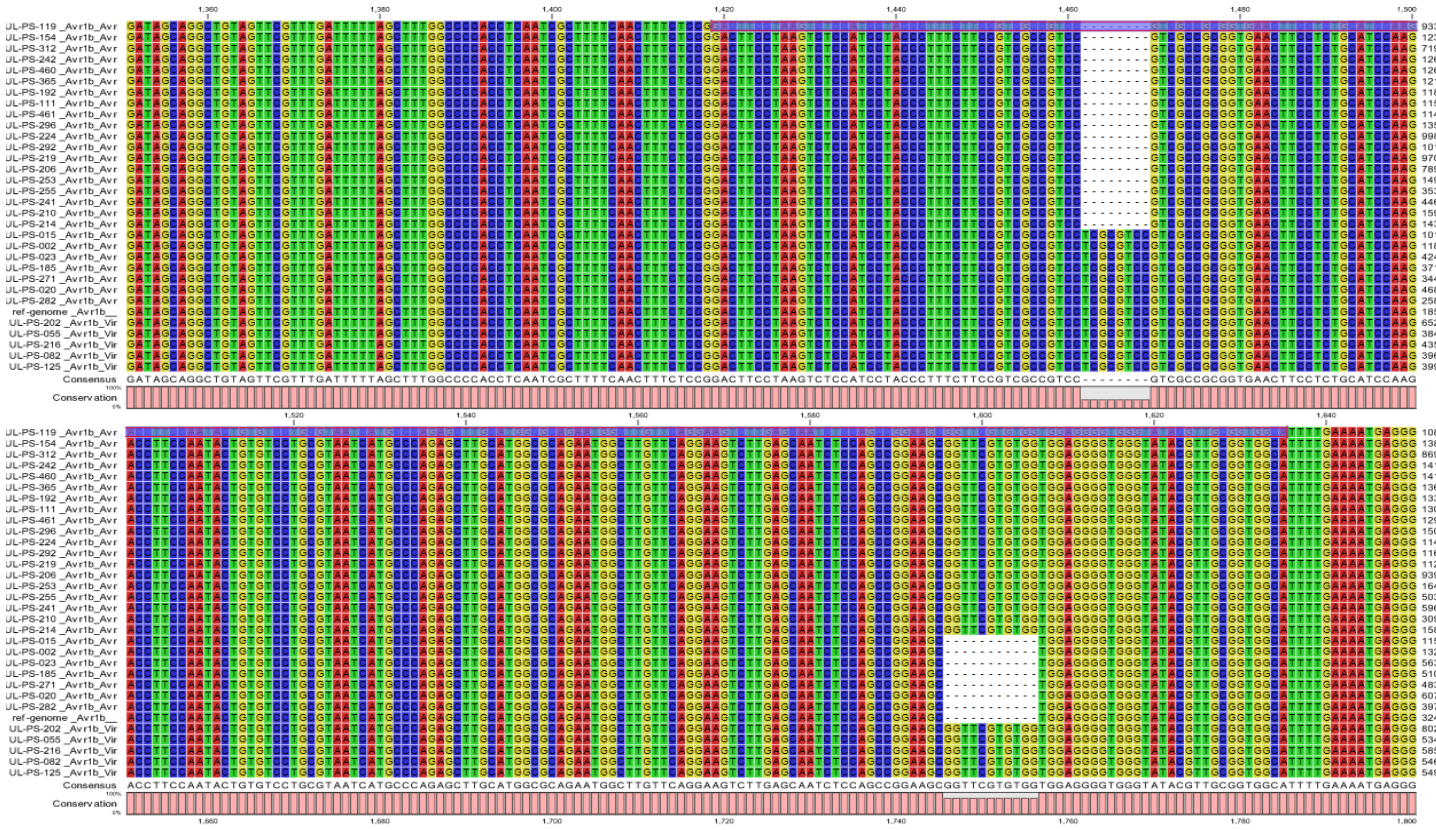

B

Avr1b-haplo A	-	GGTTCGTGTGG
Avr1b-haplo B	TCGCGTCC	-
Avr1b-haplo C	TCGCGTCC	GGTTCGTGTGG